

Dams and Reservoirs under changing Challenges

Editors:
Anton J. Schleiss & Robert M. Boes

 **CRC Press**
Taylor & Francis Group

A BALKEMA BOOK

DAMS AND RESERVOIRS UNDER CHANGING CHALLENGES

PROCEEDINGS OF THE INTERNATIONAL SYMPOSIUM ON DAMS AND RESERVOIRS
UNDER CHANGING CHALLENGES – 79 ANNUAL MEETING OF ICOLD, SWISS
COMMITTEE ON DAMS, LUCERNE, SWITZERLAND, 1 JUNE, 2011

Dams and Reservoirs under Changing Challenges

Editors

Anton J. Schleiss

*Laboratory of Hydraulic Constructions (LCH)
Ecole Polytechnique Fédérale de Lausanne (EPFL), Switzerland*

Robert M. Boes

*Laboratory of Hydraulics, Hydrology and Glaciology (VAW)
Swiss Federal Institute of Technology Zurich (ETH), Switzerland*



CRC Press

Taylor & Francis Group

Boca Raton London New York Leiden

CRC Press is an imprint of the
Taylor & Francis Group, an **informa** business

A BALKEMA BOOK

CRC Press
Taylor & Francis Group
6000 Broken Sound Parkway NW, Suite 300
Boca Raton, FL 33487-2742

© 2011 by Taylor & Francis Group, LLC
CRC Press is an imprint of Taylor & Francis Group, an Informa business

No claim to original U.S. Government works
Version Date: 20140602

International Standard Book Number-13: 978-0-203-80409-4 (eBook - PDF)

This book contains information obtained from authentic and highly regarded sources. Reasonable efforts have been made to publish reliable data and information, but the author and publisher cannot assume responsibility for the validity of all materials or the consequences of their use. The authors and publishers have attempted to trace the copyright holders of all material reproduced in this publication and apologize to copyright holders if permission to publish in this form has not been obtained. If any copyright material has not been acknowledged please write and let us know so we may rectify in any future reprint.

Except as permitted under U.S. Copyright Law, no part of this book may be reprinted, reproduced, transmitted, or utilized in any form by any electronic, mechanical, or other means, now known or hereafter invented, including photocopying, microfilming, and recording, or in any information storage or retrieval system, without written permission from the publishers.

For permission to photocopy or use material electronically from this work, please access www.copyright.com (<http://www.copyright.com/>) or contact the Copyright Clearance Center, Inc. (CCC), 222 Rosewood Drive, Danvers, MA 01923, 978-750-8400. CCC is a not-for-profit organization that provides licenses and registration for a variety of users. For organizations that have been granted a photocopy license by the CCC, a separate system of payment has been arranged.

Trademark Notice: Product or corporate names may be trademarks or registered trademarks, and are used only for identification and explanation without intent to infringe.

Visit the Taylor & Francis Web site at
<http://www.taylorandfrancis.com>

and the CRC Press Web site at
<http://www.crcpress.com>

Table of contents

Preface	xiii
Organization	xv
Sponsors	xvii
<i>Theme A: Long-term behaviour of dams</i>	
Ermenek HEPP—dam and reservoir behavior during impounding <i>E. Üzüceck, R. Kohler, J. Linortner & S. Güven</i>	3
A new approach for large structures monitoring: SCANSITES 3D® <i>H. Lançon & S. Piot</i>	11
Maintenance and operation of aged dams <i>Y. Kita, S. Ariga & M. Katayama</i>	19
Estimation of rockfill dam behavior during impounding by elasto-plastic model <i>N. Tomida, N. Sato, H. Soda, S. Jikan, K. Ohmori & H. Ohta</i>	27
The investigation method of hydroelectric facilities by using digital camera <i>S. Wada & Y. Kono</i>	35
Situation and developing trend of defective reservoir reinforcing technology in China <i>G. Dashui & T. Jiexiong</i>	43
Long term behavior of the concrete dams drainage system and ageing phenomena <i>D. Stematiu, R. Sarghiuta & A. Constantinescu</i>	51
Unpredictable behaviour of a large arch dam in South Africa <i>L.C. Hattingh & C. Oosthuizen</i>	59
Performance of a high rockfill dam during construction and first impounding—Nam Ngum 2 CFRD <i>S. Moll & R. Straubhaar</i>	65
Intensified monitoring of Emosson arch dam during construction of Nant de Drance pump storage scheme <i>H. Stahl</i>	73
Dam embankment deformation and face slab movement monitoring of Nam Ngum 2 concrete face rockfill dam <i>P. Khamwongkhong & W. Mairaing</i>	79
Analysis on the operating performance of Sanbanxi CFRD <i>Z. Xu, G. Deng & C. Zhao</i>	91
Numerical modelling investigation of an existing crack within an arch-gravity dam <i>A. Mellal, A. Koliji & M. Balissat</i>	99

Distributed fiber optic temperature measurements in embankment dams with central core—new benchmark for seepage monitoring <i>M. Aufleger, M. Goltz, J. Dornstädter & O. Mangarovski</i>	107
Performance of dams affected by expanding concrete <i>F. Amberg</i>	115
Warning systems—basic components of Hidroelectricita's emergency management system <i>I.D. Iacob & D. Zachia</i>	123
A risk based approach to dam safety management in New South Wales, Australia <i>P. Heinrichs</i>	129
Dam safety in Slovakia <i>P. Panenka & A. Kasana</i>	137
Improvement of safety of Swiss dams on the basis of experience <i>H. Pougatsch, R.W. Müller, T. Sonderegger & A. Kobelt</i>	145
Concept of safety and safety requirements for dams <i>P.A. Zielinski</i>	153
Alkali-Silica Reaction in Japan <i>H. Koga, T. Hyakutake, H. Watanabe & T. Sakamoto</i>	163
Experimental study on the detection and inhibition of alkali aggregate reactivity for dam concrete <i>C. Zhiqing, L. Xingping, Y. Jie, L. Shisheng, W. Ling & L. Han</i>	171
Expanding concrete in dams—long term challenges <i>R. Charlwood & K. Scrivener</i>	179
Re-assessment and treatment-design of an ASR-affected gravity dam <i>R. Leroy, L.I. Boldea, J.-F. Seignol & B. Godart</i>	187
The integrity of old style post tensioned anchors in dams—a real dam safety issue <i>R. Herweynen</i>	195
Development of geomembrane systems for watertightness of dams in Europe <i>A.M. Scuero & G.L. Vaschetti</i>	203
Development of small hydropower plant utilizing pumped storage power plant's dam <i>H. Watabe & N. Arai</i>	211
A study of the grouting at the bottom of the Yashio dam reservoir and the evaluation of the leakage by grouting <i>F. Kawashima, Y. Kimura & M. Nishigaki</i>	219
Filter design for the heightening of a high earth core rockfill dam <i>S. Messerklinger & R. Straubhaar</i>	229
Rock treatment around morning glory spillway of Sefidrud dam <i>A. Faghihimohaddess, R. Naghibian & A. Bashash</i>	239
Rehabilitation and upgrade of Giudea dam <i>G. Baldovin, E. Baldovin & G. Morelli</i>	247
Assessment of small gravity dam heightening <i>T. Hofmann, M. Wickenhäuser & W. Gabl</i>	255
Deriner double curvature arch dam—foundation consolidation and curtain grouting <i>K.A. Ross & M. Kaleli</i>	263

Application of grouting technique for stabilization of coarse materials—Karkheh storage dam experience, Iran <i>M. Heidarzadeh, F. Eslamian & A. Mirghasemi</i>	271
Dam safety and operational efficiency improvements in Sri Lanka <i>A. Sorgenfrei & M. Friedrich</i>	279
Strengthening of Les Toules arch dam <i>A. Wohnlich & O. Müller</i>	287
 <i>Theme B: Dams and climate change</i>	
Long-term behavior of the Yashio dam, asphalt faced rockfill dam <i>T. Tsukada, M. Doi, K. Yoshizawa & T. Kikuchi</i>	297
Some long-term problems associated with suffusion in the foundation of embankment dams <i>A. Soroush & P.T. Shourijeh</i>	305
RCC dams—is there a limit to the height? <i>M.R.H. Dunstan</i>	313
Numerical analysis of water reservoir dam—prediction of long term performance of Versetal dam (Germany) <i>M.M. Zimmerer, T. Schanz, Y. Lins & V. Bettzieche</i>	321
Dam and hydropower in a changing world <i>J. Jia, J. Ma & C. Zheng</i>	331
Sedimentation of Polish reservoirs—characteristics and significance of the phenomenon and procedures of its control <i>A. Kosik, J. Kloze & A. Wita</i>	339
Innovative sediment handling to restore reservoir capacity <i>H. Schüttrumpf & M. Detering</i>	345
Sediment management strategies for sustainable reservoir <i>T. Sumi & S.A. Kantoush</i>	353
An experimental study on turbid water coagulation method using natural coagulant <i>H. Umino & N. Hakoishi</i>	363
Burrowing-type sediment removal suction pipe for a sediment supply from reservoirs <i>T. Sakurai & N. Hakoishi</i>	371
Upper Missouri River mainstream reservoirs: Sedimentation and sustainability issues <i>M.J. Teal</i>	379
Flood retention in alpine catchments equipped with complex hydropower schemes—a case study of the upper Aare catchment in Switzerland <i>M. Bieri, A.J. Schleiss, F. Jordan, A.U. Fankhauser & M.H. Ursin</i>	387
Controlled sediment flushing of Cancano reservoir <i>P. Espa, M.L. Brignoli, A. Previde Prato, E. Castelli, G. Crosa, G. Gentili & F. Bondiolotti</i>	395
Sediment bypass tunnel design—review and outlook <i>C. Auel & R.M. Boes</i>	403
Numerical simulation of flow and sedimentation transport in the early stage of the Three Gorges Reservoir (TGR) <i>R. Huang, X. Zhang & Y. Huang</i>	413

Hybrid modeling of sediment management during drawdown of Räterichsboden reservoir <i>G. Möller, R.M. Boes, D. Theiner, A. Fankhauser, M. Daneshvari, G. De Cesare & A.J. Schleiss</i>	421
Aras transboundary river basin cooperation perspective <i>A. Heidari</i>	429
An example of sedimentation and proper management of flushing operation since 45 years: The Kashm El Girba reservoir on the Atbara river <i>C. Guilbaud, O. Cazaillet, P. Cochet & C. Odeyer</i>	437
Future glacier evolution and impact on the runoff regime in the catchments of Alpine reservoirs: The Aletsch area, Switzerland <i>D. Farinotti, A. Bauder, R.M. Boes, M. Huss, G. Jouvet & F. Widmer</i>	449
Decision Support System for the hydropower plants management: The MINERVE project <i>J.G. Hernández, A.J. Schleiss & J. Boillat</i>	459
Incorporating climate change scenarios into new operating rules for large reservoirs: A transnational assessment in the Meuse basin <i>B. Dewals, S. Detrembleur, P. Archambeau, S. Erpicum, M. Piroton, G. Demny, T. Rose, C. Homann, J. Lange, N.P. Huber, M. Kufeld, B. Sinaba & H. Schüttrumpf</i>	469
The flexible flood control capacity exploration and its relevant extra benefit estimation of lower Jinsha River cascade reservoirs <i>J. Xu, J. Chen, Z. Yin & C. Yang</i>	479
Impact of climate change on the management of water resources in mountainous regions—case of the Lake Annecy basin in the French Alps <i>M. Cottet, C. Freissinet & B. Graff</i>	487
Optimized and adapted hydropower management considering glacier shrinkage scenarios in the Swiss Alps <i>S. Terrier, F. Jordan, A.J. Schleiss, W. Haerberli, C. Huggel & M. Künzler</i>	497
Future challenges for dams under climate change <i>D.-K. Koh & J.-H. Park</i>	509
Study on rational control model for excess flood by utilizing rainfall prediction <i>A. Yamamoto, S. Mitsuishi, T. Ozeki & T. Sumi</i>	517
Effective flood control through integrated and collaborative dam operation at three dams in the upper Nabari River <i>T. Matsumura, H. Kamiya & N. Yoshida</i>	525
Global warming and design flood: The case study of Bagatelle dam, Mauritius <i>S. Le Clerc & H. Garros-Berthet</i>	533
Study on the Pan-basin optimization of West route engineering of South-to-North water transfer <i>J. Zhang, S. Peng, Y. Wang & H. Wang</i>	541
Impact of climate change on hydro-energy systems: An overview <i>R.P. Brenner</i>	551
The Upper Paunglaung RCC dam—design and construction <i>U. Myint Zaw, U. Thaug Han, Ch. Rohrer & K.M. Steiger</i>	559

Theme C: Dams and natural hazards

Damage to the Ishibuchi dam by the Iwate-Miyagi Nairiku earthquake in 2008 and seismic assessment <i>H. Yoshida, A. Nakamura, N. Matsumoto & T. Kasai</i>	569
Effects of vertical earthquake motions on deformation of Newmark sliding analysis <i>N. Matsumoto, T. Sasaki, K. Shimamoto, Y. Sugiura & H.Q. Zhao</i>	577
Earthquake-induced settlement analysis for rockfill dams using cumulative damage theory <i>Y. Yamaguchi, H. Satoh & K. Shimoyama</i>	585
Shaking table test of concrete dams with penetrated cracks and DEM analysis simulation <i>T. Iwashita, T. Kirinashizawa, Y. Yamaguchi, H. Kojima & Y. Fujitsuka</i>	595
Effects of the Iwate-Miyagi Nairiku earthquake in 2008, Japan, on a central clay core rockfill dam <i>T. Ohmachi & T. Tahara</i>	605
Seismic stability of a Peruvian tailings earth-rockfill dam with liquefiable foundation <i>M. Seid-Karbasi, H. Hawson & U. Atukorala</i>	613
Simplified methodology for estimating seismic coefficients for the pseudo-static slope stability analysis of earth dams <i>A.G. Papadimitriou, K.I. Andrianopoulos, G.D. Bouckovalas & K. Anastasopoulos</i>	621
Dam shape adaptation resulting from strong earthquake context <i>B. Tardieu, A. Si-Chaib, M. Marouk & M. Bibi</i>	629
Seismic safety of Chancy-Pougny dam <i>M. Ferrière, J.-P. Person, H. Charif, O. Vallotton, S. Rossier & P. Lestuzzi</i>	637
Behavior analysis of soil-structure interaction of a composite dam using geo-centrifuge test <i>J.Y. Lim & I.S. Ha</i>	645
Swiss expertise in North Africa focusing on flood protection <i>N. Nilipour & K. Essyad</i>	653
Risk assessment for the critical regimes of Chaira dam stilling basin <i>J. Tadjer & H.T. Falvey</i>	661
Design and hydraulic modelling of a fuse plug spillway <i>L. Schmocker, E. Rühli, V. Weitbrecht, R.M. Boes, P.A. Mayor & S.M. Springman</i>	669
Inflow Design Flood and dam safety <i>P.A. Zielinski</i>	677
Combinations of earthquake and flood hazards together with other factors <i>D.N.D. Hartford</i>	685
Measures to reduce dynamic plunge pool pressures generated by a free jet <i>Th. Berchtold & M. Pfister</i>	693
Impulse waves at Kühtai reservoir generated by avalanches and landslides <i>H. Fuchs, R.M. Boes & M. Pfister</i>	701
Numerical simulations of water waves due to landslides <i>Z. Jiang, J. Han & Z. Cheng</i>	709

Hazard and risk assessment of rock slide tsunamis in lakes and reservoirs <i>C. Harbitz, F. Løvholt, U. Domaas, S. Glimsdal & B. Romstad</i>	717
Characteristics study of Gorge reservoir landslide <i>X.L. Tang, X.L. Tang, D.Y. Liu & H.B. Feng</i>	725
Goescheneralp dam—impact of natural hazards on construction site and freeboard optimisation <i>T. Dietler</i>	733
Design and construction of asphalt facing in cold heavy snow region <i>S. Abe, H. Seto & H. Watanabe</i>	741
 <i>Theme D: Dams in a sound environment</i>	
Identification of hazardous zones for development of tourism industry: A case study in Taleghan dam catchment area <i>N. Ahmadi & H. Ahmadi</i>	753
How to maintain the bad reputation of dam projects <i>R. Zwahlen</i>	761
Measures for vegetation restoration on modification sites at Takizawa dam <i>N. Takemoto, Y. Takahashi & M. Hirose</i>	769
Building dams in a sound environment: Development of La Romaine HEP, situated in Northern Québec, Canada <i>B. Soucy, V. Alicescu & J.-P. Tournier</i>	777
Methodological approach and artificial intelligence application as a solution for environmental conflict related to large dams <i>S. Stevovic, M. Stamatovic & G. Ivanovic</i>	785
Introduction of cost-benefit evaluation of the environmental impacts and mitigation measures in hydropower production and water supply service sectors <i>A. Kryżanowski & M. Gorišek</i>	791
Environmentally rehabilitation of dam Bitdalen <i>A.M. Ruud & L. Lia</i>	799
The conservation measures on rare and endemic fish during the construction of cascaded hydropower projects in downstream of Jinsha River <i>X. Zhao, Z. Sun, Y. Chen, D. Wang & Y. Gao</i>	807
Application of MIKE 11 model in the prediction of water pollution accident in the Three Gorges Reservoir <i>Y. Fang & Y. Min</i>	813
Protection of the National Mayanghe Natural Reserve in development of Wujiang Panshui Hydropower Station <i>G. Jiang, H. Li & Y. Li</i>	821
Implement water diversion measures to ease the ecological water demand of the Yellow River Delta <i>X. Li, L. Sun & X. Meng</i>	829
Study on river ecological compensation of China <i>B. Ruan & Y. Fu</i>	835

Impacts of dam on Key Biodiversity Area in southwest China based on integrated map <i>L. Chong, P. Jing & W. Hao</i>	843
A model for the dry closure of tailings dams <i>J.L. Justo, P. Durand, M. Vázquez, A. Morales & F.A. Jiménez</i>	849
A holistic approach to reduce negative impacts of hydropeaking <i>W. Gostner, C. Lucarelli, D. Theiner, A. Kager, G. Premstaller & A.J. Schleiss</i>	857
The new Muttssee dam (Switzerland) <i>F. Tognola & M. Balissat</i>	867
Post-audit of Alqueva reservoir's water quality: Lessons learned with the comparison between forecast and reality <i>P.A. Diogo, A.C. Rodrigues, P.S. Coelho & M. Almeida</i>	875
Keyword index	883
Author index	885

Preface

This book contains 106 papers selected by the reviewers out of 170 accepted papers for the International Symposium on “Dams and Reservoirs under changing Challenges” held on June 1, 2011 during the 79th Annual Meeting of the International Commission on Large Dams in Lucerne, Switzerland.

In today’s globalized world, many things seem to be changing ever faster. Even for the very ancient art of building dams, the largest man-made structures of great longevity, some boundary conditions are indeed different nowadays from what they used to be. In particular, besides the technological part in the dam planning, construction, operation and maintenance processes, ICOLD’s mission to also adequately deal with the environment and related infrastructure has become increasingly important and challenging. In the frame of global climate change, altered water cycles as well as more extreme weather conditions and an increasing number of natural hazards clearly affect the safe and economical operation of dams and reservoirs. Moreover, emission-free hydropower production as the most important form of “liquid” solar energy and the provision of water for irrigation and potable water supply is becoming more and more important to meet the world’s fast growing demand for energy and food in a sustainable way.

These reflections led us to divide the symposium into four main themes, namely

- Long-term behaviour of dams
- Dams and climate change
- Dams and natural hazards
- Dams in a sound environment.

This book gives an overview on current case studies, design applications, construction, maintenance and operation experience as well as research and development activities related to the mentioned themes from around the world.

The editors gratefully acknowledge the contribution of the authors, the work of the reviewers and the support of the international scientific as well as the local organizing committees. Special thanks go to Dr. Michael Pfister (LCH) and Lukas Vonwiller, Jeannette Gabbi and Renata Müller (VAW) who managed the review process and the submission of the final papers and prepared the print-ready version of these Proceedings.

Moreover, the support and sponsorship of our partners and sponsors are kindly acknowledged.

Anton J. Schleiss
Laboratory of Hydraulic Constructions (LCH)
Ecole Polytechnique Fédérale de Lausanne (EPFL)
Conference chair and Chairman of the Swiss Committee on Dams

Robert M. Boes
Laboratory of Hydraulics, Hydrology and Glaciology (VAW)
Swiss Federal Institute of Technology Zurich (ETH)
Conference chair

Lucerne, June 2011

Organization

CONFERENCE CHAIRS

Prof. Dr. Anton J. Schleiss, *Switzerland*
Prof. Dr. Robert M. Boes, *Switzerland*

SECRETARY GENERAL

Dr. Bernard Joos, *Switzerland*

LOCAL ORGANIZING COMMITTEE

Marc Balissat, *Switzerland*
Dr. Peter Billeter, *Switzerland*
Hans Bodenmann, *Switzerland*
Dr. Roger Bremen, *Switzerland*
Dr. Peter Brenner, *Switzerland*
Ian Clarke, *Switzerland*
Dr. Georges Darbre, *Switzerland*
Dr. Walter Hauenstein, *Switzerland*
Dr. Harald Kreuzer, *Switzerland*
Laurent Mouvet, *Switzerland*
Dr. Bastian Otto, *Switzerland*
Andreas J. Siegfried, *Switzerland*
Karl Steiger, *Switzerland*
Dr. Martin Wieland, *Switzerland*

INTERNATIONAL SCIENTIFIC COMMITTEE

Prof. Dr. Markus Aufleger, *Austria*
André Carrère, *France*
Jean-Jaques Fry, *France*
Patrick Le Delliou, *France*
Michel-Marc Lino, *France*
Michel Poupart, *France*
Dr. Giovanni Ruggeri, *Italy*
Prof. Dr. Peter Rutschmann, *Germany*
Dr. Pietro Sembenelli, *Italy*
Prof. Dr. Peter Tschernutter, *Austria*
Prof. Dr. Silke Wieprecht, *Germany*
Prof. Dr. Gerald Zenz, *Austria*

PROCEEDINGS

Dr. Michael Pfister, *Switzerland*, Management of review process and proceedings
Lukas Vonwiller, *Switzerland*, Assistance to formatting

SECRETARIAL OFFICE

Rachel Niedermann, *Switzerland*

Sponsors

PARTNERS

ETH

Eidgenössische Technische Hochschule Zürich
Swiss Federal Institute of Technology Zurich

Lombardi

EPFL

ÉCOLE POLYTECHNIQUE
FÉDÉRALE DE LAUSANNE

LUZERN+
TICEVME
THE CITY. THE LAKE. THE MOUNTAINS.

WALO

Walo Bertschinger

swiss

Swiss
International
Air Lines



AF-Colenco AG

MAIN SPONSORS

YKWO
GRIMSELSTROM

STUCKY



Marti Holding AG
Baunternehmungen

BKW ⚡
BKW FMB Energie AG

Schweizerische Eidgenossenschaft
Confédération suisse
Confederazione Svizzera
Confederaziun svizra
Bundesamt für Energie BFE
Office fédéral de l'énergie OFEN
Ufficio federale dell'energia UFE
Swiss Federal Office of Energy SFOE

PÖYRY

HUGGENBERGER AG
SINCE 1908

ewz
Die Energie

ALPIQ

SPONSORS

REPOWER

Ofima
Maggia Kraftwerke AG

**Grande
Dixence**

Holcim

CO-SPONSORS



Theme A: Long-term behaviour of dams



Grande Dixence Dam, Switzerland (285 m, 1961).

Ermenek HEPP—dam and reservoir behavior during impounding

E. Üzüceck

Devlet Su İşleri (DSİ), Yucetepe, Ankara, Turkey

R. Kohler

Pöyry Energy GmbH, Salzburg, Austria

J. Linortner & S. Güven

Pöyry Energy GmbH, Ankara Branch Office, Ankara, Turkey

ABSTRACT: An Austrian—Turkish Consortium is constructing the hydro power plant Ermenek in Turkey for the Turkish State Hydraulic Works, DSI. The project is located in the South of Turkey, at the Ermenek river, and has an installed capacity of 300 MW with an estimated annual energy output of 1000 GWh. The project consists of an arch dam, a large grout curtain, a pressure tunnel, a power house and appurtenant structures. The 218 m high double curved thin arch dam is located in a mega-block (Olistolith) of Nadire limestone. The highly karstified limestone is sealed at both sides of the dam by a huge grout curtain of 682.00 m². The performance of this grout curtain together with the drainage curtain in the vicinity of the dam abutment is of high importance for pore water pressure and consequently the dam stability. In addition the grout curtain should reduce the seepage to a minimum. Further on the tightness of the reservoir itself is of high interest due to the low water inflow (yearly average 42.3 m³/s) compared with the reservoir volume of 4600 mio m³.

1 INTRODUCTION

1.1 General

The concreting works for the dam started in September 2007 and could be finalized in October 2009. For the 218 m high dam, only 300,000 m³ of concrete and about 363,000 m³ of rock excavation were necessary due to the extreme steep and narrow gorge with a natural width at the base of 20 m and about 110 m at the crest. The thickness of the structure at the center line is at the dam's base 25 m and 7 m at the crest.

As the reservoir has a huge overall volume of about 4600 mio m³ it was necessary to start with the impounding already during the dam construction. Therefore, when concreting of the dam reached an elevation above 600 m a.s.l., i.e. 100 m below final crest elevation, the vertical contraction joints were grouted and the impounding started in August 2009. Due to the narrowness of the valley and the high water influx during the wet season the reservoir level increased rapidly after overtopping of the concrete cofferdam. The average increase between August 2009 and March 2010 was approximately 40 cm/day with a peak of 10 m/12 hours increase during an extraordinary flood (100 year flood event) in November 2009. By the end of September 2010 the lake reached the elevation of 625 m a.s.l., which is 135 m above foundation.

In summer-dry season the reservoir was gradually filling and the next increase of further rapid filling is expected in the winter-wet season between November 2010 and May 2011. Start of operation is expected for May/June 2011 depending on the water influx of the next coming months. The remaining additional amount of water volume for start of operation is

about 1300 mio m³. Maximum operation level can be reached only 2 years later according to longtime average influx values and the usage of water after start of operation.

The main items of interest which are influenced by the increase of the water level and mountain water table during impounding are:

- the stability of the dam and its abutments
- the tightness of the grout curtain
- the reservoir tightness itself

1.2 General geological conditions

The dam site is located in a large limestone body which is embedded in a sequence of flysch-type rock with alternating layers of sandstone and claystone. In the reservoir area the limestone is crossed by a major fault (F1) which also causes a downward displacement of the marl so that the permeable limestone (dam side) borders to impermeable Görmel marl along the F1 fault.

A second fault F2 runs parallel to F1-fault, but closer to dam site. An overview of the geological conditions at dam site is given in figure 1.

In the course of the project execution the alignment of the grout curtain was re-considered once more and therefore further investigation (geophysical and hydro-geological investigations, boreholes, etc.) were executed at the right embankment to evaluate the behavior of fault F1. Finally it could be concluded that with the new alignment the grout curtain could be shortened and anchored into the impervious Flysch rock.

In the reservoir itself, detailed hydro-geological investigations were executed by the hydro-geological department of the client, to ensure that there will be no seepage out of the reservoir.

For the dam and for the wedge stability during the dam excavation detailed rock parameter studies were performed and detailed survey and mapping of the faults and joints in the concerned area was applied before and during the progress of the works. All information gained during the excavation of the grouting galleries and tunnel with a total length of more than ... km were taken into consideration for both wedge stability calculation and grout curtain design and application.

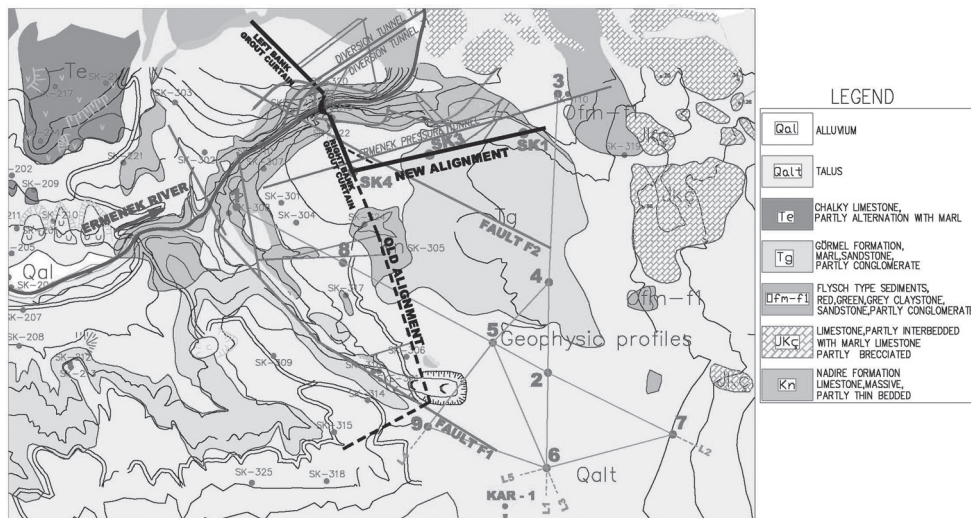


Figure 1. Geological overview at dam area.

2 EVALUATION OF THE DAM AND RESERVOIR BEHAVIOR AFTER START OF IMPOUNDING

2.1 Dam and abutments

The following picture shows the dam from a downstream view with the impounding stage in October 2010.

The grouting works in the vicinity of the dam were done in two steps: first step was consolidation grouting to improve the contact between concrete and rock and to homogenize the surrounding rock fissured due to blasting during excavation and as second step the grout curtain was drilled and injected. In addition link holes were executed in the abutments, to connect the grout curtain with the dam body concrete. In the vicinity of the dam the curtain was executed as double and partly triple row. Consolidation grouting holes and the link-holes were drilled from the inclined shafts, whereas the grout curtain was drilled from gallery to gallery. Subsequently figure 3 shows the application of the grouting works in the dam abutment.

Finally a drainage curtain at both dam abutments was drilled at the air side with a drill-hole length of 20 m. This drainage curtain was drilled from the galleries as well as from



Figure 2. Picture of the dam from downstream taken in October 2010.

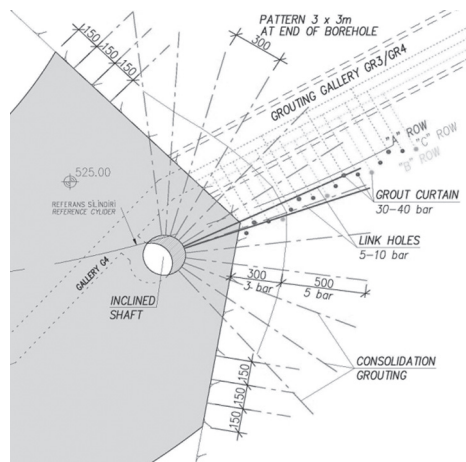


Figure 3. Application of consolidation and link hole grouting from inclined shaft.

the grouting chambers. The ones closer to the curtain are dewatering upwards, the others downwards (see figure 4). In order to observe and control the uplift pressure below the dam foundation drainage holes were drilled from the lower dam body gallery. By means of the drainage curtain in the vicinity of the dam the uplift pressure is controlled which is essential for the dam stability and also for the stability of the abutments. The total water seepage from the galleries and also from the dam abutments is measured by water flow gauging stations which are located at the gallery levels at both sides of the dam.

To monitor the deformation of the abutments, extensometers are installed at the gallery levels with depth of 5, 10, 20 and 30 m in downstream and upstream direction. Beside this the dam body is fully equipped with instrumentation of pendulum, clinometers, strain- and pressiometer, invar wires, temperature gauges, water level gauge, jointmeter, etc. (see Zenz et al. 2009).

Piezometer have been installed in addition at different levels and locations which also allow to monitor the development of the uplift pressure. The piezometer in the dam abutment at both sides have a staggered depth of 5, 15 and 30 m (see figures 4 and 5).

The evaluation of the measurement results at the Ermenek dam during the first two years of impounding, i.e. until reaching the minimum operation level of 660 m a.s.l., is done by Pöyry. As a first step Pöyry developed the work program for the measurements and focused on the improvement of the accuracy of different measuring devices. The evaluation of the records is done in 3 months intervals. So far no unusual behavior of the measured deformations and strains were observed at the dam body and abutment. The maximum deformations in the dam are actually around 3.3 mm which is below the calculated value of 4.7 mm.

From seepage point of view it can be stated that in the close vicinity of the dam (200 m on each side) the performance of the double row (-triple row) grout curtain is rather successful. No high seepage was encountered from the drainage curtain, neither in the grouting chambers nor in the gallery connection points with the dam body. Also the seepage in the gallery section is very low compared to the gallery sections with only single row curtain. In the double row curtain section only some holes are dripping and a few of them are slightly flowing.

The figures below show the locations of the piezometer and pore-water-pressures measured in the vicinity of the dam by the end of September 2010.

From uplift point of view it has to be stated that a few piezometers at the left bank showed rather high values which were already at the border of the design assumptions, in particular

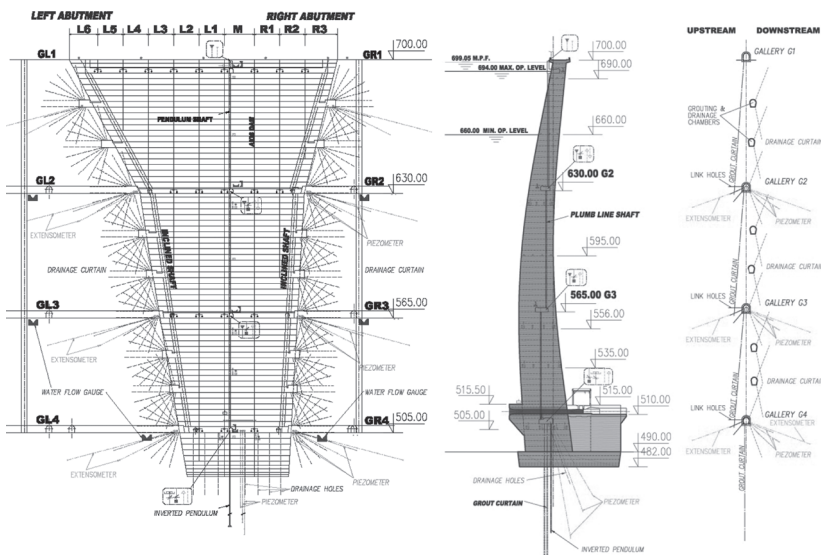


Figure 4. Dam instrumentation and drainage curtain.

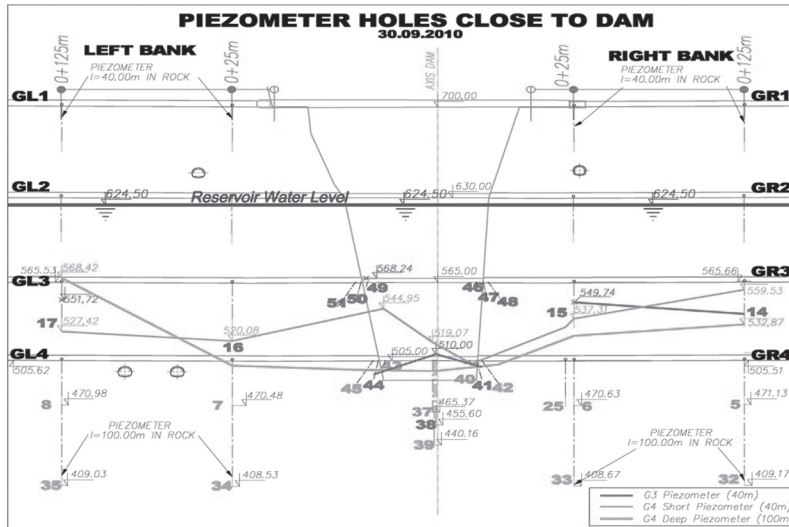


Figure 5. Piezometer measurements in the dam's vicinity.

the short (5 m) piezometer no. 43 and no. 49 next to the concrete-rock interface. Checkholes drilled into these intersection joints could not confirm the high uplift pressure. So the reason for these wrongly high recorded values might be found in the application of the piezometer installation. The uplift pressure at the dam foundation is below the design assumptions.

2.2 Application and tightness of the grout curtain

The grout curtain alignment was changed and shortened during project execution to a still remarkable total length of 2.2 km in order to anchor the curtain in the impermeable underlying flysch rocks (see chapter 1.2). About design and construction of the grout curtain it was reported in Linortner et al. (2009).

The limestone is a massive rock in moderately jointed condition. Especially at the left embankment and close to the contact to the underlying flysch rocks it could be noted that the degree of jointing is significantly lower than in general (see figure 6). In these areas it could be noted that the limestone is thickly bedded, but these bedding planes are closed and not karstified, therefore permeability and grout takes are low in these areas.

In general the rock is highly karstified. The intensity of karstification is slightly decreasing with depth. Even below the original groundwater level (of approximately 504 m) the rock is karstified, although approximately 100–150 m below the groundwater level the intensity of this process is significantly diminishing. The contact to the underlying flysch rocks is sharp, but it is not accompanied by increased karstification.

The karst cavities have been developed preferentially along the orthogonal joint system and the openings are often filled with soft clay with increased tendency of washing out closer to the surface of terrain. During grouting works it could be observed occasionally that the clay fillings have been pressed out to free surfaces from a depth of up to 70 m below gallery GR4. The fault F2 intersects the grout curtain two times, has a thickness of a few centimeters, at chainage 0 + 200 up to 1–2 decimeter, and is accompanied by parallel joints and faults of high persistence especially between chainage 470 and 770. This fault is associated with increased karstification and causes increased permeability of the rock mass so that additional sealing of the curtain had to be done.

The grout curtain is executed as an inclined curtain towards upstream from four galleries with about 70 m vertical distance, connected by link holes at the gallery levels. In general, it is a single row curtain with a final average spacing of 1.20 m. In the vicinity of the dam it is

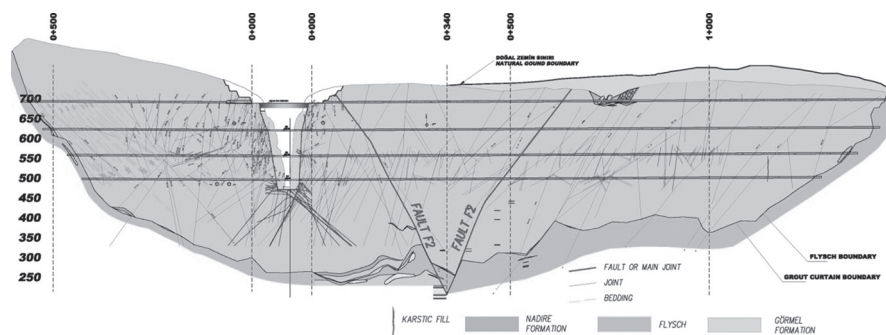


Figure 6. Geological section through the new grout curtain alignment.

executed as a double row curtain with reinforcing by a third row where necessary (based on the grout take in the first two rows). The average grout take in the grout curtain holes is 92 kg/m. The grout curtain was finalized in the lower two galleries before the impounding started. The grouting pressure applied was two times the final water pressure after full impounding.

Evaluation of the success of the grouting works was done during the grout curtain application by check holes with core recovery and Lugeon tests. The criteria for the Lugeon tests were defined by 1 to 2 Lugeon in the vicinity of the dam and 3 to 5 Lugeon in the other areas. Where these criteria could not be fulfilled additional grout holes were applied to strengthen the curtain.

Finally the drainage holes were drilled in each gallery with 12 m spacing and a depth of 10 m. For further control piezometer holes were applied, in the lower galleries with a depth of 40 and 100 m and in the upper galleries with 40 m. Prior to start of impounding the seepage and water pressure was recorded to be compared with the records during rising of the water level. Following figures show the increase of water seepage and the increase of water pressure in comparison with the rising water level in the reservoir within the first year of impounding. Total recorded seepage with end of September 2010 was recorded by 33 l/s which stays below the assumptions.

For comparison of the pressure, upstream and downstream of the grout curtain piezometer were installed, recorded and evaluated together with the piezometer installed in the galleries. The following figure shows a section about 300 m downstream of the dam through the grout curtain.

In the figure below it can be seen that the water pressure recorded downstream of the grout curtain is quit high and above the design assumptions. The reason for this is on the one hand side the high permeability along fault F2 which is also confirmed by the seepage measurements and on the other side the low permeability of the rock mass towards the gorge. To solve this problem strengthening of the grout curtain in the location of the fault and its branches is ongoing. Finally the water pressure will be released by drilling of additional drainage holes.

2.3 Tightness of the reservoir

At maximum operation level (694 m a.s.l.) the reservoir will have a surface area of 58.74 km² and a volume of 4582 mio m³. Compared to this huge reservoir, the mean water inflow of 42.3 m³/s is relatively low and therefore the tightness of the reservoir is very important. The hydrogeological investigations of the reservoir conditions were done by the geological and hydro-geological department of DSI. Mainly the geological formations and the springs surrounding the reservoir were mapped and evaluated. All springs are above the operation level of the reservoir indicating an impermeable basin. The question of waterloss out of the reservoir towards South along F1 was answered by the information gained from additional geological investigations like boreholes, seismic and

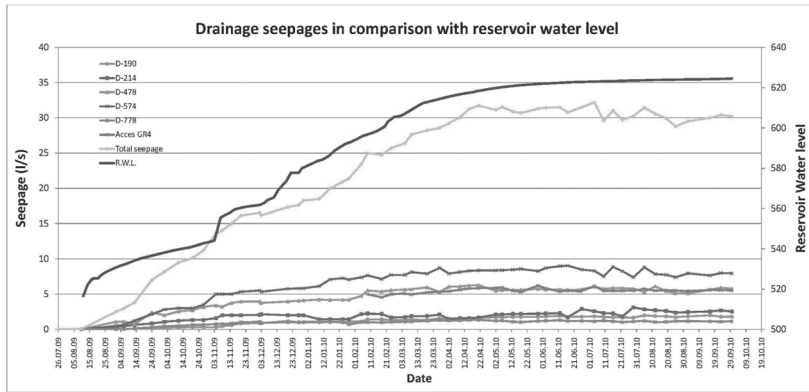


Figure 7. Seepage measurements in the galleries, single bigger seepages and total seepage.

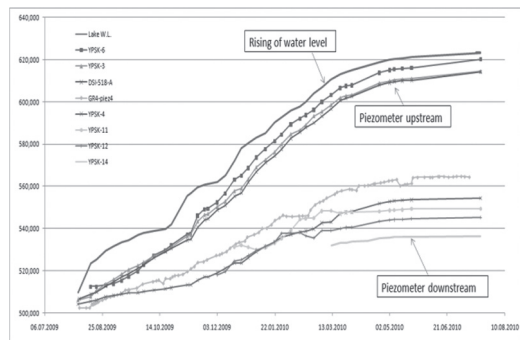
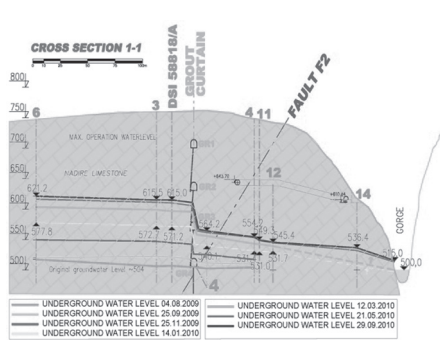


Figure 8. Section through the grout curtain. Figure 9. Development of the piezometer pressure.

hydro-geological investigations and lead to the decision that the grout curtain alignment was shortened as described in chapter 1.2.

In addition to the above mentioned investigations the contractor ordered a study at the UKAM—Hacettepe University/Ankara about possible waterloss along F1. For this study 15 wells in the concerned area were drilled and the water levels were measured during dry and wet season. Additionally to that the hydro chemical conditions (chemical analysis and electrical conductivity) have been evaluated and groundwater monitoring with tracer tests have been executed. The findings in this report did not give a clear picture but also not a clear indication of a risk for seepage towards South. Therefore Pöyry together with the local geological and hydro-geological experts A.&S. Altuğ prepared an additional study taking also the information's of the UKAM report into consideration. This study came to the conclusion that there is no indication for water loss along F1 and the chosen alignment of the grout curtain should be followed up.

Several piezometer have been installed on both embankments, up- and downstream of the grout curtain, in order to observe the increase of the groundwater level. The upstream ones show the development of the ground water table during impounding, the downstream ones give an indication of the tightness of the grout curtain. In the figure below the locations of those piezometer and some significant measurement records are shown. The general trend of bank filling can be seen from the contour lines of the groundwater level. This shape of the contour lines remained more or less constant during impounding which indicates also homogenous underground conditions in the reservoir.

The hydraulic gradient between reservoir and grout curtain is getting lower with increased reservoir filling which also indicates a gradual filling of the joint system in the banks upstream

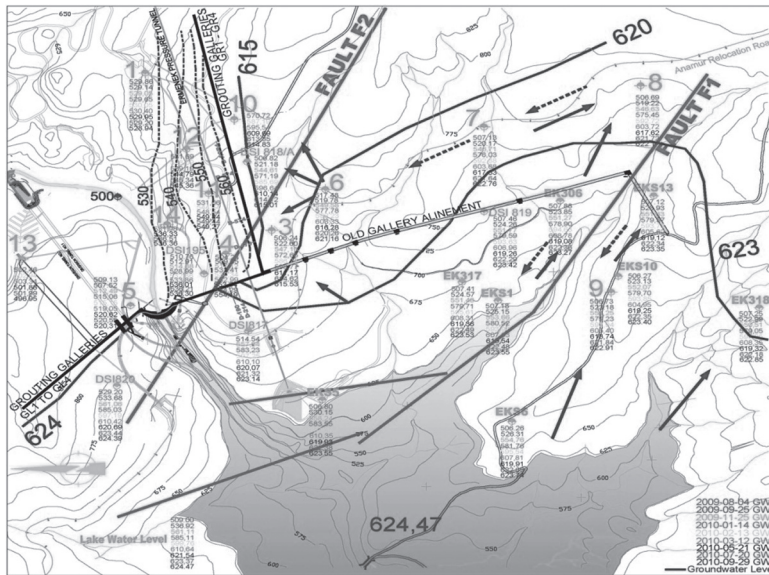


Figure 10. Field piezometer with flow directions.

of the grout curtain. This is demonstrated by the decreasing difference between the upstream piezometer and the reservoir water level as shown in figure 9. Furthermore it can be seen that the groundwater flow direction between several piezometer in the vicinity of fault F1 is changing in monthly intervals due to weather conditions which lead to increased groundwater inflow from the mountainside. This is a positive indication, as the extension of permeable rocks below the overlying Görmel marble could not be confirmed at every part of reservoir before impounding. Now it is confirmed that there is no seepage towards the South.

3 CONCLUSION

At this stage of the evaluation, October 2010, 135 m out of total 204 m are impounded. Impounding is still ongoing and start of operation is expected to be reached in May/June 2011.

So far the deformation behavior of the dam is within the expected range. For the tightness of the grout curtain and the reservoir the evaluation of the measuring results is an ongoing process. The pore pressures and seepages in the vicinity of the dam are within expected values. Higher seepages are encountered in the area of a fault zone crossing the grout curtain. The total seepage is below the assumptions, but the pressure at the downstream of the grout curtain is above the design assumptions in the area of F2. Therefore treatment of the grout curtain is ongoing in the concerned areas and additional drainage holes are ordered to be drilled. Bigger waterlosses out of the reservoir could not be recorded; even during the dry season in 2010 only smooth filling of the surrounded embankments was observed. So impounding can go on without any interruption.

REFERENCES

- Linortner J., Jung G., & Zenz G. 2009. Design and construction of the grout curtain for the Ermenek hydropower plant. Felsbau 5/2009.
- Zenz, G., Kohler, R., & Linortner J., 2009. Ermenek Dam-Construction, Instrumentation and start of Impounding, 2nd National Symposium and Exposition on Dam Safety, Eskişehir, May 2009.

A new approach for large structures monitoring: SCANSITES 3D®

H. Lançon & S. Piot

SITES Company, Rueil-Malmaison, France

ABSTRACT: Dams' monitoring needs to take care of walls' deformations and degradations. New technologies provide some modern tools to produce some detailed and numeric visual inspection and geometric surveys. The SCANSITES 3D® was developed to provide, in a multilayer file associated to a database, a high density survey and a detailed inspection. Two case studies show the method's results.

1 INTRODUCTION

Since decades, among the existing monitoring devices and methodologies, two are widely used for large dams' safety management: visual inspection and geometric survey. The first is usually carried out with empiric methods, and the second is realized using accurate but discrete methods such as geodetic micro-triangulation.

This paper introduces a new approach, using an exhaustive and numeric method called "SCANSITES 3D®".

The SCANSITES 3D® is based on a combination of the SCANSITES® method, which is an advanced tool to provide numeric defects inspection on large structures, and a new wide ranged Lidar technologies aiming to deliver geometric exhaustive mapping, and photogrammetric coverage.

In the first part of this paper, we will describe the SCANSITES® method, in a second part the Lidar coverage and in the third one, the photogrammetry. We will explain how the combination is performed and which data can be extracted on large structures. Before concluding, we will extend this paper with additional data which could be overlaid, such as thermographic pictures.

2 SCANSITES® OVERVIEW

By the past, many owners weren't completely satisfied with the traditional defects mapping process, using binoculars or rope access. The main drawback is the difficulty to produce a scaled defects map enabling an accurate and reproducible monitoring (crack evolution...). To answer this problem, the SCANSITES® was developed in 1990's. This system aims to produce a numeric defects mapping connected to a database which is working as a true real-time G.I.S. (Geographic Information System). It's composed of:

- An hardware tool with a robotized inspection head and its controllers (Fig. 1).
- A software suite including a database and several dedicated inspection tools.

The whole system is designed to operate in-field, without heavy carriage. Several dozens of dams have been surveyed by the SCANSITES® and SITES Company team across the world (Figs. 2, 3).



Figure 1. SCANSITES® head.

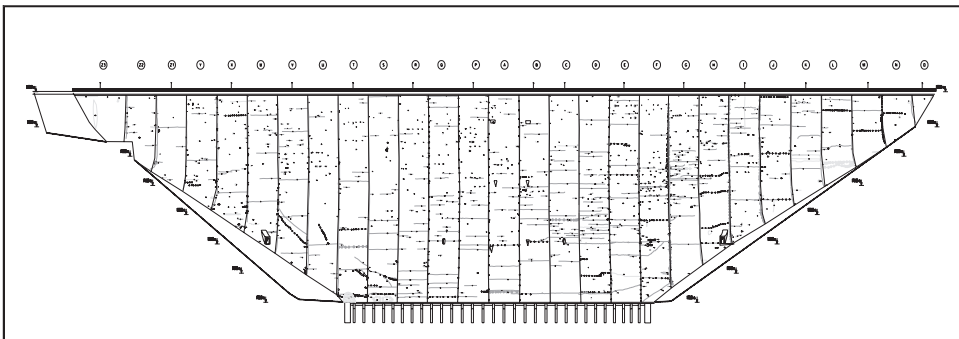


Figure 2. Defects mapping.



Figure 3. Picture of defect captured with SCANSITES®.

3 LIDAR OVERVIEW

The Lidar (Fig. 4) is a device which aims to produce some high density surveying in 3D coordinates. It's based on two angular coders and a remote electronic distance measurement device. The system works with enough velocity to acquire thousands of points each second. To cope with most of dams, a wide range Lidar is used. It is able to scan structure, up to 1000 meters onto surfaces, with less than 20% reflectivity.

The result of a Lidar survey, called “point cloud” (Fig. 5.), is usually composed of tens million points known in XYZ. The average density ranges from 1 point each 5 to 20 mm.

4 PHOTOGRAMMETRIC OVERVIEW

In this case, the photogrammetric coverage aims to deliver exhaustive and high definition pictures of the structure. The goal is to be able to produce a visual inspection, using 3D referenced pictures. The camera and lenses used can give a pixel equivalent to few millimeters onto the structure, which is enabling to detect the main defects. As photos' orientation is known, each photo can be projected on 3D mesh to texture it (Fig. 6). Next step is to project the textured 3D mesh on a primitive projection (plane, cone, and cylinder) to obtain a map. This projected image is called orthophotography.



Figure 4. Lidar in operation.

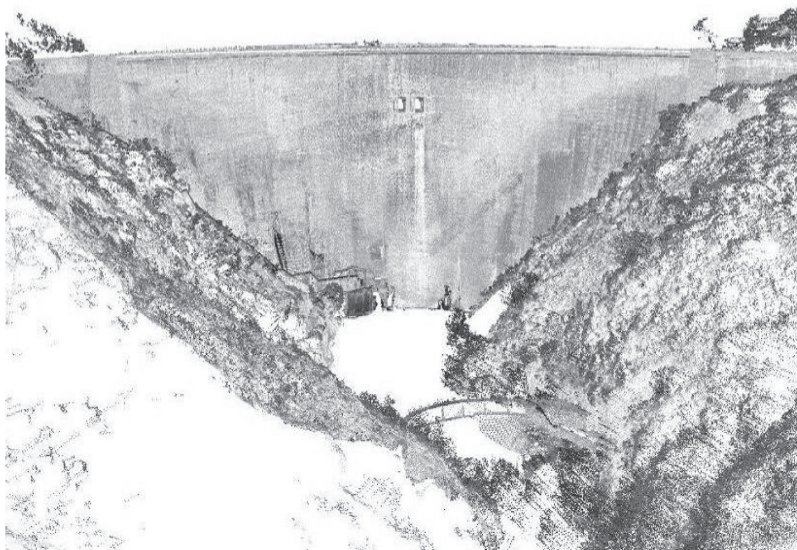


Figure 5. Point cloud of a dam.



Figure 6. High accuracy picture of degradation captured with the camera.

5 OPERATIONS

In this section, we will explain the different steps required to produce a SCANSITES 3D® survey. As said before, all data are known in a 3D referential. For that, the method can use the one established for the traditional survey (targets, pillars). In case where there is no available network, it is necessary to create one, based on singular points on the structure and determined with traditional survey operations.

Concerning the visual inspection, each dam's owner has its own requirements. It deals with defects, which have to be surveyed, and the associated classification. One of the most important parameter is the minimum opening for crack that needs to be surveyed. It mainly impacts the focal length used during the inspection (up to 4 meters!) and widely, the total number of defects stored. All those considerations enable to prepare the mission, mainly the database and the inspection software.

At this step, in-field operation can begin.

SCANSITES® and Lidar are set at different locations in order to cover the structure's surface. The high gain video camera and quality lenses of the SCANSITES® enable it to work with low ambient luminosity. The Lidar, as for it, can work without light.

With the Lidar, a complete scan is realized. Based on this point cloud, a triangular mapping (Fig. 7) is generated and converted in a 3D shape. The first use of this 3D shape is to enable the SCANSITES® to locate the defects in 3D.

With those incoming data, we proceed to the visual inspection. The technician scans the entire wall moving the inspection head with a joystick. When a defect is seen, it is caught. The 3D map is updated in real time with defects and the database is filled in, with its characteristics and coordinates.

In parallel to the scanning operation, a complete high definition photogrammetric coverage is done.

6 TREATMENTS

The treatments aim to produce, on a multilayer file, a map containing all defects caught, the geometric deflections and the photogrammetric coverage.

The first step is to compare the dam's 3D shape to the theoretical shape or to a previous survey. The 3D deflections are extracted, and a map is generated. Two ways of representation are possible. One is a coloured map: each colour depending on deflection value. The other way is to carry out a contour line representation.

The second step is to overlay the defects surveyed with the SCANSITES®, using the referential network.

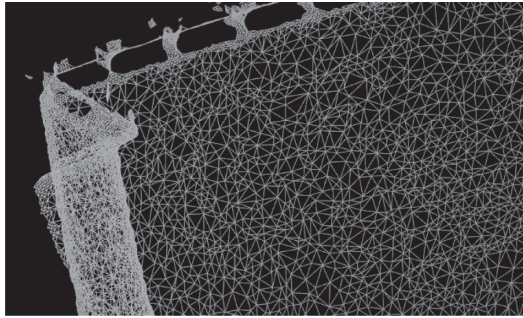


Figure 7. Triangular mapping.

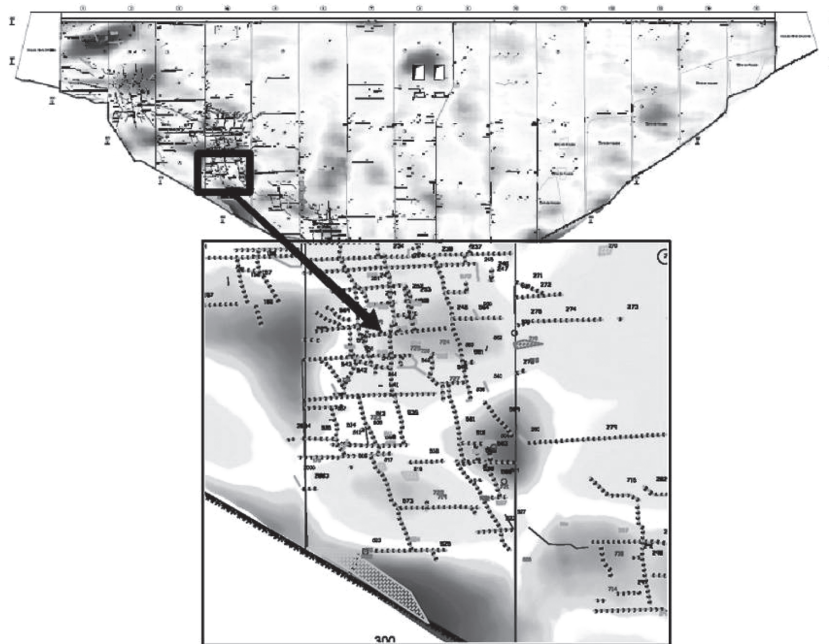


Figure 8. Map overlaying deflection/defects and magnifying.

The last step is to overlay the pictures directly on the structure's 3D shape enabling to produce an orthophotography. With that file, many views can be generated such as composite views: defects/deflections, defects/pictures, or thematic views (based on database queries).

6.1 Case study: dam N°1

The SCANSITES 3D® method was applied on a dam, located inside EU. Its main figures are 87 meters high and 180 meters long along the crest. The aim of this job was to connect the geometric deflections to the defects surveyed. Both upstream and downstream facings were monitored.

The Lidar survey required 12 million points, and the defect total quantity was near to 300.

The map (Fig. 8) shows a colored layer of the downstream facing deflections vs. defects drawing (mainly cracks).

6.2 Case study: dam N°2

The second case study concerns a dam also located in EU but slightly larger: 120 meters high and 250 meters long along the crest. The average distance between SCANSITES 3D® points of view and the downstream facing were about 200 meters (Fig. 9).

On this dam, two parts are distinguished: a sensitive part, located near to the banks and the bottom, and a common part which is the remainder.

The aim of the job is to get dam geometric deflection, a very accurate visual inspection onto the sensitive part, a less detailed inspection onto the common part and a global photogrammetric coverage.

As carried out on the previous case study (Dam n°1), a Lidar point cloud was generated representing tens million points. In parallel, we covered the whole facing with pictures, projected it on 3D shape, and then on projection cylinder, for a total quantity exceeding 3 billion pixels (Fig. 10).

Concerning the visual inspection, the SCANSITES® was used for the sensitive part. For the common part, all defects were caught directly on the 3D textured model.



Figure 9. Lidar and SCANSITES® in operation.

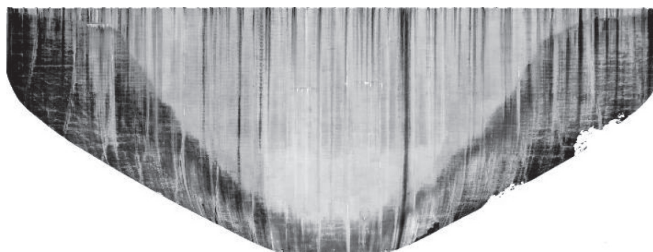


Figure 10. Orthophotography (cylindrical projection).

7 RESULTS

Concerning the visual inspection, the main difficulty for traditional methods, such as rope access or binocular inspection, is to produce a map enabling a good location of defects and their evolutions. SCANSITES 3D® provides some numerical results: a scaled defect map and defects database. The first result is to produce an accurate report emphasizes defects evolution between two inspections, and the number of defects classified by zone (Fig. 11). This is helpful for establishing an accurate bill of quantities for restoration works, like total crack length to be treated, total corroded bar amount for passivation treatment...

The Lidar coverage is a guideline for defects analysis, for instance to see if cracks are correlated, or not, with geometrical distortions.

Another interesting point is its use on parts covered of vegetal moss. Scanning one way we get structural information whereas visual inspection is inefficient. It is also helpful to know where a structural diagnosis has to focus on (with concrete sample or testing core for example).

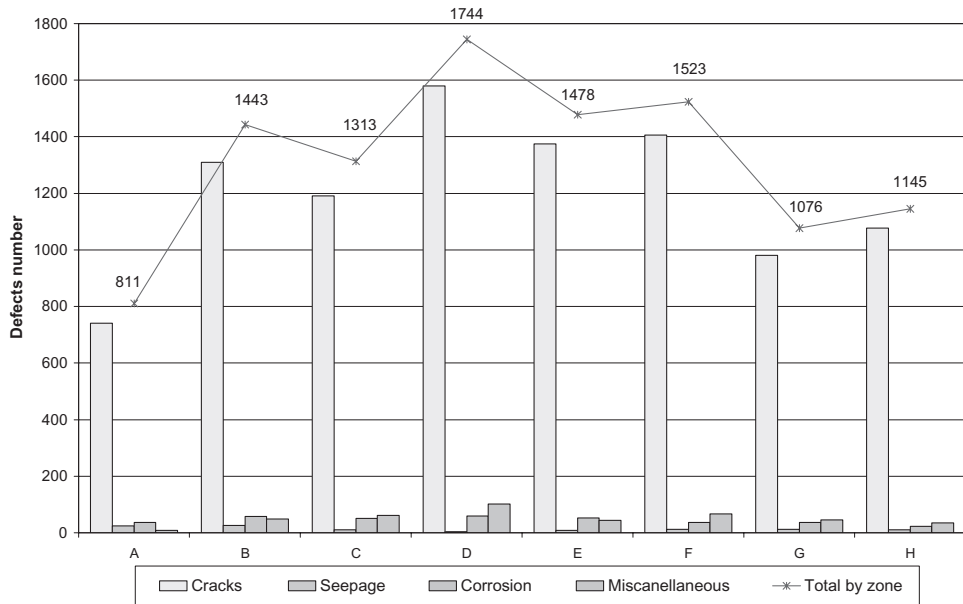


Figure 11. Number of defects by family and zone.

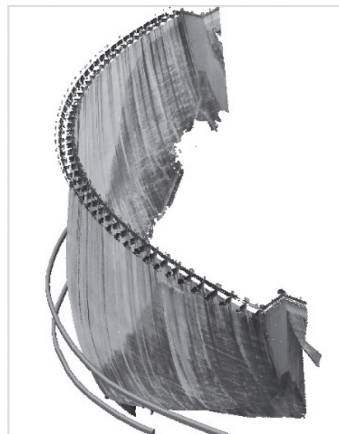


Figure 12. 3D textured shape of a downstream with a surveying of galleries.

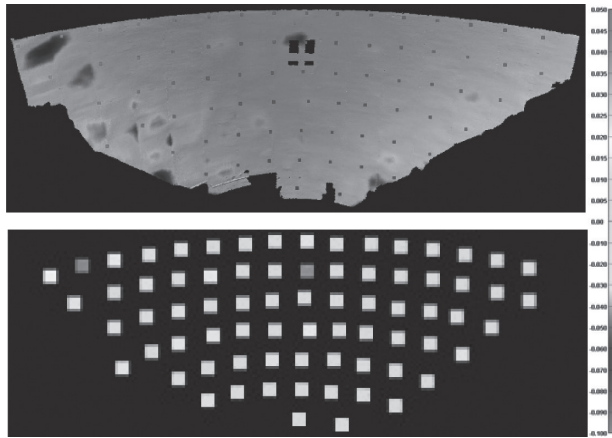


Figure 13. Scanner distortion map superposed to classical surveying targets, and classical surveying targets distortions.

As the accurate 3D shape of the dam is known, data for planning sensor installation or wells location can be easily computed (Fig. 12).

Traditional geometric survey uses theodolites and well-known microtriangulation methods. It presents the advantage to provide some results close to the best possible accuracy (near to 1 mm). However, the drawback is to be a “discrete” method, because it focuses on limited number of points, usually few tens (target, reflectors), not necessary placed on critical parts.

Even if SCANSITES 3D® is less accurate, the high density scan produces some surface definitions near to 3–4 mm uncertainty. Usually working with few millions points, it provides a global information. It widely improves the sensitivity of the geometric diagnosis, showing all details (Fig. 13).

The last advantage is these methods work on every structure, even if there is no surveying equipment such as targets.

All data (photo, geometric survey, defects maps, evolutions) are overlaid on a same file. The engineer gets a faster way to make his diagnosis compared to the fastidious data fusion imposed by separated reports.

The last result is to store all collected data in a database, offering efficient tools to measure the structure ageing and widely a “fleet” of structures.

All these jobs are performed without rope access, increasing dramatically the safety conditions.

8 CONCLUSION

We’ve presented a new and modern approach for visual inspection and geometric survey, here focused on dams, with the SCANSITES 3D®. This method is particularly adapted to every structure which needs the resuming of its monitoring program, because it provides an exhaustive inventory. It also permits to readjust an existing monitoring program by completing the lacks forgot by classical approach. Not only is this method adapted to concrete structures, but it can also be used on old constructed works, masonry-work, clay works. The correlations between the defects and deflections are finally some precious information to locate the areas where geodic surveying and sensors have to focus on. Moreover, besides useful results for the monitoring, the SCANSITES 3D® provides as-existing mappings which are often lacking on old structures. This method is widely applicable on large structures such as cooling towers but also skyscrapers, chimneys. The next step (in progress) is to overlay a high accuracy thermographic imagery survey. The aim is to study the possible gain in diagnosis, mainly on cracks.

Maintenance and operation of aged dams

Y. Kita, S. Ariga & M. Katayama

Electric Power Development Co., Ltd, Tokyo, Japan

ABSTRACT: In this paper, our approach for extending the lifetime of the aged dams is described. The main problems of the aged dams are structural deterioration and disappearance of records. The extraction work of the problem was conducted based on the failure mode analysis of the dam for structural deterioration. Consequently, there was no urgent problem connecting with the dam failure. But, it turned out that information such as monitoring records had not been used effectively enough for maintenance of dams. It was reconfirmed that the periodical check and the measurement were the most important for the operation and maintenance of the dam, and various approaches for the improvement of the dam safety have commenced.

1 DAMS OF EPDC

1.1 *History of EPDC*

EPDC (Electric Power Development Co.,Ltd.) was established in 1952 to accomplish the large-scale power generation projects suitable for a rapid increase in the power demand of Japan after World War II. The first large-scale electric power development that EPDC had handled was the Sakuma Dam of the concrete gravity type of 155.5 m in height in 1956. Then the domestic construction standard of a large-scale dam in Japan was not provided. So it was designed by adopting an overseas technology and the standard, and constructed by using imported construction equipments. Afterwards, the Okutadami Dam (concrete gravity type, 157.0 m, 1960) and the Miboro Dam (rock-fill with inclined impervious core, 131.0 m, 1961) which was called "Pyramid in the Orient" at that time were developed. The large-scale hydro power projects have been accomplished in a short term, and now EPDC subsequently owns and operates 48 Dams in Japan. The major EPDC dams show in Table 1, and those locations in Figure 1.

1.2 *Current situations and issues of hydro power plant*

Recently, Japan's economic growth is at low level after the high-growth period had been maintained after World War II, and also the expansion of the power demand has stagnated. The number of domestic new hydro power projects has decreased, and the scale is also smaller than before. However, the hydro power as renewable energy performs the key role in accordance with highlighting the value of global environment. Moreover, Japan's self-sufficiency ratio of the energy resources is the lowest in the advanced countries, and importance of the hydro power that is a pure domestic energy is quite high. Effective use of the existing hydro power is the national proposition in term of energy security.

The history of the hydro power development in Japan is so old that the half number of existing hydro power stations passed 60 years or more after construction, and various repair works, big and small, of the old hydro power plants are increasing in recent years. It is big problem for the electrical power companies in Japan how aged hydro power plants will be operated efficiently for a long time. The 73% of EPDC dams also passes 40 years or more (Fig. 2). The mission of EPDC is changing from the large-scale hydro power development into adequate maintenance to extend its dams' lifetime.

Table 1. Major EPDC dams.

Name	Type	Hight (m)	Crest Length (m)	Storage Capacity (m ³)	Since
Nukabira	Concrete-gravity	76.0	293.00	193,900,000	Jan-1956
Sakuma	Concrete-gravity	155.5	293.50	326,848,000	Apr-1956
Akiha	Concrete-gravity	89.0	273.40	34,703,000	Jan-1958
Kuromatagawa I	Concrete-gravity	91.0	276.00	42,845,220	Feb-1958
Tagokura	Concrete-gravity	145.0	462.00	494,000,000	May-1959
Kazaya	Concrete-gravity	101.0	329.50	130,000,000	Oct-1960
Okutadami	Concrete-gravity	157.0	480.00	601,000,000	Dec-1960
Miboro	Rock-fill	131.0	405.00	370,000,000	Jan-1961
Sakamoto	Arch	103.0	256.30	87,000,000	Apr-1962
Ooshirakawa	Rock-fill	95.0	390.00	14,200,000	Dec-1963
Kuromatagawa II	Arch	82.5	235.21	60,000,000	Jan-1964
Ikehara	Arch	111.0	459.96	338,000,000	Sep-1964
Yanase	Rock-fill	115.0	202.00	104,625,000	Jun-1965
Misakubo	Rock-fill	105.0	258.00	30,000,000	May-1969
Kassa	Rock-fill	90.0	487.00	13,500,000	Jul-1978
Futai	Rock-fill	87.0	280.00	18,300,000	Jul-1978

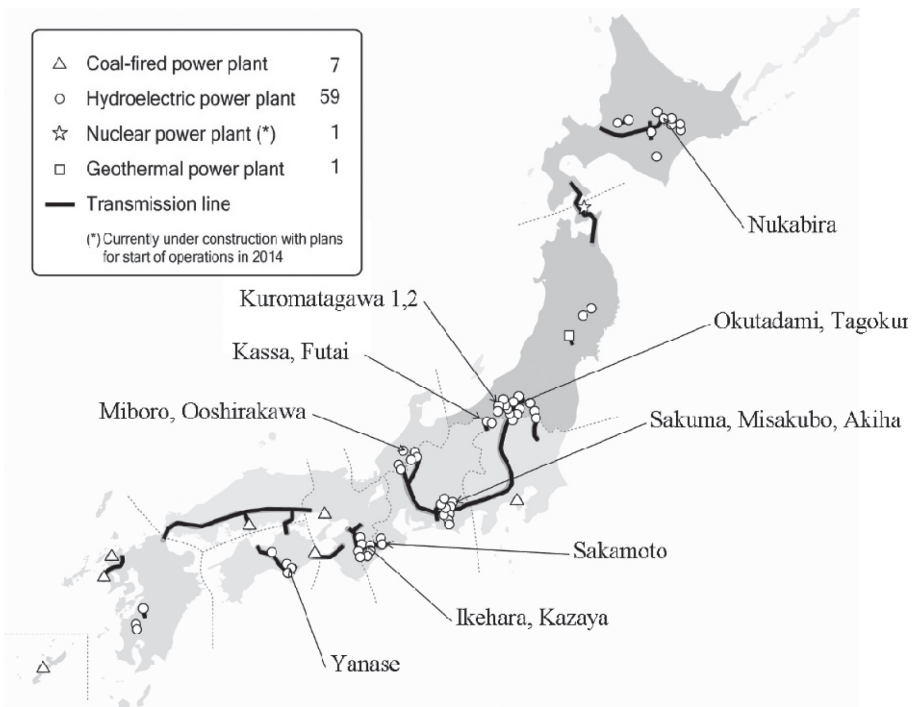


Figure 1. Locations of EPDC dams.

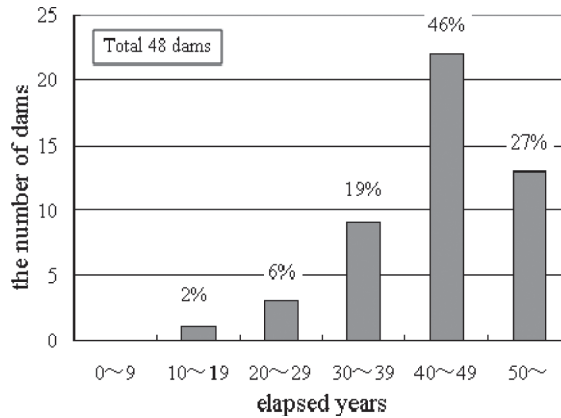


Figure 2. Elapsed years distribution of EPDC dams.

2 THE APPROACH FOR SAFETY MANAGEMENT OF DAM

2.1 Problems in safety management of dam

Although structural remarkable damage is not observed, partial deterioration of dams that EPDC manages begins to appear. For example, the water stop in construction joint deteriorated, and the surface materials of rock-fill dam weathered although those phenomena cause neither critical nor dysfunctional damage immediately. The dam has a complicated and organic function to store the river water, to generate the power utilizing the storage water, to supply the water to the industry, the public and for irrigation, and to control the flood. The steel structure such as the gates and the mechanical devices are maintained preventively based on the elapsed time. However, the fixed quantitative evaluation of the degradation phenomenon is difficult, because the dam is composed of various structures. It is necessary to understand that deterioration mechanism is different among each dam and it is important to make an appropriate diagnosis to an individual dam and to maintain it in the most effective way.

Moreover, when dealing with the aged deterioration, the problem is not only structural deterioration but also disappearance of information. The important information such as geological features and technological methods during construction was rarely recorded systematically at that time, and only a part of it was described explicitly in the construction records. A lot of information necessary for dam maintenance is disappearing as time goes by. That is the cause to make the dam safety management difficult.

2.2 The systematic approach for dam safety evaluation

The monitoring and the measurement are the most important work for managing the dam safety. The maintenance team at the site office has executed a repair work in a small-scale based on the daily monitoring and the measurement. On the other hand, a large-scale refurbishment has been conducted by the head office. Recently, as the deterioration of the most of dams is proceeding, it becomes more difficult for site office to evaluate the degree of deterioration and the most effective investment cost, which requires a high-level engineering judgment. Considering that situation, we are trying to create the system (Fig. 3) to manage the dam efficiently.

2.2.1 The risk analysis for dams

First of all, we tried to understand the current state of the dam, and to extract the risk connecting with the dam failure, then we referred the technique of the dam failure mode analysis used by Federal Energy Regulatory Commission (FERC)¹⁾, after comparing domestic and foreign standards. Secondly, we made the risk scenario (Fig. 4) taking into account the dam

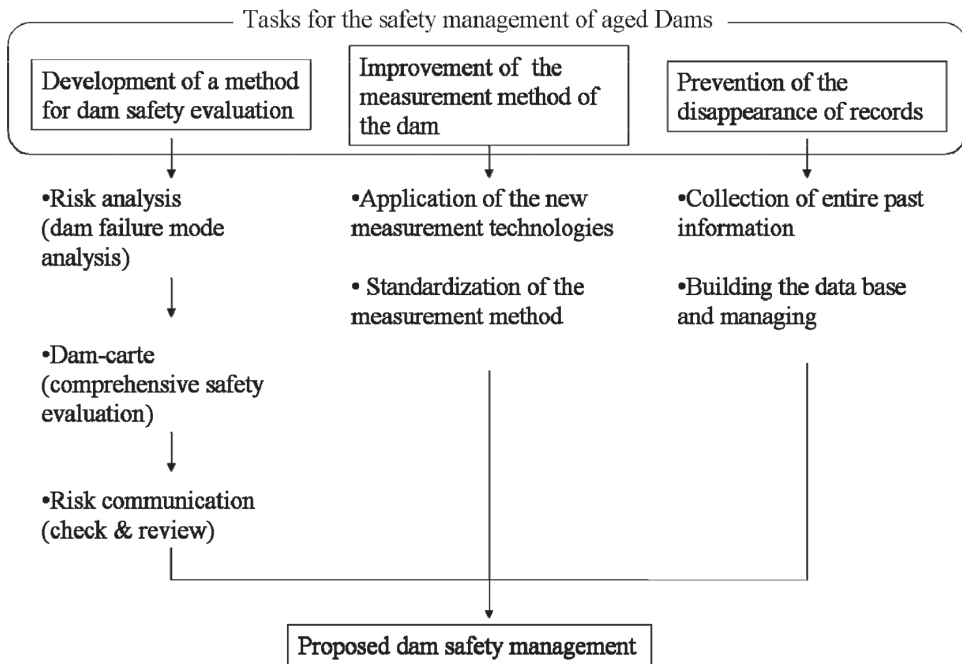


Figure 3. Approach for the safety management of dams.

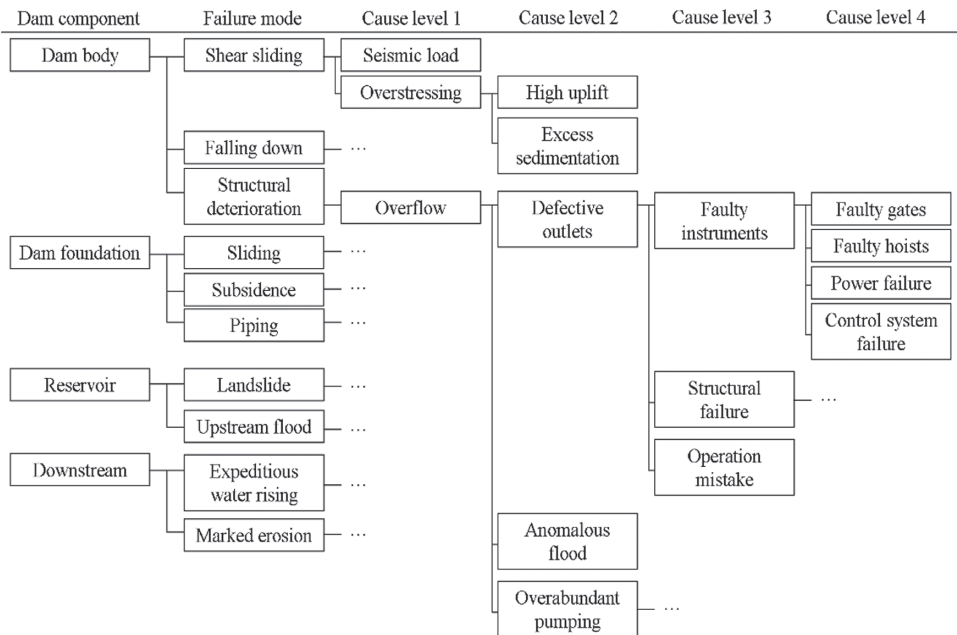


Figure 4. Tree diagram of dam failure mode and cause level.

failure modes and causes by each types of dam. According to the risk scenario, the chief engineer for each dam checks whether there is an event to meet the scenario or not. If there are any items to meet the scenario, they will collect and arrange the evidences, such as the pictures and the monitoring data. They can relate the events occurring in the dam to the dam failure mode, and can improve the knowledge of risk management by doing this analysis.

2.2.2 The dam-carte (comprehensive safety evaluation)

The dam-carte is the record of a series of information including the extracted problems by the risk analysis, the countermeasures, the progress, and the verification of the result. In the dam-carte, the extracted problems are prioritized according to the degree of influence and its emergency. And those problems are classified into two categories. One is the small-scale and a short term problem and the other is the large-scale and a mid/long term one. All of the related parties from the chief engineers for each dam to the engineers belonging to the head office have a common view through the dam-carte, and use it as the judging source for the capital investment.

2.2.3 The risk communication (check & review)

The risk communication is held to check the propriety of the dam-carte in order to make procedure, and to plan the countermeasures and those priorities. It is organized by the local managers, engineers in the regional offices, and the engineers at the head quarter including the external experts (Fig. 5).

2.3 Problems and countermeasures led from the result of risk analysis

2.3.1 Outline of the risk analysis result

As a result of the risk analysis done for 48 all dams that EPDC had, there was no critical problem connecting with the dam failure at the moment. However, it turned out that the dam measurement data that was the important information to evaluate the dam condition has not been verified enough so far. For instance, there was the volatility of the data seemed to be the movement of the reference point for the dam measurement, and the loss of the data caused by the plugging of the uplift measurement hole. Thus, there were some cases that the data was not verified regarding the reliability and the measurement method.

On the other hand, the steel structures such as the gate and the electrical control devices etc. were maintained periodically, so there was no problem to keep its quality.

2.3.2 The problems of the dam measurement

2.3.2.1 Seepage from the concrete dam

The total volume of the seepage from the concrete dam is measured together with the seepage from the joints and from the drain holes. The total amount of the seepage from some old dams over 50 years tended to increase gradually. It was too difficult to point out the reason of the increase when the measurement of the seepage from the joint and the drain holes was not separated. If it was separated as shown in Figure 6, it shows clearly that the seepage from the

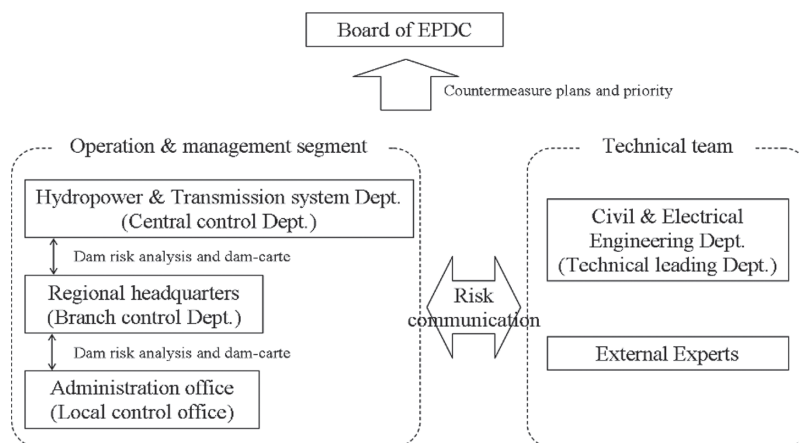


Figure 5. Risk communication in EPDC.

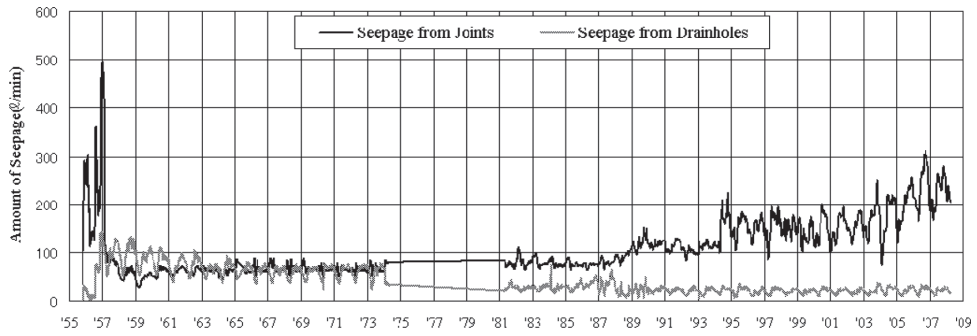


Figure 6. Seepage chart in a concrete-gravity dam.

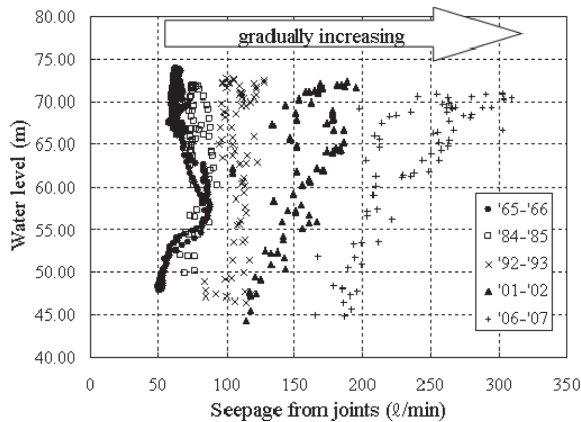


Figure 7. Correlation between seepage from joints and water level.

joints is gradually increasing, and one from the drain holes is decreasing. Figure 8 also shows the linear relation between the seepage from drain holes and the water level recently, so the hydraulic characteristic of the foundation of the dam is thought to be stable.

2.3.2.2 Uplift measurement

There were some cases where the uplift of a concrete-gravity dam showed “0”. In this case, it is necessary to check the reason why the instrument doesn’t react, for example, the breakdown of the meter, or the plugging of the drain holes. After the soundness of the devices is confirmed, it will be able to judge whether the uplift shows “0”, or the uplift water level doesn’t reach the top of the hole. An appropriate uplift measurement can be done only after those confirmation works are done.

2.4 Improvement of dam measurement

In case of the measurement of the dam displacement, it is necessary to treat the reference point as fixed point to survey a relative position and the movement of the dam. Several decades have passed since the dam construction, and there are some possibilities that the immobility of the reference point is doubted. Since the reference point is believed to be stable, the main reason of the dam displacement is thought to depend on the measurement error. However, the GPS technology is developed and prevailing, and an absolute position can be specified now. We are attempting to confirm the immobility of the reference point by using the GPS technology.

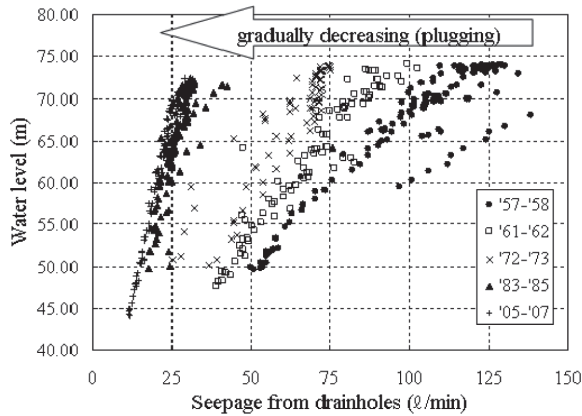


Figure 8. Correlation between seepage from drain holes and water level.



Figure 9. GPS installed on a rock-fill dam of EPDC.

Moreover, an industrial fiberscope can be applied to check the internal condition of the drain holes of the concrete dams, now. When it is plugged by the efflorescence and the function of the drain holes is damaged, measures to recover its function such as cleaning and the re-boring, etc. should be examined.

It is recognized again that it is important to understand that the original purpose of the measurement work is to confirm the stability of the dam, to detect the fault, and to maintain the appropriate environment for the measurement to reflect the dam's condition. And, we are trying to make an in-house standard of the dam measurement that shows the purpose of the dam measurement, the method, and the application of the new technologies.

2.5 Prevention of the disappearance of records

The development of the electronic information technology, information processing technology, and the telecommunication technology are improving the handling of the measuring data and the recorded information. Records of the past are uniformly managed and all information is shared among related parties through the data base system. This data base has a probability to make it more convenient to explore the similar events when some troubles are observed at any dams.

3 CONCLUSION

In Japan, after the age of large-scale infrastructure construction, it entered into the age of maintenance, when existing facilities should be maintained adequately for a long time. The dam is the compound and organic structure composed of the foundation, the dam body, and the associated equipment structure, and maintenance methods of dams are different from those of the mechanical and the steel structure. The improvement of the measurement technique makes it possible to specify the dam condition quantitatively and visibly which has not been observed so far. However, the monitoring is one of the most important works for the safety management for the dam. We have to change the consideration about the existing measurement methods, and to examine the new method in order to keep the dam safety. At the same time, we have to prevent the experiences accumulated so far from weathering, and aim to improve the maintenance technology as well as the construction technology.

REFERENCES

- Federal Energy Regulatory Commission: *Engineering Guidelines for the Evaluation of Hydropower Projects, Chapter 14, Dam Safety Performance Monitoring Program*, July 1, 2005.
U.S. Dept. of the Interior Bureau of Reclamation: *Safety Evaluation of Existing Dams*, 1983.

Estimation of rockfill dam behavior during impounding by elasto-plastic model

N. Tomida, N. Sato, H. Soda & S. Jikan

Japan Water Agency, Saitama, Japan

K. Ohmori

Ridge Research Institute of Digital Geo-Environment, Kanazawa, Ishikawa, Japan

H. Ohta

Research and Development Initiative, Chuo University, Tokyo, Japan

ABSTRACT: Tokuyama dam is one of the largest rockfill dams in Japan, which JWA constructed across the Kiso River. Since width of the central core of Tokuyama dam was re-designed to be thinner than the original design. Therefore, evaluation of the safety of the core zone during the impounding period was carried out by both numerical analysis and observed data. In this report, following the actual construction process of embankment and impounding, an elasto-plastic soil/water coupled consolidation analysis is carried out to find the rise of pore water pressure and change of effective stress in the core zone. The safety level of the core zone during the impounding period was evaluated by Seed standard.

As a result, numerical analysis and observed data matched closely, which confirmed the validity of the analysis. The safety of the core zone during the impounding period was confirmed by both observed data and numerical analysis.

1 INTRODUCTION

Tokuyama dam is a multi-purpose dam constructed by JWA. It is one of the largest rockfill dams in Japan with the dam height of 161 m, the dam volume of 13,700,000 m³ and the gross storage capacity of 660,000,000 m³.

Figure 1 shows the location of Tokuyama dam. The construction work started in March, 2000, and completed in the end of November, 2005. The first impounding commenced on September 25, 2006. The water level in the reservoir reached surcharge water level on April 21, 2008, followed by the completion of the first impounding on May 5, 2008.

In Japan, the bottom width of the core zone of rockfill dams is normally around 40–50% (Ministry of Construction River division, 1987) of the dam height. The final design of Tokuyama dam applied thinner shape, and its bottom width of the core zone is 36% of the dam height. Due to adopting the thinner core zone than normal design, the stress reduction was concerned. So the appropriate estimation on safety against failure during the impounding period was necessary.

In this report, an elasto-plastic soil/water coupled consolidation analysis was carried out to simulate the physical behaviors within the dam body based on the actual construction process of embankment and impounding in Tokuyama dam. A comparison of the numerical analysis and observed data shows similarity, which proved the validity of elasto-plastic soil/water coupled consolidation analysis. The safety of the core zone during the impounding period was also estimated by using the results of this analysis.



Figure 1. Location of Tokuyama dam.

2 OUTLINE OF THE ANALYSIS

The analysis predicts the pore water pressure and minor principal stress of the core zone as the following procedures, in order to evaluate the safety level for hydraulic fracturing during the first impounding. Firstly, the rise and dissipation of pore water pressure of the core zone during the embankment is predicted. After that, the dam body behavior during impounding is analyzed in the initial conditions of the first impounding decided by the first prediction. During the impounding period, the elasto-plastic soil/water coupled consolidation analysis is carried out to estimate the rise of pore water pressure, the rise of osmotic pressure at the upper part of the dam body, the change of the effective stress and the dam body behavior. In the above analysis, the elasto-plastic soil/water coupled consolidation model is adapted as the model of the embankment material of dam.

The elasto-plastic soil/water coupled consolidation model employed a stress-distortion relationship (constitutive law) of Sekiguchi-Ohta model (Sekiguchi and Ohta, 1977) which can cover embankment material with anisotropy and predict the volume change of soil induced by compression stress and shear accurately. Figure 2 shows the conceptual diagram of elasto-plastic model. Table-1 shows main parameters used for analysis.

The analysis parameters of filter material and core material are set based on material test whereas that of rock material is based on both material test and observed data at site. The earth pressure coefficients at rest K_0 of each material is 0.7.

Figure 3 shows the relation between coefficient of permeability and void ratio of core material in Tokuyama dam. The coefficient of permeability of saturated soil obtained from consolidation test is 10 times larger than that of unsaturated soil obtained by consolidation test. The coefficient of permeability obtained from permeability test on embankment surface at site matches closely with that of saturated soil obtained by consolidation test. The coefficient of permeability used for the analysis is set based on the result of consolidation test of unsaturated soil, since the core material is unsaturated during embankment. The initial coefficient of permeability is obtained by consolidation test in which void ratio of the material was adjusted to the average void ratio in embankment area at site. Because the material of core with small void ratio tends to have lower permeability, coefficient of permeability is changed according to the change of void ratio obtained from the analysis, using the relationship between the coefficient of permeability and void ratio obtained from the consolidation test shown in dotted line in Figure 3. In the analysis, the coefficient of permeability is changed in every embankment stage.

Figure 4 shows the cross section of Tokuyama dam used for the analysis. Tokuyama Dam has the height of 161 m, upstream slope gradient of 1:3.0, downstream slope gradient of

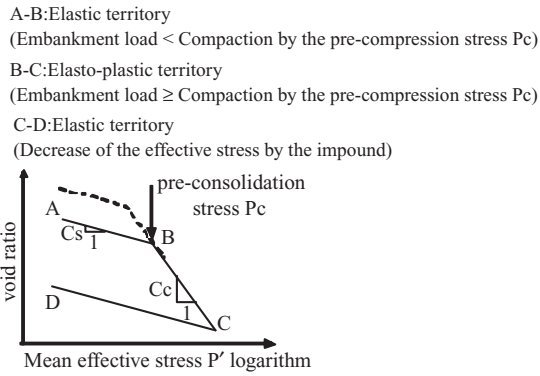


Figure 2. Conceptual diagram for elasto-plastic model.

Table 1. Material parameter for the analysis.

Category	Unit	Rock material	Filter material	Core material
Swell index (C_s)		0.0375	0.0033	0.0045
Compression index (C_c)		0.0860	0.0140	0.0215
Pre-consolidation stress (P_c)	(kPa)	820	920	132
Friction angle (ϕ')	(degree)	43.3	39.4	37.8
Coefficient of permeability	cm/sec	3.05×10^{-1}	8.0×10^{-4}	1.93×10^{-7}
Critical state parameter (M)		1.78	1.61	1.54
Irreversibility ratio (λ)		0.564	0.764	0.791
Coefficient of dilatancy (D)		0.00317	0.00234	0.00928
Effective poisson ratio (ν')		0.412	0.412	0.412

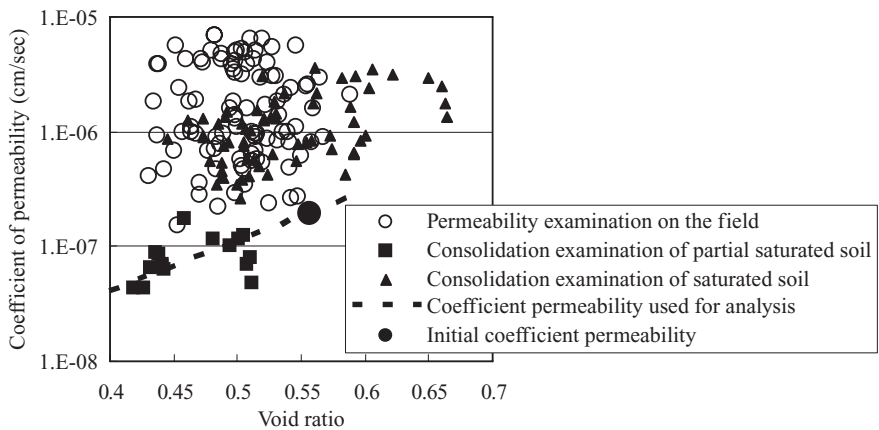


Figure 3. Relation between core material's coefficient permeability and void ratio.

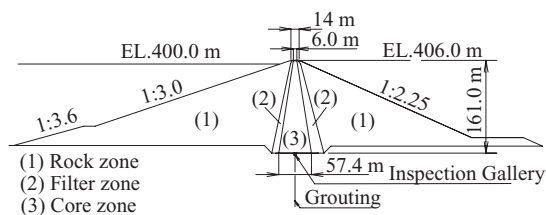


Figure 4. Cross-section.

1:2.25, and its symmetric core slope has a gradient of 1:0.16. The analysis is implemented for the dam body and the foundation. The analysis horizontal range is about the double of the base width and the vertical range is about the double of the dam height. The number of elements is 5524 in the finite elements method. As the boundary conditions, the horizontal displacement at the side of the foundation is 0 and that at the underside is fixed. As the hydraulic boundary conditions, the distribution load and hydrostatic pressure based on the reservoir level is set on the upper face of the dam. Also the vertical load based on the difference between the wet density and saturated density is set at the dam body under water. The pore water pressure at the lower rock zone is set as 0 during the embankment and impounding period. As the boundary conditions, the water pressure based on the reservoir level at the upper side of the foundation, the hydrostatic pressure at the lower side of the foundation and the undrained condition at the underside are set respectively.

In the embankment analysis, in order to represent the actual embankment process, the elements of dam body are accumulated successively based on the embankment process as shown in Figure 5.

In the impounding analysis, the effective stress is numerically predicted by an unsteady-state seepage analysis in saturated soils with a time dependent boundary condition of escalating water level in reservoir.

The fracturing pressure of the core zone is evaluated by “(Seed and Duncan, 1981)”. Seed suggests a quantitative evaluation method of hydraulic fracturing which defines the condition of soil destruction with crack by the following formula.

$$u_f = \sigma_3 + \sigma_t \quad (1)$$

where u_f = hydraulic fracturing pressure; σ_3 = minor principal stress in total stress; σ_t = tensile strength of soil.

In this report, the generation of hydraulic fracturing of core material is based on the Seed standard. Local safety factor against hydraulic fracturing (Fsh), is obtained by formula (2), neglecting tensile strength of soil to evaluate in a severer condition.

$$Fsh = (\sigma_3 + \sigma_t) / \Delta u \quad (2)$$

where Δu = pore water pressure.

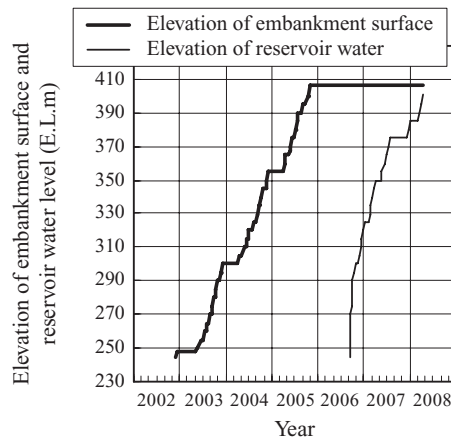


Figure 5. The process of embankment and impounding turned into a model by FEM analysis.

3 INVESTIGATION AND CONSIDERATION ON RESULT OF DAM BODY BEHAVIOR ANALYSIS COMPARED WITH ACTUAL VALUE

Figure 6 shows the comparison of settlement value at the same location between numerical result and data measured by settlement gauge A-2. The comparison shows close similarity when the water level reaches the maximum water level.

Figure 7 and Figure 8 show another comparison at the same location between numerical results and data measured by vertical earth pressure gauge, E-14 set up in the upper side of middle elevation of core zone and E-15 set up in the center part. The comparison of the value at E-14 between numerical results and data measured at site shows a close similarity, whereas that of E-15 does not. At E-15, earth pressure is numerically predicted larger by 30% than observed data.

Figure 9 and Figure 10 show a comparison of pore water pressure between numerical results and measured data at the time of maximum water level during the first impounding.

Residual pore water pressure exists after the completion of embankment, but the osmotic pressure in the core rises due to the impounding. Both observed data and numerical prediction show the dissipation of pore water pressure when the water level reaches the maximum water level, leaving the profile of pore water pressure high at the upper stream and low at the downstream.

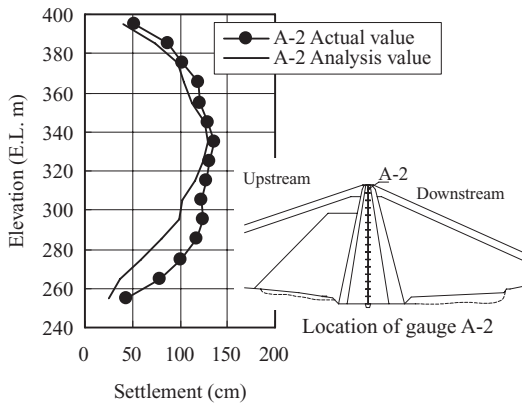


Figure 6. Actual value and analysis value by differential settlement gauge (Maximum water level).

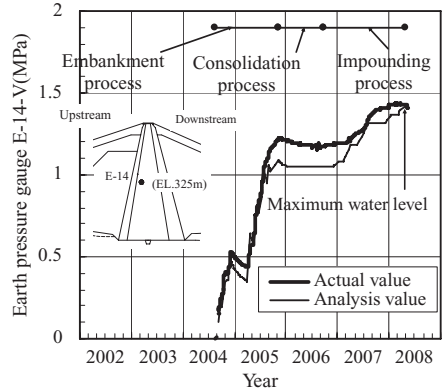


Figure 7. Chronological change of Vertical Earth Pressure.

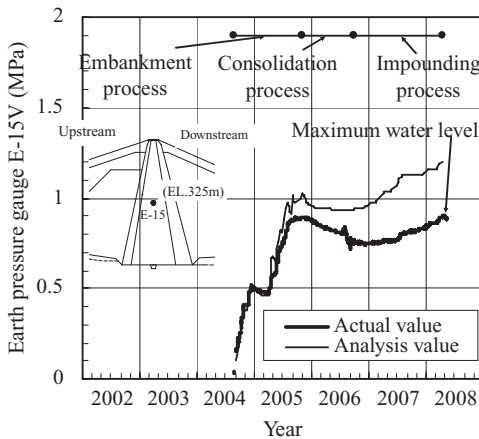


Figure 8. Chronological change of Vertical Earth Pressure.

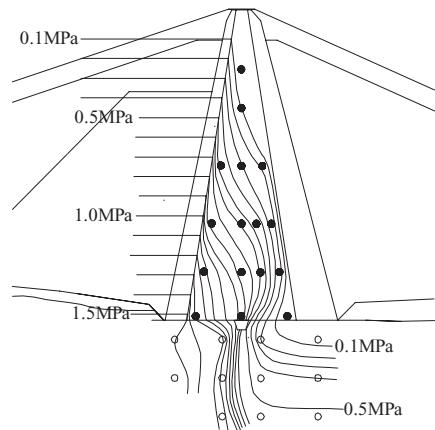


Figure 9. Distribution map of Pore water pressure on highest high-water level (actual value).

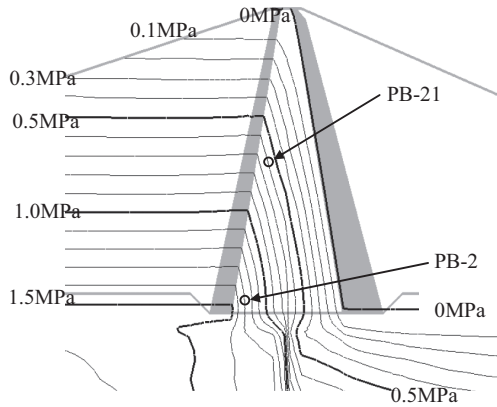


Figure 10. Distribution map of Pore water pressure on highest high-water level (analysis value).

Figure 11 and Figure 12 show a comparison of pore pressure at the same location between numerical prediction and observed data measured by pore pressure gauge at PB-21 set up in the upper side of middle elevation of core zone and PB-2 set up in the lower elevation. It shows similarity between numerical result and observed data of pore water pressure during the process of embankment and at the time of the maximum water level. Differences between numerical prediction and observed data are seen from November, 2005 to March, 2007. During this term, observed data tends to be larger than numerical prediction. The dissipation of water pressure is calculated by seepage analysis, on the assumption that the core is saturation. On the other hand, the core is unsaturated during this term, so the coefficient of permeability is small, seemingly resulted in the delay of dissipation of pore water pressure.

Figure 13 shows distribution contour of major effective principal stress at the end of embankment obtained by the embankment analysis. The generation of arching phenomena due to the difference of rigidity between core zone and filter zone leads the stress reduction in the core zone.

Figure 14 shows a comparison of the major principal stress σ_1 , minor principal stress σ_3 and pore water pressure at the same location between numerical prediction and data measured at E-14. Observed major principal stress σ_1 and minor principal stress σ_3 are calculated based on the data from trihedral earth pressure gauge. The numerical prediction is successful to simulate the qualitative trend of pore water pressure inside of the core, major principal stress in total stress σ_1 and the minor principal stress in total stress σ_3 , to increase parallel with the water level in the reservoir. Observed data and numerical prediction of minor principal stress σ_3 shows a close similarity. In addition to that, major principal stress in total stress σ_1 and minor principal stress in total stress σ_3 surpass pore water pressure in every point.

4 CONSIDERATION ON THE SAFETY AGAINST THE HYDRAULIC FRACTURING

Figure 15 shows the distribution contour of safety factor against hydraulic fracturing at the core zone obtained by the analysis at the time of the maximum water level. The safety factor against hydraulic fracturing becomes the smallest at the border of the core zone and the filter zone at the height of 1/3–2/3 of the dam height. The smallest safety factor is approximately 1.3.

On the other hand, Figure 16 shows both the safety factor against hydraulic fracturing in the core zone obtained from the observed data and that from the analysis. The smallest safety factor obtained by the observed data is 1.56, and that of numerical prediction is 1.42. Although observed data is a little larger than numerical prediction, safety factors in the core zone are nearly equal.

From these points, smallest safety factor against hydraulic fracturing at the core zone in Tokuyama dam is 1.56 based on observed value and 1.4 from numerical prediction, which confirms “safety factor ≥ 1.0 ” in every point.

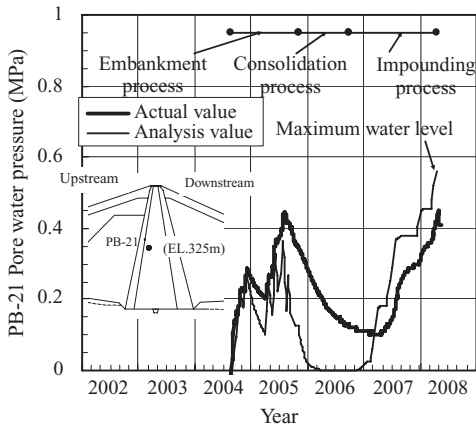


Figure 11. Chronological change of pore water pressure.

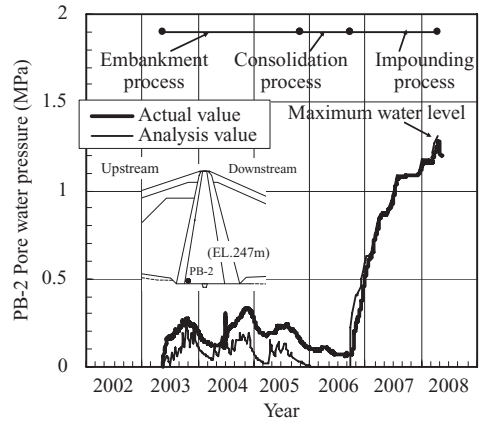


Figure 12. Chronological change of pore water pressure.

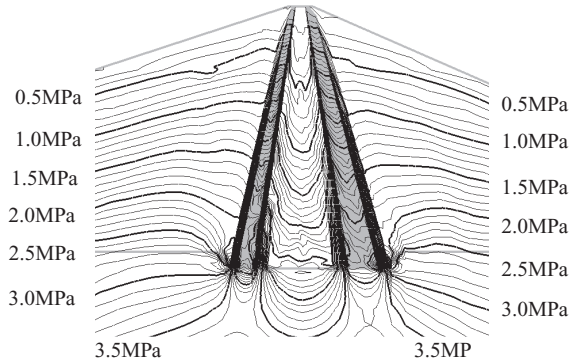


Figure 13. Distribution map of major effective principal stress when the embankment was completed (analysis value).

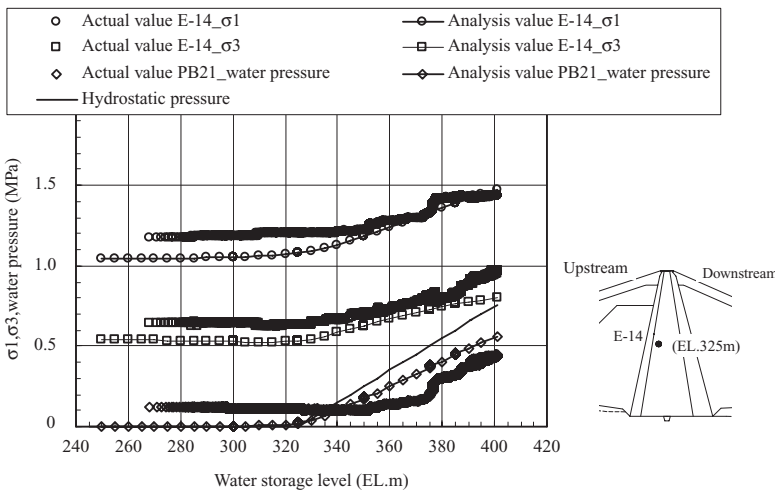


Figure 14. Chronological change of major, minor principal stress and Pore water pressure on E-14.

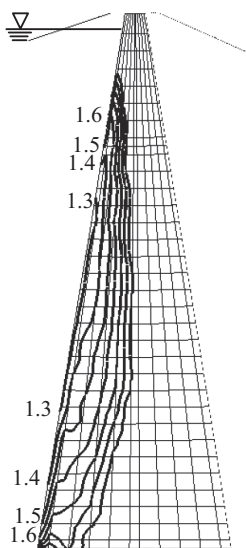


Figure 15. Distribution contour of safety factor against hydraulic fracturing in the core when the water level reached maximum water level (analysis value).

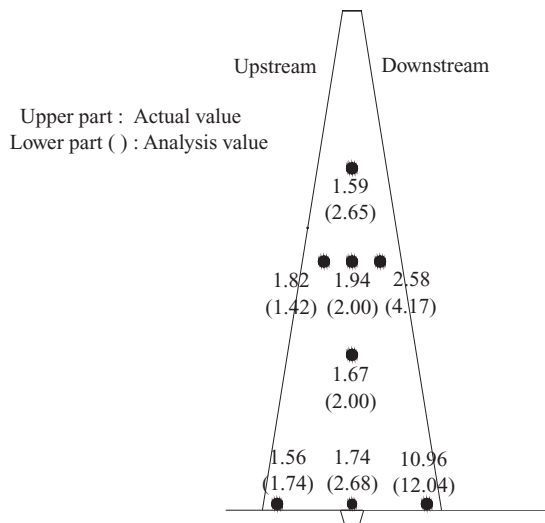


Figure 16. Safety rate against hydraulic fracturing of central core.

5 CONCLUSION

In this report, the numerical prediction of dam body behavior based on actual construction process of embankment and impounding in Tokuyama Dam is implemented by using elasto-plastic soil/water coupled consolidation analysis which can cover the rise and dissipation of pore water pressure and rise of osmotic pressure. As a result, the numerical prediction of settlement and vertical earth pressure from embankment to impounding are similar to that of observed data. The numerical prediction of pore water pressure is similar to that of observed data during the process of embankment and when impounding is completed. The numerical prediction is successful to simulate the qualitative trend of pore water pressure, major principal stress and minor principal stress in the core zone to increase parallel with the water level in the reservoir.

From these points, numerical prediction of dam body behavior in Tokuyama Dam is successful to prove the validity of elasto-plastic soil/water coupled consolidation analysis. The smallest safety factors against hydraulic fracturing at core zone in Tokuyama Dam are approximately 1.56 based on observed data and 1.4 based on numerical prediction. Safety against hydraulic fracturing is also confirmed since the smallest safety factors surpass 1.0 in both values.

Observed data during the first impounding did not show any abnormal phenomena in permeability and deformation of dam. The results of the numerical prediction matched with those observed data.

REFERENCES

- Ministry of Construction River division (Supervisor), 1987, Constructions of multi-purpose dam, 4th volume: 84. Tokyo: Dam Engineering Center foundation (in Japanese).
- Seed, B. & Duncan, J.M. 1981. The Teton Dam Failure- A Retrospective Review, Proc. of 10th ICS-MFE: 1-20.
- Sekiguchi, H. & Ohta, H. 1977. Induced anisotropy and time dependency in clays, Proc. of 9th ICS-MFE: 229-239.

The investigation method of hydroelectric facilities by using digital camera

S. Wada & Y. Kono

The KANSAI Electric Power Co., Inc., Osaka, Japan

ABSTRACT: In surface investigation of the concrete structures, an investigator has to often access a high place. In such a case, methods such as temporary scaffold and rope access are adopted. However, these methods are expensive, and dangerous. In recent years, the performances of a digital camera and image processing technology have accomplished remarkable progress. So the authors attempted to apply the photographic image measurement technique both for the surface of a dam and the concrete lining of a tunnel.

1 INTRODUCTION

The KANSAI Electric Power Co. (hereinafter called KEPCO), own 149 hydroelectric power plants in Japan and the total output of hydropower is about 8195 MW. KEPCO has Inspection and Monitoring System divided into three portions, such as patrol, inspection and deterioration diagnosis. The patrol is conducted daily and monthly, and the inspection is conducted annually. The deterioration diagnosis is conducted once in several years and we assess the conditions of facilities in total.

KEPCO conducts deterioration diagnosis at our concrete dams once every 10 years, and we conduct crack monitoring of the concrete structures in the deterioration diagnosis. In conventional investigation methods, investigators have to often access a high place. In such a case, methods such as temporary scaffold and rope access (Figure 1) are adopted. These methods, however, are expensive and time consuming, and danger is accompanied. Therefore, the improvement of the investigation methods is required.

Then, the authors developed a photographic image measurement system to check the surface of concrete, and KEPCO adopts the system in actual investigations since 2009.

This newly developed system is a combination technology of a total station and a digital camera (Tsugio et al. 2008). First, images taken with a digital camera are transformed into the images viewed from the front on the PC, based on three-dimensional coordinate data obtained by a total station. Secondly, the individual front view images are stitched into a total image of the structure. Finally, the crack locations, the crack total lengths and the crack widths are found from the stitched image.

KEPCO has conducted the photographic image measurement at 16 dams and a waterway tunnel in 2009 and 2010. Authors report the investigation results here.

2 PRINCIPLE OF PHOTOGRAPHIC IMAGE MEASUREMENT TECHNIQUE

In the beginning, authors explain the principle of the image measurement technique. This technique provides synthesized front view images of the components of the structure. The technique uses images taken by high resolution digital camera and the coordinates measured by an automatic surveying instrument so called total station (Figure 2), and compensates angle, curvature and scale, then synthesizes images by image processing unit (Figure 3). Then the lengths of the cracks are measured by tracing the recognizable cracks on a synthesized

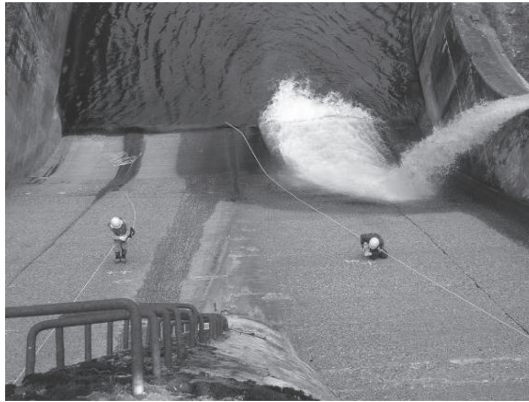
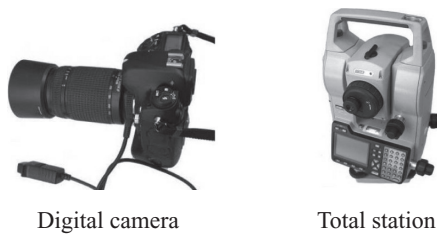


Figure 1. Dam surface inspection by rope access.



Digital camera

Total station



Figure 3. Image processing unit.

Figure 2. Image measurement equipment.

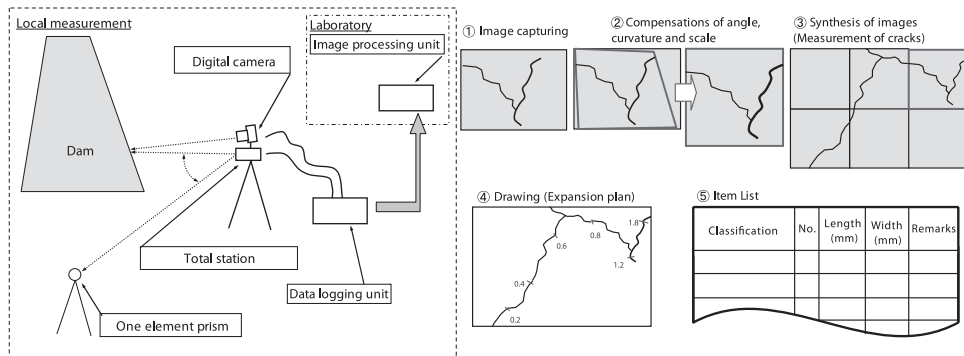


Figure 4. Flow of image measurement technique.

image displayed on a monitor and the widths of the cracks at the position that can be recognized on the cracks with the naked eye are evaluated (Figure 4). Main instruments of the system are a single-lens reflex digital camera, a non-prism total station (instrumental tolerance equals plus or minus 3 mm and plus or minus $[2 \times 10^{-5} \times \text{distance}]$), an image processing unit and a data logging unit (Table 1).

The quality of an image mainly depends on the resolution of the digital camera and the telephoto lens. When same area is captured, the quality of the image becomes higher if the digital camera is equipped with more pixels. The resolution of a pixel (the length of a side of a pixel) of the digital camera equipped with $2,900 \times 4,350$ pixels (12.6 million pixels) is around 1.4 mm when the rectangular surface of a concrete structure with the dimensions of $4 \text{ m} \times 6 \text{ m}$ is captured. Figure 5 shows an evaluation method of crack width. Since the individual pixel of the digital image usually has 256 gradation steps for each three primary color (RGB), the width of

Table 1. Specification of main equipments.

Equipment	Specification
Digital camera	Single-lens reflex digital camera: 12.6 million pixels
Telephoto lens	Autofocus (24–85, 80–400 mm)
(Non-prism) Total station	Instrumental tolerance: $[3 + \text{or} - 2 \times 10^{-5} \times \text{distance}] \text{ mm}$
Data logging unit	Note PC (CPU: Core Solo U1300, Memory: 1 GB, HDD: 60 GB)
Image processor unit	Desktop PC (CPU: Pen4, 3.2 GHz, Memory: 2 GB, HDD: 250 GB)

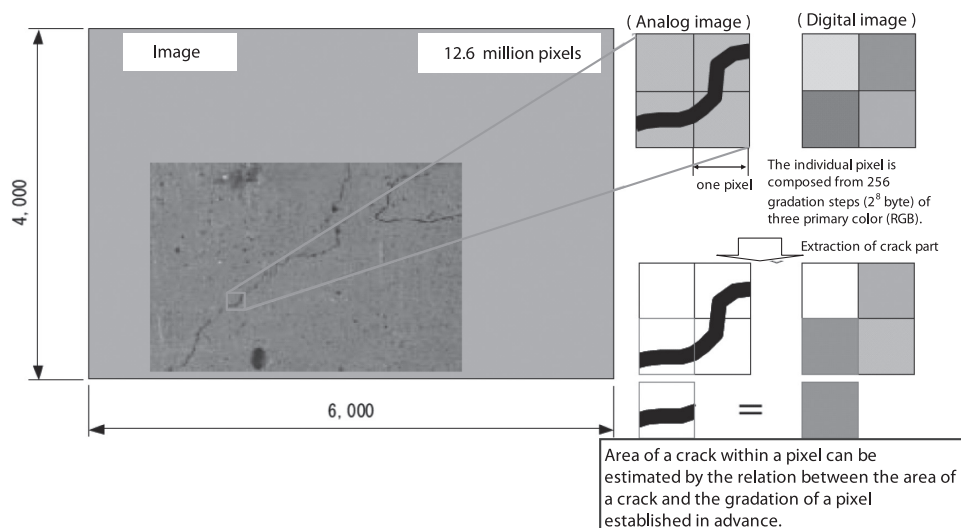


Figure 5. Evaluation method of crack width.

a crack which is narrower than the resolution can be measured if the relation between the ratio of the crack over to one pixel and the gradation level of the pixel is established (Hiroshi 2004).

In the case of using digital single-lens camera which is attached 400 mm telephoto lens, it is possible to identify the crack width of 0.2 mm if the image is taken 120 m away. The detection ratio of cracks of 0.2 mm width or wider is more than 90% by limiting the angle of view narrower than 7.3 m.

3 APPLICATION EXAMPLE OF PHOTOGRAPHIC IMAGE MEASUREMENT TECHNIQUE

3.1 Dam deterioration diagnosis

KEPCO conducts crack monitoring of the concrete structures in the dam deterioration diagnosis by using this photographic image measurement technique since 2009. KEPCO has already conducted the initial investigation in 16 dams out of 39 concrete dams owned by KEPCO. Here are the results to verify whether the photographic image measurement has an advantage over the conventional method by rope access.

The photographic image measurement technique was applied to aerial surfaces of two dams with a different size (surface areas of the two dams sum up to about 10,000 m² in all). Images were captured from where a captured image area was smaller than a rectangle of 4 m × 6 m, the angle to the subject was smaller than 45 degrees and distance from the subject was closer than 150 m. About 1,500 images of the two dams were captured in seven days. Figure 6 shows

distant view on the dam downstream side. Compensations of angle, curvature and scale were carried out to all the images, and these images were synthesized into several front view images. Cracks of 0.2 mm width or wider could be found individually while stains, concrete joints and formwork marks were checked on a monitor. Figure 7 shows an example of a sketch of cracks on a synthesized image after the compensation of angle, curvature and scale.

Moss and stain did not prevented any cracks from being found in the verification. Some painted concrete areas with reflection of sunlight prevent some cracks from being found. In such cases, images were captured again at other time considering the reflection of sunlight. Comparing all found crack lengths of the two dams with opening of 0.2 mm width or wider with those found by the conventional method, each deviation was within plus or minus 10% in about 97% of all cracks and the deviation of accumulated length of individual components of the dams varies from minus 2.1% to plus 6.2% (Table 2, Figure 8). The deviation of width of the cracks was within plus or minus 0.1 mm in about 98% of all cracks.

The photographic image measurement also has another advantage that degraded area is easily calculated because each pixel of a subject is accompanied with coordinates.



Figure 6. Distant view on the dam downstream side.

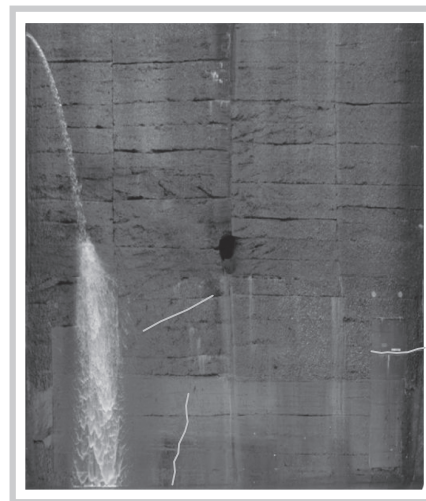


(Image processing area: about 378m² (The number of images:28))

Figure 7. Dam downstream side image after image processing.

Table 2. Comparison results of the crack of the two dams.

Crack	No.	Length (mm)		Deviation (%)	Maximum width (mm)		Deviation (%)
		Conventional method	Image measurement		Conventional method	Image measurement	
	1	8,100	8,006	-1.2	0.2	0.2	+0.0
	2	7,050	6,964	-1.2	0.2	0.2	+0.0
	3	2,750	2,981	+8.4	0.3	0.2	-33.3
	4	2,500	2,406	-3.7	0.2	0.2	+0.0
	5	2,500	2,393	-4.3	0.2	0.2	+0.0
	6	2,200	2,245	+2.1	0.2	0.2	+0.0
	14	8,850	8,881	+0.3	0.3	0.4	+33.3
	15	3,250	3,379	+4.0	0.2	0.2	+0.0
	16	5,050	4,886	-3.2	0.2	0.2	+0.0
	17	2,450	2,268	-7.4	0.3	0.2	-33.3
	18	2,700	2,883	+6.8	0.2	0.2	+0.0
	19	1,850	1,720	-7.0	0.2	0.2	+0.0
	20	3,300	3,328	+0.8	0.5	0.4	-20.0
Total / average		93,450	91,987	-1.6	0.275	0.240	-10.3

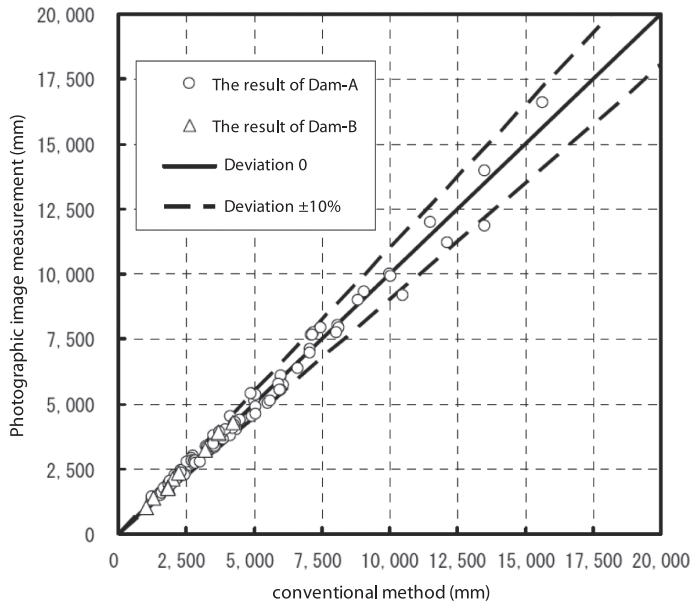


Figure 8. Comparison results of crack length.

The image measurement costs approximately 30% lower than the conventional method judging from the rough estimate of labor costs. Now we are conducting more detailed cost evaluation of the photographic image measurement.

We are also developing a database system with a retrieval function in which electronic data such as digital images and crack information are linked to drawings of the facilities. We expect the system help and save our maintenance work such as the comparison with the previous investigation.

3.2 Waterway tunnel inspection

Next, authors show an application example for a waterway tunnel inspection. The KANSAI Electric Power Group is engaged in an O&M consulting business of an overseas hydropower IPP, the San Roque Multi-purpose Project in Philippines, and in the waterway tunnel inspection of the San Roque power plant, the photographic image measurement has been conducted in 2009. Table 3 and Figure 9 show the outlines of the San Roque Dam and a longitudinal section profile of the waterway tunnel. Because the inside diameter of the waterway tunnel, which is pressure tunnel with concrete lining, is 8.5 m, it is necessary to set up a tall temporary scaffold for visual monitoring of cracks in order to observe the crown of the tunnel in detail. Since dewatering period of the waterway tunnel is a very short time, and a hatch of the waterway tunnel is less than 1 m in diameter from which inspection equipment are brought in. It is difficult to carry out enough research in a short time, so KEPCO introduced the photographic image measurement. The image measurements were carried out at sections where the bedrocks were weak and many cracks were found. Two locations were selected for the photographic image measurement, which were 29 m wide and 3 m high, 21 m wide and 3 m high respectively, with a total area of 150 m². Because the surface of the tunnel was stained with the mud, images were taken after cleaning the surface by high-pressure water washing. The measurement was completed in about three days. After bringing back the images to Japan, authors conducted image processing in our laboratory. Because the waterway tunnel has a simple circular cross section and the concrete surfaces had formwork marks, the image syntheses were relatively easy.

Table 4 and Figure 10 show comparison results of some of the data obtained from the image measurement in 2009 and 2010. As for the results of 2010, authors couldn't distin-

Table 3. Outlines of the San Roque Dam.

Item	Outline
Dam type	Center Core type Rock fill Dam
High (m)	200
Crest length (m)	1,130

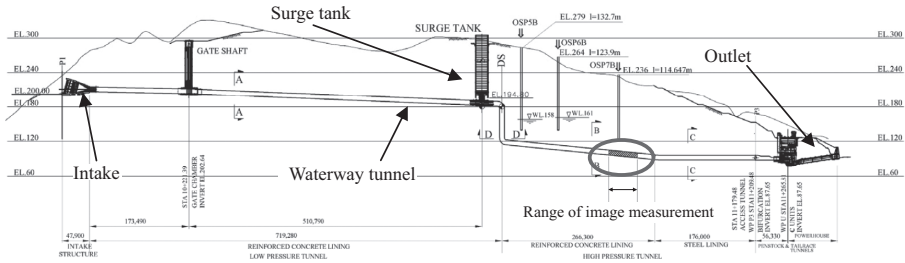


Figure 9. Longitudinal section profile of the waterway tunnel.

Table 4. Comparison of waterway tunnel crack data.

No.	Length (mm)		Deviation (%)	Maximum width (mm)		Deviation (%)
	2009	2010		2009	2010	
1	1167	1220	4.3	0.2	0.2	0.0
2	1138	1131	-0.6	0.6	0.6	0.0
3	1999	2030	1.5	0.4	0.4	0.0
4	1725	1691	-2.0	0.2	0.2	0.0
5	9959	9516	-4.7	0.8	0.8	0.0
6	1255	1178	-6.5	0.8	0.8	0.0
7	7150	7443	3.9	0.8	0.8	0.0
8	6995	8077	13.4	0.8	0.8	0.0
9	3940	4337	9.2	0.8	0.8	0.0
10	1765	1905	7.3	0.4	0.4	0.0
11	3084	3150	2.1	0.6	0.6	0.0
12	1833	1723	-6.4	0.2	0.2	0.0
13	-	954	-	-	0.4	-
Total/average	42010	44355	5.3	0.508	0.538	5.7

guish any change of crack width. But authors found slight progress of the length of the some cracks, and found one new crack. Seeing images of 2009 much more closely, authors could find a tiny sigh of a crack at the new crack position. Since the slight cracks were confirmed when images of the previous year were investigated in detail, it is assumed that the finding of the new crack is due to using a higher resolution camera (from 12.6 million pixels to 16.0 million pixels) or the different condition of the wall washing. Therefore, authors finally judge the tunnel keeps sound conditions.

Since the San Roque Power Plant, of which operation was started in 2003, is a relatively new power plant, significant degradation progress was not observed in the inspection. KANSAI could record the concrete condition at a relatively early stage. This data will be very useful at future stage in which degradation of the plant will advance.

The photographic image measurement at the San Roque waterway tunnel is the first-time experiment for KANSAI to conduct the measurement more than twice at the same point. We are firmly convinced that the database system is very useful by reconfirming as much as by comparing the past data.

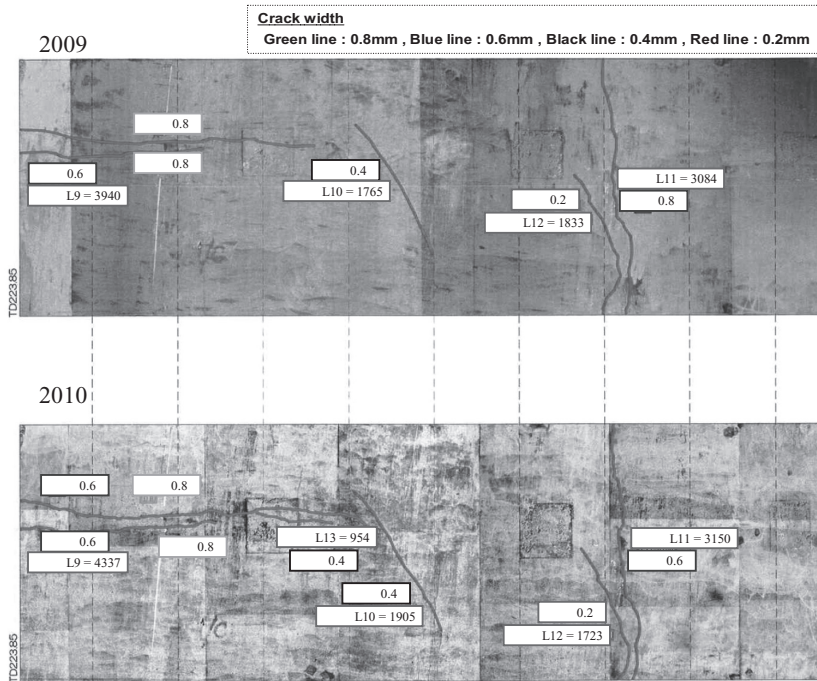


Figure 10. Result of waterway tunnel image analyses.

Authors have given on-the-job training of taking the images to the local civil engineer of the San Roque Multi-purpose Project. From now the local engineers will take and send the images to us and authors will conduct image processing in our laboratory. KANSAI can share the wide variety of the database both in Philippines and in Japan, and it makes the O&M more reliable and effective.

4 CONCLUSION

In this study, we have developed the photographic image measurement applying both for the surface of a dam and the concrete lining of a tunnel and have confirmed the availability with a certain level of the accuracy. We believe the new measurement ensures the safety of field works, the accuracy of observe data and economic efficiency.

With the information obtained from this new method, we are attempting to establish more reliable operation and maintenance of concrete structures. We are also going to pursuing more laborsaving method and expand applicable objects of the photographic image measurement by modifying the equipment and devising methodology of measurement and data processing.

We think a subject of future investigation is how to detect the depth of cracks, which is one of key factors to the soundness of concrete structures.

REFERENCES

- Hiroshi, K. 2004. Digital Imaging Process for Inspection, Diagnosis Concrete Structure. *Journal of the Japan Welding Society* 73(7): 510–513.
- Tsugio, Y., Yukihiro, K., Mashahiro, I. & Hiroshi, K. 2008. Dam Surface Investigation by Digital Camera. *Journal of Japan Society of Dam Engineers* 18(2): 118–125.

Situation and developing trend of defective reservoir reinforcing technology in China

G. Dashui & T. Jiexiong

Changjiang Institute of Survey, Planning, Design and Research, Wuhan, China

ABSTRACT: China has built more than 87,000 reservoirs, 40% of which are defective. In recent years, central government put huge amount of money into reinforcing projects from more than 7500 defective reservoirs, thus improving reservoir and dam safety situation throughout China. Through developing database information system of defective reservoirs reinforcement, and turning to mathematical statistics methods, our study systematically illustrates the characteristics and causes of diseases in certain aspects such as flood control, dam seepage, structural safety and seismic safety. We carry out statistics analyses on quantity, proportion and cost for reservoir reinforcing projects in China, according to size, dam type, structure, and disease form. Based on given examples, this article figures out technical features on dam reinforcing, summarizes various reinforcing methods, technical points, scope of application, and puts forward prospective direction for research and study in China.

1 GENERAL INSTRUCTIONS

According to “National Special Plan for Defective Reservoir Reinforcement”, China possesses 87,076 reservoirs at present, of which 508 are large reservoirs, 3209 medium-sized, 15,842 small (level one), and 67,517 small (level two). There are 38,019 defective reservoirs, of which 288 are large reservoirs, 2145 medium-sized, 9,133 small (level one) and 26,453 small (level two), accounting for 56.7%, 66.8%, 57.6%, 39.2% respectively.

Such a great number of defective reservoirs not only affect efficiency and benefit of reservoir, but also seriously threaten property safety and people’s life. Nowadays, defective reservoirs gradually become a significant weakness and potential safety hazard of the overall flood control system. Defective reservoir reinforcement is in critical need and urgency.

Because of large number and wide geographical distribution of defective reservoirs in China, engineering information management is a complicated and heavy work. Moreover, local capacity for defective reinforcement diversify quite a lot, so The Eleventh Five-Year National Technology Support Program launched a subject named Study on Technical Patterns on Information Management and Technology for Defective Reservoir Reinforcement,^[2] focusing on developing a engineering information management system for defective reservoir reinforcing projects, summarizing domestic technologies on defective reservoir reinforcing, and aiming to increase our comprehensive capacity in this field. This article gives a brief introduction of part of our research results.

2 GENERAL FEATURES OF DEFECTIVE RESERVOIRS IN CHINA

According to statistics, 95% of reservoirs in China are consisted of earth-rock dams,^[3] mostly built from the 1950s to the 1970s. Constrained technically and economically then,

low compaction, incomplete foundation clearance, ineffective seepage control treatment are rather common is during dam construction, which left potential hazards of dam seepage, piping, soil erosion, contact scour, even dam crack, landslides and other problems after dam and reservoir was put into operation.

For stone masonry dam, concrete dam, spillway and aqueduct and so on, carbonization, crack, Re-bar exposure, peeling, scouring, lixiviation, leakage may appear due to the poor construction quality or imperfect foundation treatment with increasing years in operation. These problems actually affect structural and seepage control safety.

Generally speaking, causes of diseases in defective reservoirs can be summarized into following aspects:

1. Unsafety in flood control standard

Main problem is lower crest elevation or insufficient discharge capacity, that is, flood control standard can not meet requirement of relevant regulations. Statistical data^[4-5] from Chinese Ministry of Water Resources in 2004 shows that, 51 large, 196 medium-sized and 14,000 small reservoirs of the total defective reservoirs have this problem.

2. Unsafety in dam seepage control

Main problems are seepage in dam body or foundation; piping, erosion and contact scour in earth-rock dam; lixiviation in masonry and concrete dam. Statistical data^[5] (the 1st and 2nd batches of 26 defective reservoirs before 1998 not included, the same hereinafter) shows that, of the 46 homogeneous earth dams in large defective reservoirs, 10 have seepage risks; 17 have serious foundation seepage; 8 have by-pass seepage and contact seepage; and 11 have serious seepage at downstream dam slope. Of the 55 core-wall-dams in large defective reservoirs, 5 have seepage risks; 19 have serious foundation seepage; 9 have by-pass seepage and contact seepage; and 11 have quality problems in core wall. In addition, there are 16,000 small reservoirs which have seepage control problems.

3. Unsafety in Dam Structure

Main problem is structural strength and sliding stability of the dam cannot meet regulatory requirements. Statistical data^[6] shows that, of the 46 homogeneous earth dams in large defective reservoirs, 3 have insufficient cross-section size; 12 have unstable slope; and 14 have problems in slope protection form. Of the 55 core-wall-dams in large defective reservoirs, 13 have unstable slope; 7 have problems in slope protection form. In addition, there is a wide slotted concrete gravity dam and a stone masonry gravity dam having problem in sliding stability.

4. Unsafety in Anti-Seismic Standard

Main problem is anti-seismic standard for reservoir and dam cannot meet regulatory requirements. Statistical date^[4] shows that, 13 large defective reservoirs cannot meet anti-seismic requirements of relevant regulations. There are also a considerable number of medium-sized and small reservoirs have this problem.

5. Unsafety in Water-Delivering and Flood Discharge Structures

Main problem is structural strength and stability of water-delivering and flood discharge structures cannot meet regulatory requirements.

6. Unsafety in Metal Structures and Electromechanical Equipments

At most defective reservoirs, their metal structures and electromechanical equipments have been running for 30 to 50 years, over or close to the depreciation period. Aging and rust corrosion drive them out of normal operation, seriously affecting safety of the reservoir.

7. Inadequate Management Facilities

Most defective reservoirs do not have adequate hydrological measuring and reporting and dam monitoring systems, especially small reservoirs, which usually have no such facilities at all. Management facilities at many reservoirs are very old and out of date. There are low-level or even no highways for flood control use.

Table 1. Reinforcing cost for different structures unit: million RMB yuan.

Item	Scale		
	Large	Medium	Small
Dam Body	3046.85	1064.8	244.60
Dam Seepage Control	1640.77	420.18	90.22
Dam Related Structures	1406.08	644.60	154.37
Spillway	1337.60	475.63	83.97
Water-Delivering Structures	453.73	161.95	44.50

3 STATISTICS OF MODERN TECHNICAL PATTERNS ON DEFECTIVE RESERVOIR REINFORCEMENT IN CHINA

Based on specific information of 2311 defective reservoir reinforcing projects assigned by the Central Government collected from document literature,^[2] we established project management information databases for the above 2311 reservoirs and professional technical databases for another 206 reservoirs. Turning to modern statistic analysis methods, we summarize contemporary technical patterns in China on defective reservoir reinforcement as follows:

1. Of the above 2311 defective reservoirs already reinforced, 58 are large reservoirs, accounting for 2.5%; 744 medium-sized, 32.2%; 1509 small, 65.3%. Sorted by dam type, 93.3% are earth-rock dams, 5.6% stone masonry dams, and the rest concrete dams. Among earth-rock dams, homogeneous earth dam takes the largest proportion, that is, 66%; followed by clay core dam, 30%; clay sloping core dam and concrete face rock-fill dam accounts for 3.5%, 0.5% respectively.
2. Unit capacity reinforcing cost varies from one another for different scale of defective reservoir. The average cost is 0.17 RMB yuan for large reservoir, 0.45 RMB yuan for medium, and 0.67 RMB yuan for small. The total cost goes into different reinforcing items, with over 60% into dam seepage control and structure safety, 28% into spillway and 10% into water-delivering structures. See Table 1.
3. Among all the reinforcing approaches for raising flood control standard, heightening of dam is the most widely used in specific projects, with a proportion of about 48%. Next are building wave wall and increasing discharge capacity, accounting for about 29% and 18%. Integration of heightening of dam and increasing discharge capacity take a proportion of 6%.
4. As for dam seepage control reinforcement approaches used in projects, concrete cut-off wall accounting for 52%; jet grouting cutoff wall 5%; geomembrane 3%; and foundation curtain grouting 36%. Principal measures dealing with seepage problems existing in concrete and stone masonry dams are adding new concrete slab and grouting.
5. For dam slope reinforcement, especially for upstream slope reinforcement of earth-rock dams, removing and rebuilding accounts for 46%; partly repairing 20%; partly rebuilding 12%; and no treatment 22%.
6. For spillway reinforcement, partly removing and rebuilding accounts for 73%; total discarding and rebuilding 4%; and no treatment 23%.
7. For water-delivering structures reinforcement, intake tower reinforcing or rebuilding accounts for 85%; tunnel reinforcing 66%; outlet energy dissipation structures reinforcing 10%; and metal structures and hoist equipments replacing or repairing 82%.

4 PHOTOGRAPHS AND FIGURES

4.1 *Increasing reservoir flood control capacity and heightening of dam*

In response to general features of unsafety in defective reservoir flood control, we take measures to improve reservoir flood control capacity that can be categorized into two major

classes: ① heighten the dam to increase reservoir flood storage capacity; ② expand scale of flood discharge structures to increase discharge capacity. In China, a number of large and medium-sized reservoirs have taken the above two approaches to increase their overall flood control capacity since “75.8” flood in the 1970s to the 1980s.

4.1.1 *Heighten the dam*

4.1.1.1 *Earth-rock dam*

1. Add wave wall

For dams which do not have wave walls, we prefer to add a new wave wall on the dam crest after we carry out calculation and make sure that dam body itself can meet basic requirements for normal operation. The wave wall is usually 1.0 to 1.2 meter tall.

2. Heighten the dam

Generally, it is favorable to heighten the dam on downstream slope without emptying reservoir or compromising operational benefit. However, supposed the dam slope was unstable, we should consider heightening the dam either at the upstream or downstream slope in view of dam slope stability condition.

4.1.1.2 *Concrete dam*

Heightening of concrete dam has two ways: ① pour concrete on dam crest, meanwhile increase dam cross section at upstream or downstream side; ② combine new concrete with old dam body and foundation through the vertical prestressed anchor cable. In order to guarantee bearing capacity of the joint structure, dig key seat, insert rebar and apply bonding adhesive at the concrete interface.

1. Increase dam cross section

Construction of Danjiangkou Water-Control Project is divided into two stages. The second stage serves for the South-to-North Water Transmission Project, with the main job of increasing dam cross section by 14.6 meter at downstream side. Affected by temperature changes, elastic modulus of new and old concrete diverse, and old concrete exert fairly big constraint force on new concrete, so there is great possibility that the joint structure would separate after construction. Original design for the first stage reserve key seats for later heightening at downstream dam slope, but dam face concrete carbonize as time pass by. During the second stage construction, we remove the carbonized concrete layer by 2 to 3 centimeter, dig new key seats where there is no seat reserved beforehand (new key seat size is 70 centimeter long, 40 centimeter wide, 30 centimeter deep; the downside forms an angle of 23.19° with original dam surface; and center interval of seats is 1.5 meter.), and insert anchor (diameter 25 millimeter, 4.5 meter long, 2 to 3 meter into old concrete, alternate with long and short anchor, interval distance 2×2 meter, mortar strength grade M20) at concrete interface for higher bond strength and better joint bearing performance. Still, we properly raise grade of new concrete to achieve relatively consistent elastic modulus of new and old concrete.

2. Heighten the dam with prestressed anchor cable

Fixing vertical prestressed anchors on the upstream side of a heightened dam can improve anti-sliding stability and anti-bending performance. In this way, there is no need lowering normal reservoir operational water level, and economic benefit will not decrease. We implemented this approach on Fengman Reservoir, resolving foundation seepage problems and heightening the dam by 1.2 meter. Shiquan Reservoir was adopted this way to solve the dam stability problems, while we heightened the dam 14.6 m. The Shiquan Reservoir is another example of this technology and its design flood standard was increased dramatically.^[7]

4.1.2 *Increase discharge capacity*

Besides exploring potential capability of flood discharge structures, we can also broaden or deepen original spillway or build a new one. For example, Miyun Reservoir in Beijing chose to build a new spillway. Another way is to build new emergency spillway. For example, Lucun Reservoir in Anhui builds two emergency spillways when reinforcing, which highly improve its flood control capacity.

4.2 Seepage treatment measures for earth-rock dam

Seepage is one of the primary diseases existing in defective earth-rock dams. We have multiple treatment measures such as concrete cut-off wall, high pressure jet grouting, fractured grouting, stable cream seriflux grouting, geomembrane, etc.^[2] This article just introduces three types of anti-seepage technologies.

1. Concrete cut-off wall

This methodology is to build a concrete cut-off wall along the axis of the earth-rock dam. The wall can be put inside dam body or stretch into the foundation for a certain depth, thus cut off seepage path inside dam body and foundation. Advantages of this method include: better adaptability to various geological conditions—applicable for both dam body and foundation reinforcement; no need to emptying the reservoir during construction; and construction of wall using displacement method, which is easier for monitoring construction quality than other methods. Disadvantages include: need of wider working platform for construction; need of lowering dam crest by excavation and fill it back to design elevation; and longer construction period and higher cost.

In China, we applied this technology for the first time to Tuolin Reservoir in Jiangxi, and then to Danjiangkou Reservoir. Earlier, Uzziah Kass drilling machine was widely used for cut-off wall construction, and it costs more time and money. As construction technique developed, hydraulic grab came into practice, increasing construction speed and reducing cost. Nowadays, cut-off wall gains extensive use in reservoir reinforcing projects. Take Hualiangting Reservoir in Anhui as an example. The dam is a clay core dam with upstream sand blanket. Due to poor construction quality, serious seepage was found in dam body. So we decided to build a concrete cut-off wall inside the clay core, stretching through sand layer into rock foundation by 1 meter. The wall is 540 meter long, 0.8 meter thick with an area of 25,470 square meter and maximum depth of 66.4 meter (see Figure 1). In order to form working platform, dam crest has to be lowered by 3.25 meter. Hydraulic grab was used for cut-off wall construction assisted by drilling machine. We made full use hydraulic grab's advantage of quick pore-creating. Hydraulic grab was used for dam body and drilling machine for foundation. The cut-off wall construction of this project commenced in December 2009 and finished in just four months. Flood season in 2010 has passed, and the reinforced dam does run well without any seepage problem.

2. High pressure jet grouting

This methodology contains following procedures: drill hole with drilling machine; put jet pipe life jet pipe (with water pipe, cement pipe and wind pipe inside) into the hole; spray high pressure fluid and shock soil (cement flow and soil are mixes together); lift jet pipe and leave the mixture to solidify. The main idea of this technology is to arrange drilling holes along the axis of earth-rock dam and grout in every single hole. Grouting coagulum in adjacent holes overlaps and forms a continuous cut-off wall, finally reaching the goal of anti-seepage.

High pressure jet grouting was initially carried out in silt and sand layers, though it extended successfully into gravel layer in recent years. Take Gongshang Reservoir in Henan as an example. The earth-rock dam is of poor construction quality, with deformation and cracks on dam body. Thirty meter width's pebbly sand layer under the dam was not cleared at all. Before

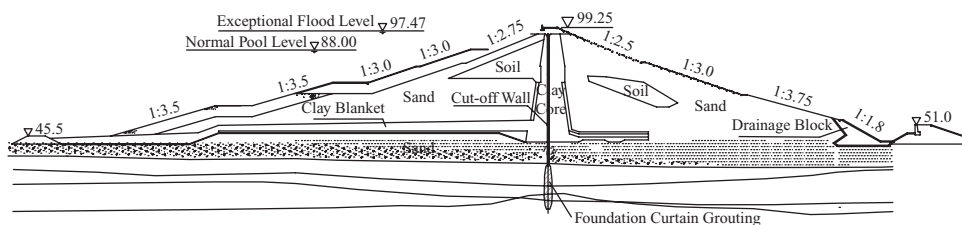


Figure 1. Sketch map of cut-off wall in Hualiangting Reservoir.

reinforcement, there was muddy water effusing at downstream dam toe—average leakage volume is 90 liter per second. In 1999, the dam was reinforced by jet grouting, and dam-toe leakage disappeared soon afterward. Advantages of this method include: no need of lowering dam crest to form wide working platform and fast construction speed. Disadvantages include: different technical parameters for different geological layers, which requires site tests and professional construction team with abundant experiences; Lower overall performance than concrete cut-off wall, for instance, difficulty of entering rock foundation, low strength in clay layer and poor durability; and high likelihood of cracking when depth exceeds 40 meter.

3. Stable cream seriflux grouting

This grouting technology is applied on coarse aggregate dam and foundation. The seriflux is liquid cement mixed with certain proportion of clay or bentonite, possesses greater viscosity and stability and is suitable for screw pump. Supported by this technology, we can build impervious curtain in rock-fill body or pebbly sand layer under macro porosity and high underground water flow rate. At Hongfeng Reservoir in Guizhou, the wood faced rock-fill dam is 416 meter long, with a maximum height of 52.5 meter. Its porosity reaches 38%. The wood face rotted after tens of years' operation, and serious seepage occurred. In order not to emptying the reservoir, we take stable cream seriflux grouting there. Based on site tests, four row of drilling holes were arranged inside the dam body to form a impervious curtain. The curtain is 4 and 14 meter thick on top and bottom respectively, and has achieved favorable performance. In 2009, Mopan Reservoir in Guangxi took this measure for its concrete faced rock-fill dam and it works very well.^[2]

4.3 Dam slope stability and anti-seismic reinforcement of earth-rock dam

1. Dam slope stability reinforcement

We usually gentle dam slope through either earth up or slope cutting, so as to increase slope stability of earth-rock dams. For steep slope at upstream side, lattice protection can be adopted. And as for slope instability caused by higher saturation at downstream side, cut-off wall may likely solve it.

Materials selected for upstream dam slope reinforcement should be rock block, rock ballast, gravel, sandy soil, which is more permeable than old dam slope ingredient and ensures quick drainage when lowering pool level. However, in some cases it is not allowed to emptying reservoir, and then we can choose rip-rap filling. When gentling downstream dam slope, we shall fill water permeable material at the bottom to lower saturation in dam body. At Lucun Reservoir in Anhui, our design for upstream dam slope reinforcement is partial rip-rap filling for slope under water, rough sand rolling filling for slope above water; for downstream slope, we use lattice protection. According to monitoring data during three years after reinforcement, we can judge that the dam slopes are all stable. At Qingshan Reservoir in Hubei, cut-off wall was built inside its dam to solve seepage problems of seepage and downstream slope instability.

2. Slope protection reinforcement

Upstream slope protection for earth-rock dam could be rock block, cast-in-place concrete and precast concrete, while downstream could be vegetation, lattice plus vegetation, rock block, cast-in-place concrete and precast concrete, etc. The Embankment dam upstream revetment to reinforce can use the revetment made in piece stone, cast-in-place concrete and precast concrete. If a reservoir is also a scenic spot, we shall choose prettified precast concrete for upstream slope, and prettified precast concrete or vegetation or lattice plus vegetation for downstream slope. Take Hualiangting Reservoir as an example. We specifically designed I-shaped precast concrete block (80 centimeter long, 30 centimeter wide, 20 centimeter thick) for its upstream dam slope. The reinforced dam slope does not only look nice, but also effectively resist waves.

3. Anti-seismic and anti earthquake liquefaction reinforcement on dam body

Liquefaction failure often occurs in sandy soil of poor denseness. Reinforcing methods for this kind of material include replacement, densification and weights. ① Replacement means

removing all sandy soil within liquefaction area and refill with anti liquefaction material like rock ballast. ② Densification means increasing density of sandy soil and its anti-liquefaction capability through vibratory percussion and compaction. ③ Weights means placing weights on surface of liquefaction area, so that it can help increase sandy effective stress and anti liquefaction capability of the sandy soil.

For instance, in the Reinforcing Project of Miyun Reservoir in 1977, without emptying the reservoir, upstream slope of Baihe earth dam was reinforced by removing the liquefaction layer, refilling with rock ballast, thickening blanket and part of sloping core.^[8] In 1998, still in Miyun Reservoir Reinforcing Project, again without emptying the reservoir, upstream slope of Chaohe earth dam was reinforced by rip-rap filling under water, replacing original sloping core with rock ballast above water. The rip-rap increased effective stress and anti liquefaction capability of the gravel layer, meanwhile, it helps gentle the slope and improve slope stability.^[8] For another example, clay core sandy shell dam of Hualiangting Reservoir have a maximum height of 58 meter, which have low density sandy soil upstream slope. The slope under water is highly likely to liquefy during a Richter scale 7 degree earthquake. After thorough study, we selected weights as reinforcement method that is placing 5.5 meter thick weights on upstream slope. In demand of water supply from local people around the reservoir, we decided not to empty the reservoir, keeping pool level at 66.5 meter elevation. The final solution is rip-rap filling for slope under water and rock ballast rolling filling for slope above water. After reinforcement, the risk of underwater slope liquefaction during 7 degree earthquake decreased a lot.^[9]

4.4 *Under-dam aqueduct reinforcement*

1. Replace under-dam culvert pipe with tunnel

At many reservoirs built earlier in China, their irrigating, generating and water-delivering structures were under-dam culverts. For different reasons such as dam body deformation, poor construction quality, deficient structure design, leakage and contact washing erosion appeared in lots of culvert, seriously threatening safety of the dam. Some culverts received reinforcement. Nevertheless, cracks did not disappear because there were deformations or current scout in dam body. Therefore, if there are leakage defects in under-dam culverts, the best disposal is to discard and block the old culvert, and build a new one at the bank.

2. Reinforced concrete lining

Adding reinforced concrete lining to the old tunnel can improve its structural and seepage safety. But this method asks for smaller tunnel cross section, slightly impacting carrying capacity. We shall pay attention to interface treatment of the old and new concrete. Inner diameter of tunnels in need of reinforcement should not be less than 2.5 meter, in case construction is impossible to proceed.

3. Steel liner

Through adding steel liner to old culverts or tunnels can improve their structural and seepage safety. By injecting cement mortar into gaps between the liner and tunnel wall, they can integrate. As the liner's roughness is relatively low, carrying capacity of the tunnel may not decrease after reinforcement. To avoid steel liner instability under high external water pressure, ribbed plate and anchorage rod can be added. Diameter of tunnel being reinforced shall not be less than 1 meter, in case it is impossible for construction.

4. High-strength carbon fiber sheet liner

Carbon fiber sheet is a tensile material with high strength and flexibility. Its ultimate tensile strength can reach up to 3,790 to 4,825 MPa, elastic modulus 220 to 235 GPa, and elongation over 1.4%. The thickness could be 0.111 or 0.167 millimeter. For tunnel concrete liner which can not meet crack resisting requirement under high internal water pressure, or have cracks and cavitations, we can paste 1 to 3 layers of carbon fiber sheet on inner surface of the tunnel to supplement its concrete strength and anti-seepage capability. For instance, at Qingshan Reservoir in Hubei, the power tunnel has a diameter of 3.5 meter and thickness

of 0.6 to 1 meter. Because of poor construction quality, cracks, scour erosion and leakage all appeared on the concrete liner, impacting safety of the tunnel itself and back massif. In view of the on-site construction conditions, we decided to use high strength carbon fiber sheet for tunnel reinforcing. Three layers of fiber sheet (0.167 millimeter thick) were pasted on lower flat and sloping sections, and two layers on upper flat and sloping sections.^[2]

5 FUTURE DEVELOPING TREND OF REINFORCING TECHNOLOGY FOR DEFECTIVE RESERVOIR IN CHINA

1. Nowadays, China has over 87,000 reservoirs, mostly built during the 1950s to the 1970s. And 44% of the reservoirs are defective, demanding more reinforcing and safety management work. Literature^[4] provides an engineering information system for defective reservoir reinforcing projects. The system has advantages of massive information processing, rapid processing speed, fine information share, easy querying and calling. It can be widely used in water administrative departments at different levels, which will improve reservoir reinforcing technology in China.
2. 95% of reservoirs in China contain earth dam. Upstream slope reinforcement is very common. Precast concrete block can better adapt to dam body deformation and prettify the slope. However, there is no requirement in regulation for precast concrete block design. Mechanically applying this technology may cause unnecessary problems. More research on this subject is needed to create systematic methodology for precast concrete slope protection and improve overall technical level.
3. Carbonization is an universal phenomenon for concrete structures in our defective dams. Currently, acrylic-emulsion cement mortar is frequently used dealing with this problem. But implementation is difficult and the ultimate appearance is imperfect. So we shall further research and develop systematic technology for treating concrete carbonization on hydraulic structures.
4. New reinforcing technologies such as fixing geomembrane, pasting steel plate and pasting carbon fiber sheet, are already used in defective reservoir reinforcing projects. Application of these technologies is still constrained by many environmental and working conditions. So further research and develop systematic technology to reduce cost and expand applied range of these technologies.

REFERENCES

- [1] Ministry of Water Resources of China, 2007. Special program of countrywide defective reservoir reinforcement [M].
- [2] TAN Jiexiong, Gao Dashui, 2010. Chiangjiang Institute of Survey, Planning, Design and Research. Special report on technical patterns on information management and technology for defective reservoir reinforcement. The Eleventh Five-Year National Technology Support Program, 2006BAC14B01.
- [3] Zhang Yanming., 2001. Professional technical paper collection on defective reservoirs and sluice in China [M]. Beijing: China Water Resource and Hydropower Press.
- [4] Zu Leiming, 2004. Safety management of defective reservoir in China [M]. Safety evaluation and reinforcement of hydro-engineering. Wuhan: Changjiang Press.
- [5] Shen Hailian, Zhang Hua, Xu Li, 2008. Present situation and reinforcing measures for small reservoirs in China [J]. *Water saving and irrigation*, 2008(8): 71–75.
- [6] Lv Guoliang, Cen Zhikang, Zheng Guangjun, 2009. Engineering design of Danjiangkou dam heightening works for South-to-North Water Tansmission Project. Yangtze River, 2009(12): 81–84.
- [7] Gao Dashui., 2004. Application of prestressed anchorage technology and statistics of technical parameters [J]. *Journal of Yangtze River Scientific Research Institute*, 2004(6): 87–90.
- [8] Fu Lei, 2000. Anti-seismic design for earth dam of Chaohe Reservoir [J]. *Journal of Hydraulic Engineering*, 2008(8): 16–20. (in Chinese).
- [9] Gao Dashui, Ye Junrong, 2008. Study of anti-seismic performance and reinforcing measures for sandy shell dam of Hualiangting Reservoir. *Journal of Geotechnical Engineering*, 2008(12): 1921–1924.

Long term behavior of the concrete dams drainage system and ageing phenomena

D. Stematiu & R. Sarghiuta

Technical University of Civil Engineering Bucharest, Romania

A. Constantinescu

Freelance consultant

ABSTRACT: During service of a concrete dam the upstream watertightness and efficiency of the drains generally decrease. An ageing of the dam often entails ageing and clogging of the drains. The most common approach in assessing the decrease of the drainage efficiency is based on the monitoring of the uplift pressures and the seepage collected by drains. Several case studies of uplift evolution revealed by complex monitoring of dams have shown that the abnormal behavior can not be attributed entirely to the drainage clogging but also to site geology and foundation rock properties. Poiana Uzului dam is selected to underline the concept. The dam is a buttress dam, 80 m high that presented several behavior incidents as a consequence of the sudden uplift increases that in their turn were induced by tensile cracks in the grout curtain at the dam upstream toe and over passing of the drainage system capacity.

1 INTRODUCTION

An ageing of the dam often entails ageing and clogging of the drains. The most common approach in assessing the decrease of the drainage efficiency is based on the monitoring of the uplift pressures and the seepage collected by drains. However, the current approach does not cover all the particular conditions of a dam. Several cases from the Romanian dam portfolio present this particular behavior. Iron Gates overflowing gravity dam on Danube River has systematically lower uplift forces than assumed not as a consequence of the intensive drainage but due to the imperviousness of the rock as compared with the dam concrete. Golesti dam and the other dams on the Arges River cascade was provided with deep drainage drillings to control the pressure in sand layers underneath the first impervious foundation layer. Their active drainage has created in time some piping and the drainage closure did not affect the uplift pressures as expected. Poiana Uzului buttress dam has presented several behavior incidents as a consequence of the sudden uplift increases that in their turn were induced by tensile cracks in the grout curtain at the dam upstream toe and over passing of the drainage system capacity. Detailed analysis of the last dam may bring a new light on the traditional evaluation of uplift evolution.

Impoundment of the reservoir created by Poiana Uzului dam commenced in 1972. Although the dam structure allowed the operation of the reservoir up to the maximum water level during a 30 year period several incidents revealed by the monitoring system beginning with the year 1979 were caused by changes of the grout curtain and drainage system efficiency. A full set of constructive measures was established mainly aimed to improve the watertightness of the grout curtain, the drainage system hydraulic capacity and the dam-foundation interaction. The program was applied in stages monitoring the effects achieved.

2 POIANA UZULUI DAM

Poiana Uzului reservoir was performed in order to provide an active storage of $80 \times 10^6 \text{ m}^3$ for water supply in the downstream area. The dam is a concrete buttress one with a height of 80.4 m and a concrete volume of 70,000 m^3 . The dam is divided in 33 blocks out of which the three blocks in the central zone are overflowing. The buttress of each block is supported at the base b/a 15 m foundation pad, equal to the head width (Fig. 1). The pad is also used as a support for supplementary loading with fill material to provide the stability against sliding.

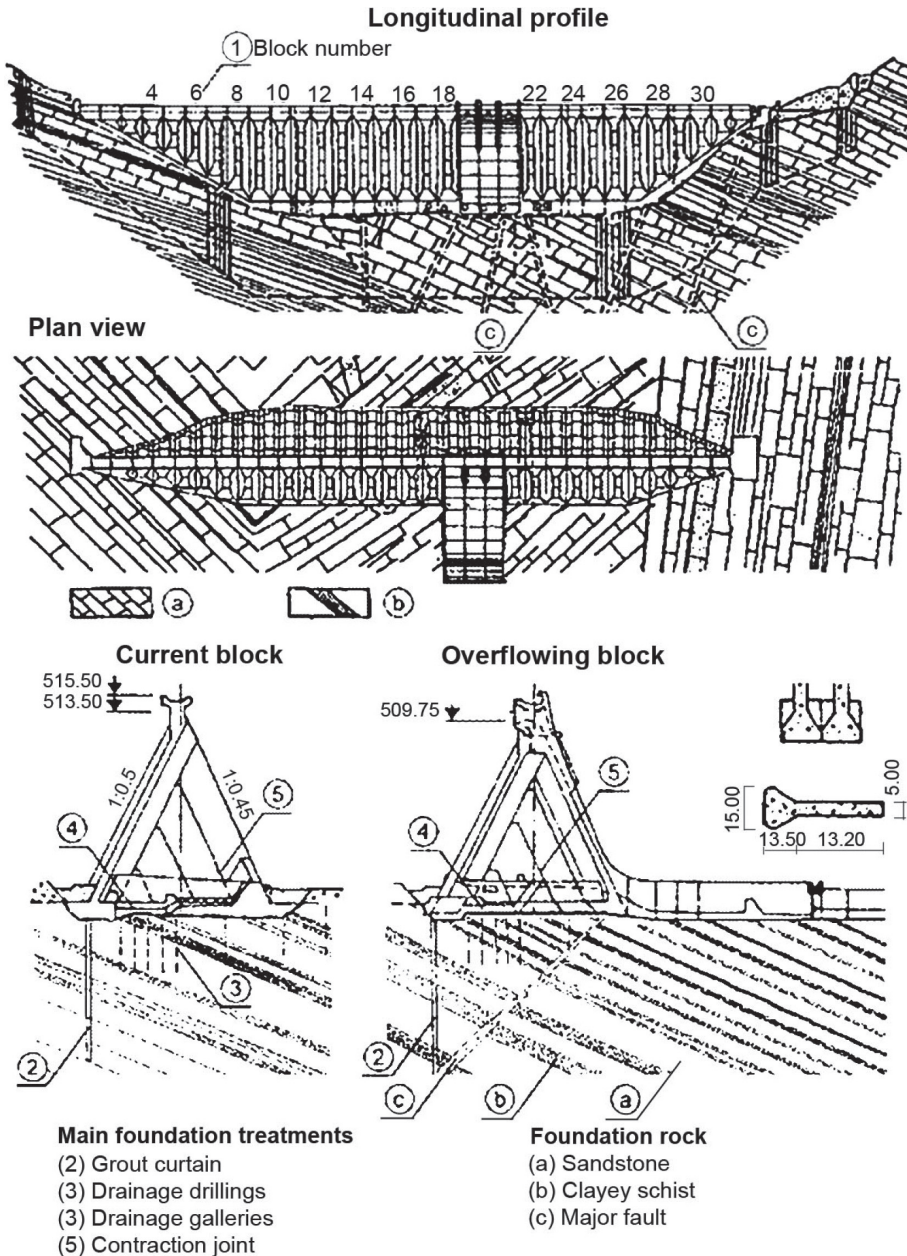


Figure 1. Poiana Uzului dam characteristics.

The buttress itself is divided into 13.2 m columns by means of construction joints oriented parallel to the downstream face. Consequently independent inclined columns transmit the load from the head of the buttress to the foundation ground. Visiting drainage galleries are provided along the contraction joints between the buttresses, at the foundation level in the upstream zone.

The concrete for the dam body was prepared with aggregates from a natural quarry formed of good quality sandstone. Due to the heterogeneity of the sand grain-size distribution about 40% of the sand was obtained by crushing. The cement content was of 250 kg/m³ and the water/cement ratio of 0.48. The laboratory tests carried out on site showed an average compressive strength of 17 MPa at 7 days and of 38 MPa at 180 days, with variation coefficients ranging between 8 and 12%. The particularly good results regarding the tensile strength—3.1 MPa in tension and 5.8 MPa in bending—should be underlined since they explain the reduced frequency of the cracks during construction (Stematiu, Constantinescu & Mircea, 1991).

The geology at the site consists of detrital sedimentary rocks: quartz feldspatic sandstones in metric layers with frequent intercalations of 2 ... 20 cm micashistous sandstones and several intercalations of 0.2 ... 4 m marly and clayey schist. Blocks of massive heavily fissured sandstone are encountered. The fissure matrix induces an increase of rock mass permeability and deformability. The site investigation has revealed a random variation of water takes in the range of 1 up to 10 lugeons, with very large values alternating to rather impervious zones. Two significant schist layers of some 3 m width are located at the base of right abutment. Six main faults accompanied by breccias with the thickness of 0.5 ... 1 m were identified during the foundation excavation.

The rock mass properties were obtained by geophysical investigations, permeability tests, compression tests as well as rock/rock and concrete/rock shear tests. The modulus of deformation ranged between 1000 and 4800 MPa about 50% of the total deformation being of elastic nature. Under the constant load of 2 ... 2.5 MPa the in time deformation stabilized in 6 ... 8 hours and the supplementary deformation level did not exceed 15%.

The watertightening of the foundation ground was performed all along the upstream toe and prolonged towards the abutment by 50 m. The grout curtain consists in three rows of drillings grouted with cement milk. During the watertightening grouting there occurred slurry pressure losses with total water circuit loss sometimes even accompanied by the cement slurry emerging to the surface. The cement uptake exceeded sometimes 1200 kg/m of drilling. The permeability-tests carried out during the grout curtain performance pointed out the existence of large discontinuities and the subsequent grouting required large cement quantities. A total of 40,000 m of drillings was performed with a mean cement uptake of 400 kg/m of drilling. The final imperviousness of the grout curtain was 1 lugeon on the upper half and up to 3 lugeons in the lower one. Mention should be made that near the right abutment, along blocks 11–14, the initial water take was significantly larger, up to 10 lugeons and the mean cement uptake was 595 kg/m of drilling.

A large number of drainage drillings was provided for uplift relief since the dam has a continuous pad foundation. Several 20 m deep drillings are located on each block, 12 ... 14 m downstream of the grout curtain. Additional five sub horizontal drillings of 40 ... 100 m length were provided in the both abutments, downstream the dam. The uplift relief is also achieved by the drainage galleries provided in between the blocks at the foundation level. The drainage galleries leave open the rock foundation along the block joint and on each side of it at the upstream end (T shape). A number of 3 ... 7 drainage drillings were performed for each gallery with a total number of 185 drillings for the whole dam. In 1977, after five years of reservoir operation 32 drainage drillings were added for the blocks 5 ... 12 located near the right abutment.

The monitoring system was designed according to the dam type and allowed a proper surveillance of the dam. Six direct pendulums and two inverted pendulums provide data concerning the relative and absolute displacements of the dam body. The rock mass displacements are measured by means of rockmeters. Survey measurements complete the total displacements monitoring and deformetric markers provides inter-blocks relative movements.

Temperatures, strains and total stresses within the dam body are measured by electric transducers located in the block 11, at the base of right abutment and in the block 24 in the central zone. Uplift values are also monitored by means of pressure cells installed in the drainage drillings.

3 INCIDENTS CREATED BY LACK OF DRAINAGE

The dam on the whole presented an adequate behavior allowing the operation of the reservoir up to the maximum level. The measured values, i.e. displacements, strains, relative movements etc. are dependent on the reservoir water level and especially on the seasonal variation of temperatures. However, several abnormal phenomena and an incident were recorded. The large settlements at the downstream toe induced by continuous increase of the foundation ground settlements were pointed out by the multiple base borehole extensometer measurements especially in the downstream toe zone.

The flows drained by drillings present very small values and occur mainly in the right abutment. During the dam monitoring up to 1984, the sudden coming into operation of the drainage drillings was recorded in some years (1979, 1981) but it was considered no special phenomenon. At the end of April 1984, the increase of the flows collected by the drillings was significantly higher, drillings that were inactive came then into operation, water jet occurred directly from the rock in the drainage galleries at joints 516 and 10/11. Simultaneously with these seepage flow increase there were also recorded abnormal displacements of the blocks (Fig. 2). Upward movements and downstream displacements higher than the previous ones were recorded at the blocks located at the base of the right abutment. A sudden change of the displacement pattern (towards downstream) in relation to the general tendency (towards upstream) was also noticed (Constantinescu, Stematiu & Hapau, 2003).

They were rendered evident by the geodesic measurements and by pendulum monitoring data. The analysis of the 1984 phenomenon led to the conclusion that it was similar to the phenomena previously recorded but its amplitude was caused by an unfavorable combination

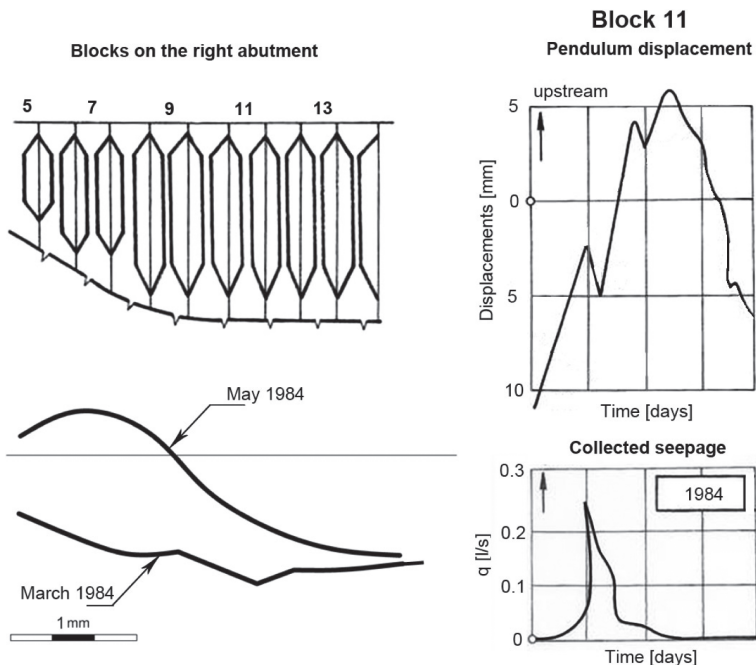


Figure 2. Change of the displacement pattern and increase of drainage flow in April 1984.

between the water load and the temperature variation. It should be noticed that the maximum water level of 1984 was exceeded in 1978 and 1983 without recording similar events. A particular role in causing the recorded phenomena was incumbent on the uplifts that occur in the foundation, due to the lack of draining capacity.

4 AGEING PHENOMENA

In the case of Poiana Uzului dam the ageing phenomena consist in loss of the grout curtain watertightness and a decrease of the drainage capacity encountered during the reservoir operation. The changes were noticed on the basis of the measurements provided by the monitoring system and by the incidents presented before.

The analysis of the dam behavior has revealed a stress dependent permeability of the foundation rock. This particular behavior was firstly pointed out by the correlation of the seepage flows with the buttress average temperature and not with the water level in the reservoir as usually happens (Stematiu & Ilie, 1992). The dependence of the drained flows on the reservoir water level is materialized only at reduced temperatures of the buttresses. For the same water level in the reservoir, the flows collected by the drainage system are larger only at reduced temperatures, when the stresses at the upstream toe decrease. From the structural point of view, tensile stresses do occur at the upstream toe of the dam under higher levels in the reservoir associated to lower temperatures in the concrete buttresses. Consequently the rock grouted fissures open. The foundation permeability increases and the drainage system are activated. Where the amount of seepage overcomes the drainage capacity the uplift increases and causes a sudden change of the displacement pattern. When the stress state in the upstream zone of the foundation is mainly compressive the fissure are closed and the seepage toward the drainage system is hindered. In between cycles of drainage reactivation a clogging of the drainage drillings occurs. Even after a large extension of the drainage system performed in 1988 similar phenomena took place (Fig. 3). The new drillings collected very

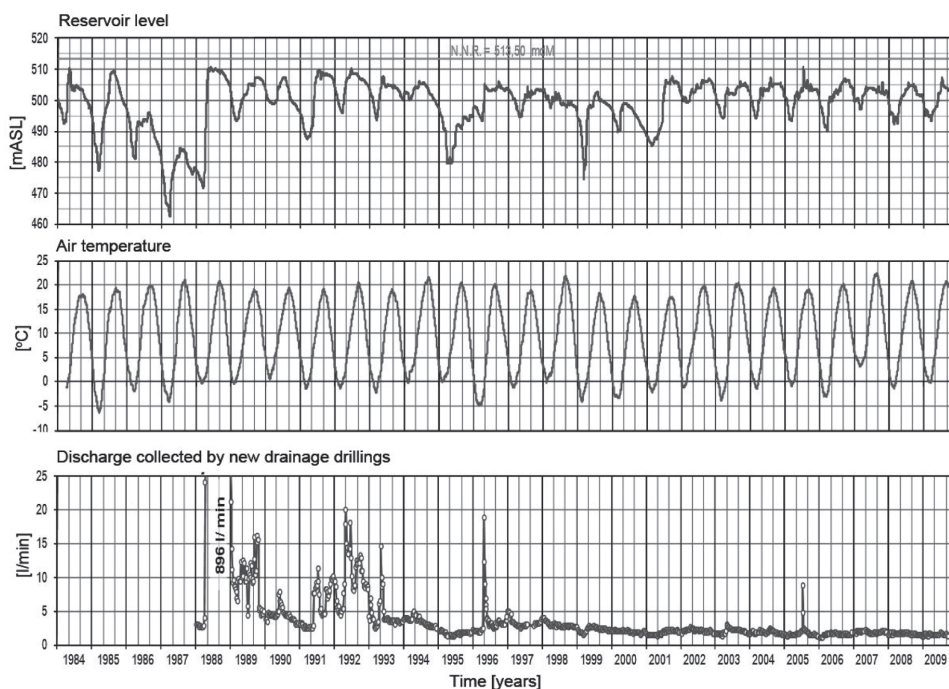


Figure 3. In time reducing the drainage flows.

high seepage flow rates and fine solid particles were carried out by the inflows. The seepage flow in the drainage gallery 8/9 has reached 4.5 ... 5.0 l/s while during the incident it was less than 0.9 l/s. Very soon the flow rates decreased and the collected seepage was clear.

The dam behavior incidents, evidenced at over 10 years from the first reservoir filling, point out once more the in time evolution induced by the unfavorable overlapping of the mechanical and thermal loadings after many cycles of the reservoir filling and emptying. The in time changes of the grout curtain watertightness and of the drainage condition are clearly an ageing phenomenon and a program of remedial works was established.

5 REMEDIAL WORKS

Subsequent to the events in April 1984 when the seepage flows collected by the drainage system increased about 30 times and were accompanied by a doubling of the horizontal displacements in the right abutment zone, a program of studies and remedial works was decided.

In a first phase, after the permeability tests using marked water rendered evident that seepages occur through the grout curtain, discharging at the upstream toe in the right abutment zone about 700 t of fly ashes performed an artificial clogging of the rock fissures. An immediate effect was obtained the seepage flows reducing significantly. After stabilizing the seepage the drainage system affected by clogging was reshaped.

In a second phase a complete program of remedial works was designed (ICOLD, 2000). It comprises (Fig. 4):

- a supplementary drainage system of the dam foundation;
- closure of preferential seepage paths through the grout curtain;

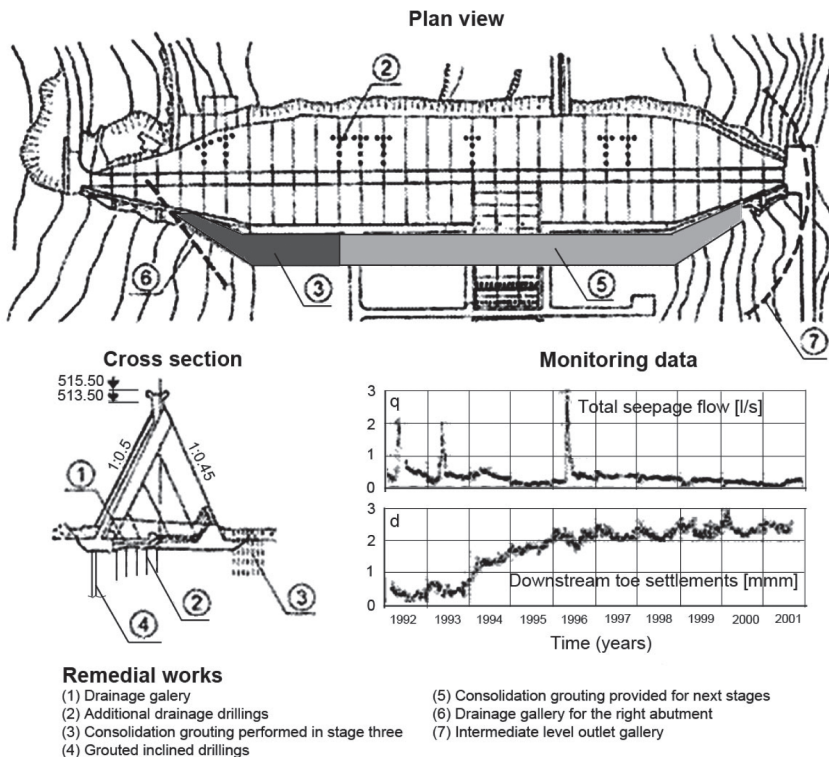


Figure 4. Remedial works program.

- consolidation grouting of the rock mass at the dam downstream toe;
- additional drainage of the left abutment;
- extension of the monitoring system dedicated to measurement of the uplift and rock deformation.

The extension of the drainage system was started immediately after the incident occurred in 1984. The first supplementary drainage drillings were performed in the blocks 8 and 9 where during the incident the water jet occurred directly from the rock. At the final stage of the drainage extension, 205 new drainage drillings were performed, with a total length of 6670 m. The total seepage flow has reached up to 11 l/s, ten times larger than before the drainage extension. The efficiency of this constructive measure is hard to evaluate in terms of dam behavior. In spite of a very large increase of the collected flows similar incidents with the one recorded in 1984 took place in 1988, 1992, 1993 and 1996.

The implementation of the uplift monitoring system was started concomitantly with the drainage extension. A total of 100 piezometric cells were installed in new drillings performed in the buttress concrete and partly in the rock. 37 cells were provided at the dam-foundation contact, 28 cells at a depth of 0.5 m under the buttress heads, 24 cells at a depth of 5 m in the rock under the buttresses and 11 cells were located at 30 m underneath the downstream toe.

The second stage of the remedial works was started in 1989 and was dedicated to cut down seepage that passes along the preferential channels through the grout curtain. Such channels have been identified by the tests performed with marked water and confirmed by the very large seepage flows collected by the drainage in the region of blocks 7 to 11. The channels closure was performed by means of 13 inclined grouted drillings that were assumed to intercept the main discontinuities. Some 3000 kg of cement was used. The results were very good, the seepage rate being cut down from 10 l/s before grouting to 1 l/s after the grouting.

The third stage was started in 1992 and consisted in consolidation grouting performed at the downstream toe of the buttresses. Due to the fact that stress state variation in the dam upstream zone are induced by temperature changes but amplified by the rock mass deformability it was decided to make the rock mass stiffer by injecting cement grout into the open fissures. Two main effects were expected. Firstly, the consolidation reduces the irrecoverable part of the deformations, and secondly, it increases the rock's modulus of elasticity. Since the abnormal behavior was recorded at the blocks 6–12, near the right abutment, the consolidation grouting were performed only for the downstream zone of these blocks. The works were performed between 1992 and 1995. A total of 207 drillings with a cement uptake in the range of 40 ... 80 kg/m of drilling were realized. The favorable effects are shown in Figure 4. The irrecoverable settlement evolution was practically stopped and only elastic movements are recorded after the year 1996.

6 CONCLUDING REMARKS

The deterioration of drainage systems in dams may become apparent when for no other reason, the seepage volume decreases, usually slowly. Sometimes this is accompanied by an increase in the uplift pressure near the drains. Other drains in the vicinity may show increased discharges.

Experience shows that the piezometric pressure underneath a gravity dam is sometimes smaller than theoretically expected. This may be the result of fine material being washed from the reservoir into the joints in the rock below the dam, or another source of increased impermeability in the foundation.

Both for the deterioration of grout curtains and clogging of drains, only detailed and long-term monitoring results of seepage and uplift pressure, starting at the first impoundment of the dam, are a sufficiently reliable tool for the detection of deficiencies.

Poiana Uzului dam behavior incidents point out the in time evolution induced by the unfavorable overlapping of the mechanical and thermal loadings after many cycles of the reservoir filling and emptying. The in time changes of the grout curtain watertightness and

of the drainage condition is considered an ageing phenomenon and a program of remedial works was established.

The staged implementation of the program of remedial works has allowed a close monitoring of the effects achieved at the end of each stage and finally a review of the proposed program. Reservoir operation that prevents the unfavorable overlapping of the water pressure and thermal loadings proved to be a very efficient solution capable to eliminate the abnormal behavior of the dam.

REFERENCES

- Constantinescu, Al., Stematiu, D., Hapau-Petcu, S. 2003. Staged implementation of the remedial works program for Poiana Uzului buttress dam. Transactions of 21 Congress on Large Dams, Q82, R20, Montreal.
- ICOLD. 2000. Rehabilitation of dams and appurtenant works. Bulletin 119. Paris.
- Stematiu, D., Constantinescu, Al., Mircea, N. 1991. Cracking of Poiana Uzului buttress dam due to unusual structural behavior. *Proc. of Int. Conf. on "Dam Fractures"*, Boulder.
- Stematiu, D., Ilie, L. 1992. Safety assessment of Poiana Uzului dam based on monitoring data and backanalysis. *Proc. of Int. Symp. on "Monitoring Technology of Dam Safety"*. Hangzhou.

Unpredictable behaviour of a large arch dam in South Africa

L.C. Hattingh

Hattingh Anderson Associates, Pretoria, South Africa

C. Oosthuizen

Department of Water Affairs & Tshwane University of Technology, Pretoria, South Africa

ABSTRACT: The behaviour of the 88 m high Gariep Dam since 1972 is discussed as well as the various regression methods used to predict behaviour. An in-depth behaviour analysis performed in 2010 revealed that the majority of so-called “unpredictable” inelastic deformations occurred as a result of prolonged periods of low water levels. The observed stepped inelastic displacements as well as possible causes are briefly discussed. In conclusion, suggestions are made for the incorporation of duration-dependent inelastic and/or semi-plastic displacements (due to e.g. surface temperature, poro-plastic and swelling action) in regression models.

1 INTRODUCTION

The 88 m high Gariep Dam is located on the Orange River in South Africa (see Figure 1). The dam comprises of a double curvature arch in the river section changing to gravity sections on the flanks and has a reservoir capacity of more than 5 000 million cubic metres (the largest reservoir in the Republic of South Africa). The dam has been monitored since completion in 1972. Due its importance an effective monitoring system has been provided that was enhanced during the 1980’s with an elaborate 3-D crack gauge system across joints and major cracks. A prediction model is part of the monitoring system to check the actual versus predicted behaviour of the structure on a weekly basis. The relative simple monitoring system includes 3D-crack gauges, pendulums as well as a geodetic survey system.

A hybrid mathematical/statistical regression model was compiled by the designers soon after first filling. At that stage there were already differences between the theoretical and actual behaviour. This regression model performed reasonably well for a number of years (requiring regular updating as can be expected). However, during the flood events of 1988 the model failed the test. The updating process proved to be laborious, and soon resulted in even more differences between expected and the actual behaviour.

The confidence levels in the particular regression model gradually dropped (to the extent that it was even doubted for loads that were not previously experienced). A neural network regression model was therefore developed during the late 1990s. Initially, the results seemed to be promising (Hattingh & Oosthuizen 1998), but soon proved to have the same deficiencies as the mathematical/statistical regression model (Hattingh 2002).

To address this problem a detailed behavioural analysis was performed in 2010 during the 5-yearly compulsory dam safety evaluation (Hattingh 2010). 5-Yearly inspections are required in terms of the South African Dam Safety Legislation that forms part of the National Water Act of 1998 (RSA 1998). The purpose of this analysis was firstly, to get a better understanding of the behaviour of the dam; and secondly, to develop a more reliable regression model for the long-term evaluation of the dam.

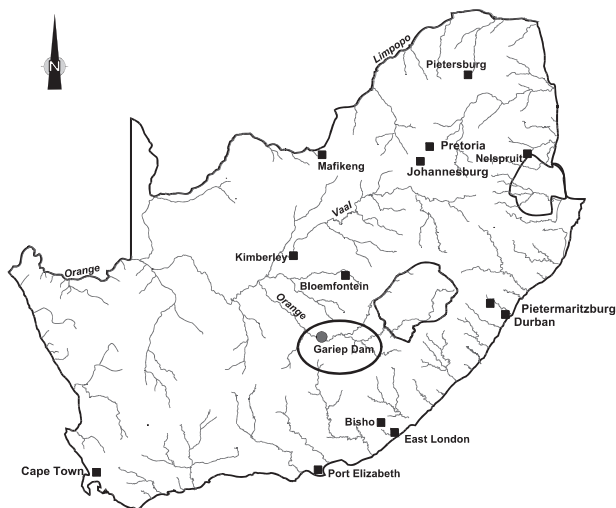


Figure 1. Location of Gariep Dam.

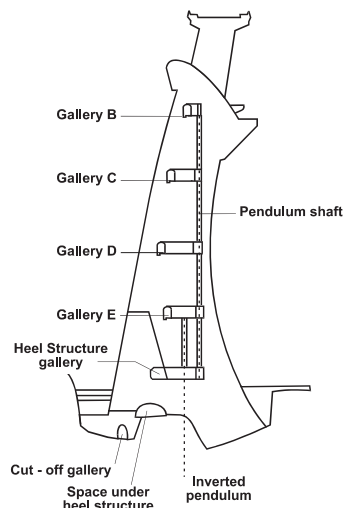


Figure 2. Section through block 1 (centre block).

2 RESULTS OF BEHAVIOUR ANALYSIS

2.1 *Pendulums*

The performance of the central part of the wall (mainly the double curvature arch) is monitored on a weekly basis by means of 7 pendulum systems (consisting of normal hanging pendulums in the concrete as well as inverted pendulums in the foundations). From these results the following were observed:

- As expected seasonal radial displacement of the structure is evident as well as the influence of water levels on the behaviour of the arch. No seasonal tangential displacement is observed; and
- Under “normal” conditions with the water levels not lower than 13 m below full supply level no abrupt inelastic radial displacement is evident. It is important to note that after the two prolonged periods of low water levels in the early and middle 1990s where the water level dropped to lower levels, it is clearly evident that some inelastic displacement in a downstream direction has occurred. This occurred gradually over a period of time—with a maximum inelastic displacement of 12 mm evident in Gallery B of block 1 i.e. the centre of the wall (see Figure 2 for a section through block 1 and Figure 4 for the radial pendulum displacements of Gallery B (top gallery) in the centre of the wall (block 1)). This observation is confirmed by the results of the geodetic survey system comprising triangulation levelling and traversing through selected galleries (see paragraph 2.2 below). This phenomenon could probably be attributed to the poro-plastic behaviour of the arch structure highlighting the importance of the effect of pore pressures in the concrete. This hypothesis is confirmed in the results of 3D-crack gauges (see paragraph 2.3 below).

2.2 *Geodetic survey*

The performance of the entire dam wall is also monitored on six monthly intervals by means of geodetic surveying done by geodetic surveyors of the Department of Water Affairs. From their results the following have been observed:

- Seasonal downstream displacements are clearly evident with the largest displacements as expected in the arch. The maximum displacement of 20 mm was observed on the bridge in the centre of the arch (see Figure 2);



Figure 3. Downstream view of Gariep Dam.

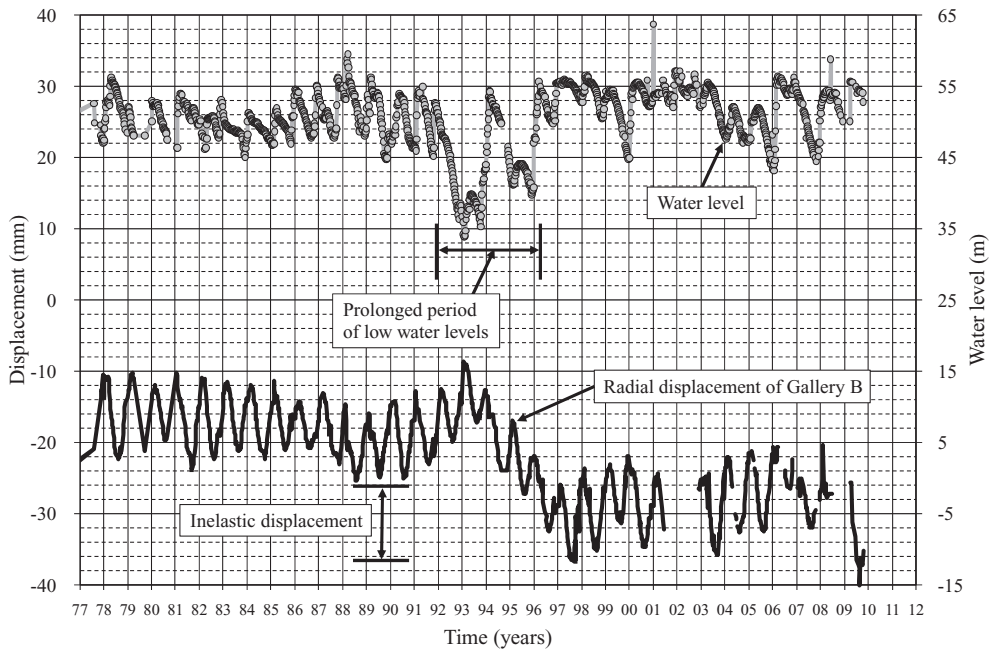


Figure 4. Radial pendulum displacement of Gallery B in the centre of the wall (block 1) (upstream movement is positive).

- The direct relationship between water levels and displacements, i.e. the behaviour of the arch, is also evident; and
- The same permanent (inelastic) downstream displacement after the two prolonged periods of low water levels in the early- and middle 1990s as shown by the pendulum results (see paragraph 2.1 above) is also evident.

2.3 3D-crack gauges

3D-crack gauges were installed in Galleries A, B and D across all the construction joints in 1992 and subsequently replaced in 2002 with DWAF 2001 type 3D-crack-tilt gauges due to the fact that an electrolytic action between the back plate and the gauge that caused corrosion leading to false displacement readings. From the results of the 3D-crack gauges the following have been observed:

- No inelastic displacement is evident after the prolonged period of low water levels from the results of the 3D-crack gauges;
- This together with the fact that the radial displacements shows seasonal cyclical movements only at the extends of the gravity flanks as well as close to the spillway in the gallery flanking the spillway confirmed the primary arch action in the spillway section, additional “stiffness” in the left flank arch section as well as the additional stiffness created by the outlet works and chute spillways; and.
- The seasonal cyclical tangential displacements are decreasing in magnitude towards the centre of the wall confirming primary arch action in the spillway section as well as additional “stiffness” in the left flank arch section.

3 REGRESSION ANALYSIS

The hybrid mathematical/statistical regression model developed during the latest dam safety evaluation only uses two (2) independent variables/regressors—the water level and the date which was transformed to time of the year variable (s) as well as time since the start of the regression analysis (t). The water level was used in its basic form while the time of the year (s) was used to represent the cyclical nature of the seasonal displacements in the form of Sine (s) and Cosine (s). Inelastic displacements were modelled using the time since the start of the regression analysis (t) in the form of e^{-t} , $e^{-t/2}$, $e^{-t/4}$ and $e^{-t/8}$. This regression model is therefore basically similar to the hybrid mathematical/statistical regression model developed during the 1970s that used water level and the date as independent variables/regressors.

3.1 Pre- 1992 analysis

When a regression period from the end of construction to the beginning of 1992 (the start of the first prolonged period of low water levels) is used for calibration purposes, it is evident that the original regression model was unreliable for the period after 1992. See Figure 5 for the regression results of the radial pendulum displacements of Gallery B in the centre of the wall. The residuals and the 95% prediction interval limits are also shown in the above-mentioned graph. The inelastic displacements as a result of the prolonged periods of low water levels are clearly visible. This regression model only made provision of a total inelastic displacement of 6 mm over a 30 year period (0.2 mm/year).

3.2 The 2010 analysis

When using a regression period from the end of construction to the beginning of 2003, it is evident that the proposed regression model predicts displacements most of the time within the 95% prediction interval limits for the residuals. See Figure 6 for the regression results of

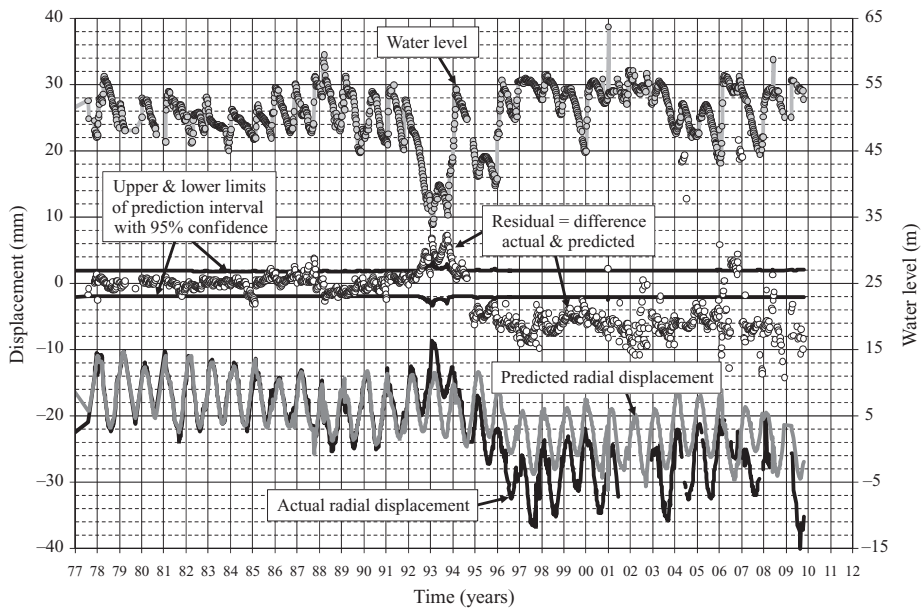


Figure 5. Regression results of pendulum displacement of Gallery B using a regression period from 1977 to 1992 (upstream movement is positive).

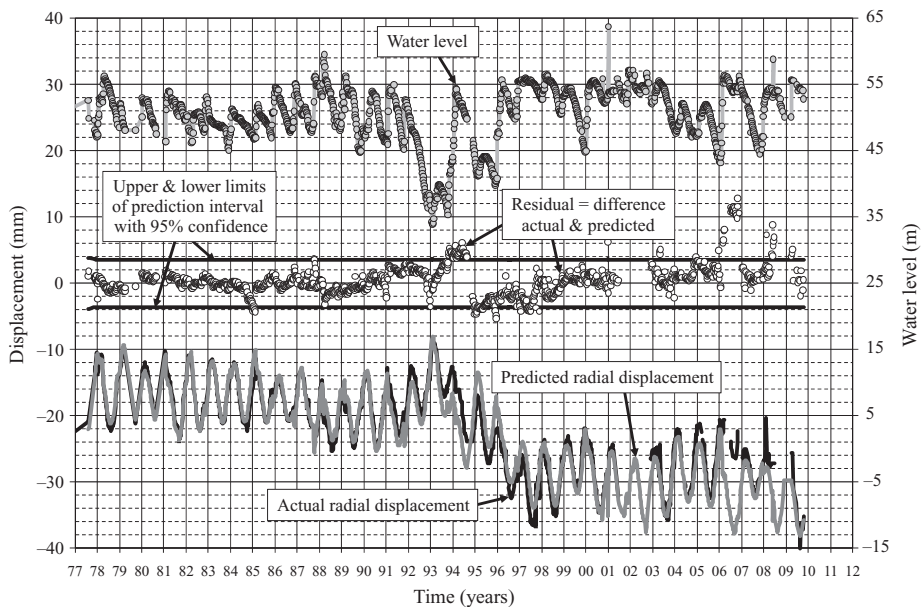


Figure 6. Regression results of pendulum displacement of Gallery B using a regression period from 1977 to 2003 (upstream movement is positive).

the radial pendulum displacements of Gallery B in the centre of the wall as well as the residuals and the 95% prediction interval limits. The improvement is mainly due to the regression model making provision of a total inelastic displacement of 14 mm over a 24 year period with the majority of the inelastic displacement taking place during the prolonged periods of low water levels.

4 CONCLUDING REMARKS

From the results of the monitoring system it is evident that inelastic deformations occurred especially in the central double curvature arch as a result of prolonged periods of low water levels. This was the main reason for the previous failure of the hybrid mathematical/statistical regression model developed in the 1970s as well as the neural network developed during the 1990s.

It must be mentioned that similar inelastic deformations are observed after prolonged periods of low water levels in several other concrete arch dams in South Africa. It is hypothesized that these inelastic deformations could be attributed to the poro-plastic behaviour of arch structures. This highlights the importance of pore pressure measurements in these dams. The importance of the results of 3D-crack gauges in making conclusions in this regard should also be emphasised.

Finally, the use of a simple hybrid mathematical/statistical regression model with only two independent variables/regressors (water level and the date as well as time since the start of the regression analysis) proved to be successful as it predicts displacements most of the time within the 95% prediction interval limits for the residuals.

ACKNOWLEDGEMENTS

The authors wish to express their gratitude to all other present and past members of Sub-directorate Dam Surveillance that contributed in some or other way to the development of the above-mentioned paper. The opinions expressed are however those of the authors and do not necessarily reflect the views of the Department of Water Affairs.

REFERENCES

- Hattingh, L.C. & Oosthuizen, C. 1998. Surveillance of Gariep Dam using neural networks. *Proceed. Int. Symp. on New Trends and Guidelines on Dam Safety*, Barcelona, Spain, 17–19 June 1998.
- Hattingh, L.C. 2002. A critical review of the use of a neural network prediction model in the surveillance of a large dam. *Proceedings of the Conference called "Dam Engineering 2002"*. Singapore, 20–22 March 2002.
- Hattingh, L.C. 2010. *Gariep Dam: Fourth Dam Safety Inspection Report*. Report No. 20/2/D350/02/D/1/22. Department of Water Affairs, Pretoria, South Africa.
- Republic of South Africa. 1998. *National Water Act. Act No 36 of 1998*. Government Printer. Republic of South Africa.

Performance of a high rockfill dam during construction and first impounding—Nam Ngum 2 CFRD

S. Moll & R. Straubhaar

Pöyry Energy Ltd., Zürich, Switzerland

ABSTRACT: The 182 m high Concrete Face Rockfill Dam (CFRD) is one of the main components of the Nam Ngum 2 (NN2) hydropower scheme in Lao PDR. Construction of the dam was essentially completed in March 2010 and reservoir impounding commenced subsequently. This paper presents the main dam design features comprising dam zoning, face slab design and instrumentation. Construction principles and rockfill properties are explained. The main observations from the dam monitoring during construction and impounding are presented. The dam deformations as monitored up to date are taken as basis for back-calculations of rockfill properties. A comparison of observed dam deformation behaviour with different rockfill deformation simulation and prediction models is made.

1 INTRODUCTION

1.1 *Nam Ngum 2 hydropower scheme*

The Nam Ngum 2 (NN2) hydropower scheme is located on the Nam Ngum river in Lao PDR, about 90 km north of the capital Vientiane and some 35 km upstream of the existing Nam Ngum 1 dam and powerhouse. With an installed capacity of 615 MW, the project will produce 2220 GWh per year energy for the Thai electricity grid. A significant component of the scheme is the 182 m high concrete face rockfill dam, with a volume of 9.7 M m³ and a crest length of 500 m. The dam impounds a reservoir with a volume of approximately 4900 M m³. A layout of the scheme is shown on Figure 1.

Construction of the NN2 Project commenced in late 2005 and was essentially completed in the second half of 2010. Rockfill placement in the dam body started in January 2008 and was completed in November 2009. Construction of the face slab, which was divided into two stages, was performed from December 2008 to July 2009 and from November 2009 to February 2010. Reservoir impounding started mid of March 2010 with the closure of the diversion tunnels. The full supply level (FSL) will be reached at the end of the rainy season in November 2010. Commissioning of the first generating unit and synchronization to the Thai grid was achieved in August 2010. Full commercial operation of the plant is scheduled to start end of December 2010.

2 DAM DESIGN

2.1 *Dam foundation*

The dam is situated in a narrow valley and is founded on sedimentary rock of variable strength. The geological formations at the dam site consist of medium bedded to massive cliff-forming sandstone, interbedded with siltstone. Three easterly trending folds whose axes are nearly perpendicular to the Nam Ngum river are present at the dam site. The cliff-forming sandstone is generally slightly jointed and fractured, whereas the interbedded siltstone is

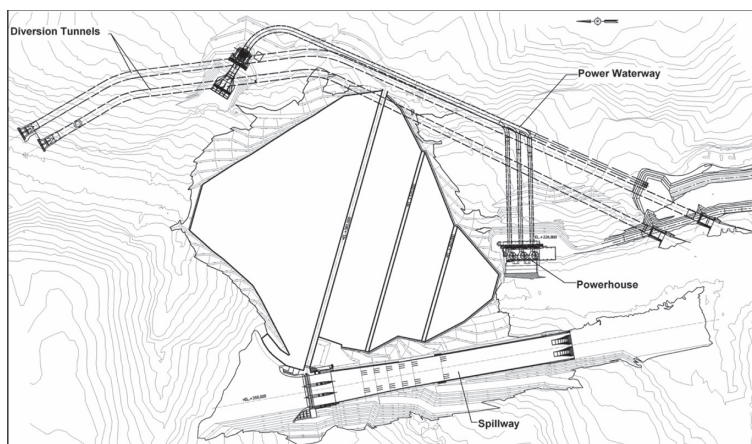


Figure 1. Project layout.

moderately to closely jointed. The typical quality of the foundation rock varies within the following limits:

- Sandstone: fresh, hard and slightly fractured, locally weathered and heavily fractured.
- Siltstone: fresh to weathered, soft and slaking.

Different foundation treatment measures have been carried out to cope with the foundation rock in particular in the upstream third of the dam.

2.2 Dam geometry and zoning

The dam has a maximum height of 182 m above the foundation at the deepest section. Both, upstream and downstream slope are inclined at 1v: 1.4 h (downstream incl. berms: 1v: 1.5 h). The dam crest is 500 m long and 12 m wide. The total dam volume is 9.7 M m³.

The dam was originally designed with a “traditional” zoning i.e. with face slab support and transition zone (2B, 3A), the main dam body of 2 rockfill zones (3B, 3C) with larger maximum size and higher lift thickness towards the downstream slope and a drainage zone (3D) at the dam bottom at the downstream 2/3 of the dam. An upstream fill (1A, 1B) is provided upstream of the face slab.

During construction it was observed that also rockfill of moderate quality and with an increased sand content was obtained from quarrying which could not always completely be separated and wasted. Therefore, the dam zoning was adjusted to permit also placement of lower quality rockfill in the central part of the dam embankment. The final dam zoning is shown on Figure 2.

2.3 Rockfill characteristics and construction principles

For the construction of the dam quarried rock of sedimentary formations were available. The source material, consisting basically of sandstone and siltstone, has been investigated by drilling, quarry trials and laboratory testing. Of particular interest were large scale triaxial and compressibility tests, which have been carried out by the IWHR¹ in China. From the results of these tests material parameters were derived which were then taken as basis for 2-D and 3-D deformation analysis. The results of the laboratory tests and also visual observations indicated a high disintegration potential of the siltstone which could lead to high dam deformations. By using only sandstone for rockfill it was concluded that the dam deformation will be within acceptable and normal limits.

1. China Institute of Water Resources and Hydropower Research (IWHR), Department of Geotechnical Engineering.

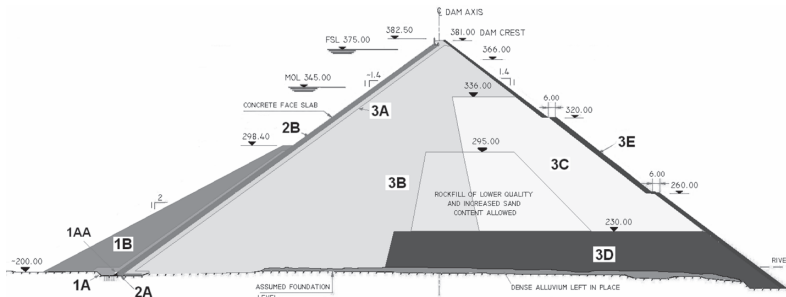


Figure 2. Dam zoning.

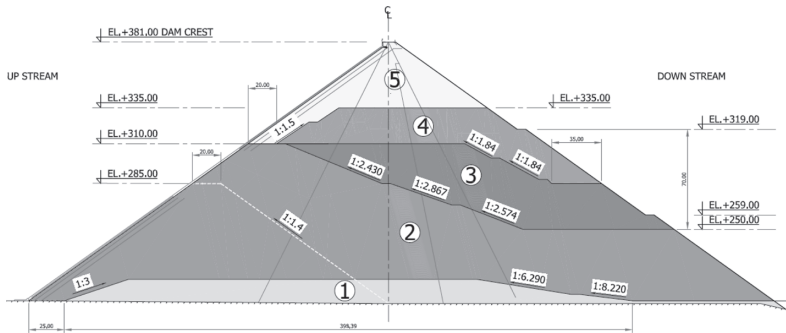


Figure 3. Dam construction stages.

For the rockfill fresh to moderately weathered sandstone was used whereby the lower quality material was placed in the central zone of the dam (see Ch. 2.2).

In general the used rockfill can be characterized as follows:

- The particle size is relatively large and particle shape is angular
- The gradation is often uniform and gap-graded, with lack of gravel-size particles
- Due to the gap-grading and increased sand content, water sluicing during placement leads to the development of a mud layer on the rockfill surface which needs to be removed
- The relative densities obtained after placement were generally adequate although areas of segregated fill occasionally occurred

The rockfill of the main dam body was placed in lifts of 0.8 m (zone 3B) and 1.2 m (zone 3C) thickness and compacted with 6–8 passes of 16 t vibrating roller compactors. The amount of water added to the fill was in the range of 100–150 l/m³.

The staging of construction is shown on Figure 3. Construction of the first stage of the face slab (up to EL 293.4 masl) commenced after completion of the rockfill stage 2. During first stage face slab construction rockfill placement continued with stage 3 and 4.

The average rockfill placement rate was about 460,000 m³/month, with a maximum placement rate of 770,000 m³/month. The total volume of 9.7 M m³ was placed in 21 month.

2.4 Face slab design and construction

The dam is situated in a steep “V”-shaped valley. The concrete face slab has an area of about 88,000 m² and the valley shape factor is $A/H^2 = 2.7$. Considering this valley shape factor, increased movements of the face slab panels towards the river bed and resulting horizontal stresses in the central face slab panels were expected and considered in the design. Figure 4 shows the valley shape factor of NN2 CFRD plotted on the graph developed by Pinto (2007).

With an assumed deformation modulus of 50 to 70 MPa the conditions at NN2 are about the same as at Campos Novos and Barra Grande CFRD where compression cracking of the face slab did occur.

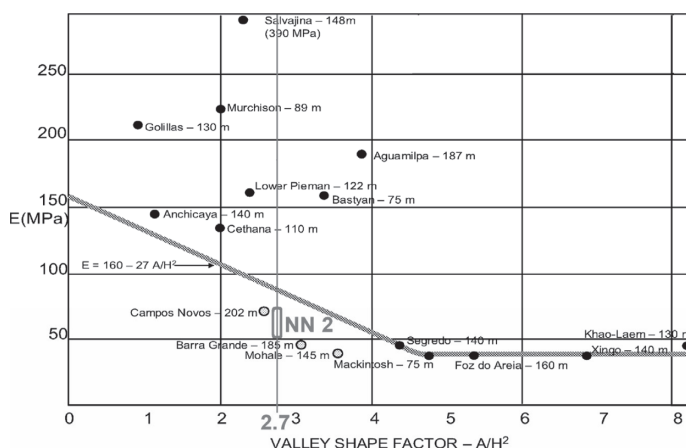


Figure 4. Graph deformation modulus vs. valley shape factor (after Pinto (2007)).

The face slab is designed with a thickness of $T = 0.3 + 0.003 H$. At the upper portion of the central slabs (above EL 293.4 masl) the thickness is somewhat increased to $0.4 + 0.0018 H$ to improve the resistance of the slab under compression. The face slab is constructed in panels of 15 m width. At the steep abutments the slab width is reduced to 7.5 m to cope with expected increased differential settlements along the relatively steep abutment slopes.

The vertical tension joints at the abutments are designed with bottom copper waterstop and GB®-surface waterstop², including corrugated waterstop, at the surface. An asphaltic bond breaker is applied on the concrete surface at the joint. The central joints are designed as compression joints with 20 mm thick compressible cork filler to allow some movement of the slabs towards the valley under compression. At the bottom a copper waterstop and at the surface a GB®-waterstop, without corrugated rubber waterstop, is provided. To maintain the designed slab thickness at the joints, the central loop of the copper waterstop is reduced and the chamfer at the slab surface is omitted. The perimeter joint is designed with copper waterstop at the bottom and GB®-waterstop system at the surface, including corrugated waterstop. A 20 mm thick bitumen painted wood filler is provided at the joint.

The face slab is constructed in two stages: Stage 1 up to EL 293.4 masl and stage 2 from EL 293.4 masl up to the top (connection to the parapet wall). The horizontal joint between the first and second stage of the face slab is constructed as movement joint with 20 mm joint filler board and bottom copper waterstop and surface GB®-waterstop. This joint will reduce the compressive stresses in slope direction.

Double layer reinforcement of total 0.4% in each direction is provided throughout the face slab. The reinforcement ratio is increased to 0.5% in each direction in an area of generally 20 m parallel to the plinth alignment and up to 40 m from the plinth at the very steep right abutment where higher stresses due to increased differential settlements are expected.

At the central slabs in an area of about 1/4 to 3/4 of the dam height, where the highest compressive forces will occur, additional stirrups are provided to prevent buckling of the upper and lower reinforcement under high compression. Anti-spalling reinforcement is provided along compression joints.

For the ease of construction the extruded curb method is used for the upstream face construction. Although constructed of lean concrete of low compressive strength (about 5 MPa), the deformability of the extruded curbs is significantly lower than that of the underlain zone 2B rockfill. Therefore, if the rockfill deforms and settles the relatively stiff curbs may not always follow the movements of the fill and potential voids may develop during dam construction.

When the concrete face is exposed to high water load (during impounding) the curbs may crack in areas of voids. In this case the concrete slab is subject to rapid deformations and high stresses.

2. GB® Waterstop Structure of Beijing IWHR-KHL Co. Ltd., China.

Therefore, the development of large voids beneath the concrete curbs must be avoided or already developed voids should be filled before impounding as e.g. done at Karahnjukar CFRD where extensive void grouting beneath the curbs and between face slab and curbs was performed.

To reduce the development of significant voids behind the curbs they should be as flexible as possible to be able to move with the rockfill deformations. In this respect cutting of the curbs into smaller pieces is promising. Therefore, at some recently constructed CFRDs in China the curbs were cut vertically at the locations of the face slab joints before construction of the face slab. At NN2 grooves were excavated into the extruded curbs during its construction on both sides along the vertical face slab joints to achieve predefined break lines in the curbs. During construction it was observed that several cracks in fact developed along these grooves.

After completion of the dam rockfill construction and during the construction of the second stage face slab exploratory holes were drilled through the face slab and curbs at defined locations. In these holes tests were performed to investigate if voids have developed between the face slab and the curbs or the curbs and the 2B fill which would have had to be grouted. No significant voids were, however, encountered.

3 INSTRUMENTATION AND MONITORING

3.1 Instrumentation concept

Instrumentation is provided to measure the behaviour of the dam during construction, reservoir impounding and long term operation. Emphasis is given towards monitoring seepage which could arise from imperfections of the face slab and from percolations through the dam foundation, and towards monitoring of embankment deformations. Seepage is indirectly monitored by piezometers installed upstream and downstream of the plinth and grout curtain, in the dam foundation and along the abutments. Seepage quantities are measured with a seepage weir at the dam toe. Deformations are mainly measured with settlement plates, embankment extensometers and inclinometers installed in the dam body and with joint-meters and tiltmeters installed at the face slab.

3.2 Monitoring and dam behaviour during construction

Dam deformations during construction were measured with hydrostatic settlement cells, fixed embankment extensometers and settlement gauges with combined inclinometer tubing. These instruments provided data of deformations along 3 sections within the dam body.

The maximum recorded construction settlement is 1.8 m, measured at both instrument levels EL 260 masl and EL 319 masl slightly downstream of the dam centre. The construction settlements measured with the instruments were used for calculating the deformation moduli during construction E_{rc} :

$$E_{rc} = \frac{\gamma Hd}{s} \quad (1)$$

where γ = unit weight of fill above settlement plate; H = height of fill above settlement plate; d = thickness of fill below settlement plate, s = recorded settlement of the settlement plate.

The back-calculated deformation moduli during construction are in the range of 70 MPa (upstream side) to 50 MPa (downstream side). Using these deformation moduli the dam settlements during construction were back-modelled using an elasto-plastic material model. The calculated dam settlements comply well with the measured settlement as shown on Figure 5. The maximum dam settlement at the end of construction is about 2.2 m which corresponds to 1.2% of the dam height.

3.3 Monitoring and dam behaviour during first impounding

The first reservoir impounding started in March 2010 just after the completion of the second stage face slab construction and about 4 months after completion of the dam fill. Until December 2010 the reservoir was filled up to about 98% of the full supply level (FSL). Seepage quantities

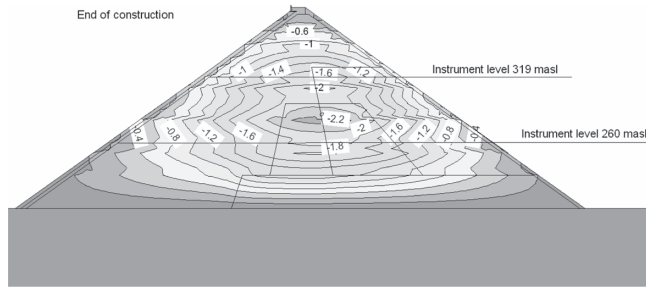


Figure 5. Dam settlements (in m) at the end of construction.

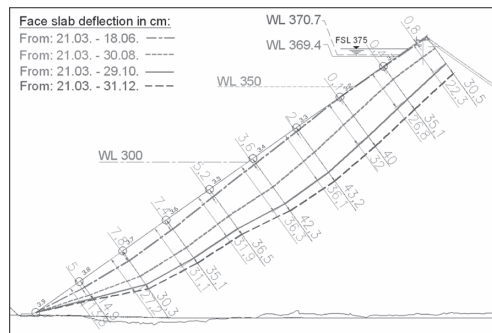


Figure 6. Face slab deflection derived from tiltmeter readings.

recorded with the seepage measuring weir have increased relatively linearly with the rise of the reservoir level until September 2010 when the reservoir level 360 masl (approx. 90% of FSL) was reached. Since then the recorded seepage quantity was stable at 80–90 l/s and it was suspected that the maximum capacity of the measuring system was somehow exceeded. After rectification works at the system had been performed a seepage quantity of about 300 l/s was measured.

Post-construction dam deformations generally occur due to the following reasons:

- Increased load from the reservoir
- Creep; softening of the rock due to wetting/water saturation

The increasing water load during reservoir impounding mainly acts on the dam face and causes the concrete face and the upstream part of the rockfill to deform. The face slab deflection is measured by tiltmeters (electro-levels) installed on the face slab and by geodetic survey of surface displacement points.

The face slab deflection at different reservoir levels as measured with the tiltmeters installed at a central face slab panel is shown on Figure 6. The face slab deflection has significantly increased after the water level exceeded EL 300 masl. At a reservoir level of 371 masl (corresponding to about 98% of FSL) the maximum face slab deflection since start of impounding is in the order of 43 cm and occurs at about half height of the dam.

From the deformation monitoring data of the downstream side of the dam body where the reservoir load has only little or no impact quite pronounced creep settlements are observed. Data from the settlement cells in the downstream part of the dam body and geodetic survey data of the downstream shell indicate a settlement rate of 20–40 mm/month.

4 DAM DEFORMATION PREDICTION AND BACK-CALCULATION

Several methods for predicting dam deformations during construction and first reservoir impounding exist. Such methods range from simplified deformation estimates based experience, up to mathematical modeling with various constitutive models.

For the Nam Ngum 2 dam 2-dimensional and 3-dimensional numerical stress and deformation analyses have been performed by IWHR³ prior to the construction of the dam. The analyses were performed using the non-linear hyperbolic material model. The used rockfill parameters were based on results from large scale triaxial tests carried out on samples from the quarry with gradations downscaled to suit the testing equipment. Additional calculations have been performed using adjusted rockfill properties. The used rockfill parameters are listed in Table 1.

In Table 2 the displacements obtained with the 3-dimensional analysis using the above sets of material parameters are summarized. It is noticed that the computed displacements are considerable lower than the actual displacements, indicating that the embankment materials behave softer than assumed based on triaxial testing.

It should be noted that the maximum settlement at the end of construction is observed in the central downstream part of the dam which is not much influenced by the water load acting on the concrete face.

After completion of the dam construction 2-dimensional numerical analyses have been performed using deformation moduli E_{rc} , back-calculated from the settlements measured with the instruments during construction. For the analysis an elasto-plastic constitutive model was used.

As shown in chapter 3.2 the back-calculated dam deformations at the end of construction coincide well with the monitored deformations (see chapter 3.2, Fig. 5). If the same parameters would be used for calculating the face slab deflections due to impounding, a value of 1.1 m would be obtained.

However, the deformation moduli to be used for estimating face deflection are normally higher. A simple and practical way of predicting the maximum face slab deflection is to consider the deformation modulus E_T of the rockfill evaluated in the direction of the face

Table 1. Material parameters used for numerical analyses.

Materials	γ_d (g/cm ³)	K	K_{ur}	n	R_f	K_b	m	c (kPa)	ϕ_0 (°)	$\Delta\phi$ (°)
Case 1: Zone 2B*	2.15	1600	3200	0.38	0.918	2800	-0.27	-	44.1	4.2
Zone 3A*	2.15	1040	2080	0.31	0.820	1000	-0.06	-	45.9	5.7
Zone 3B*	2.15	1000	2000	0.38	0.864	1680	-0.29	-	46.5	6.2
Zone 3C*	2.10	630	1260	0.37	0.802	520	0.0	-	45.1	5.4
Case 2: Zone 2B	2.15	1000	2000	0.35	0.918	500	0.20	-	44.1	4.2
Zone 3A	2.15	1000	2000	0.35	0.820	500	0.20	-	45.9	5.7
Zone 3B	2.15	630	1260	0.37	0.864	400	0.10	-	46.5	6.2
Zone 3C	2.10	630	1260	0.37	0.802	400	0.10	-	45.1	5.4

* Derived from triaxial test results.

Table 2. Results of 3-dimensional analyses.

Case	Case 1	Case 2
Settlement end of construction (cm)	96	140
Settlement after impounding (cm)*	98	149
Face slab deflection due to impounding (cm)	20	34

* Including construction settlements.

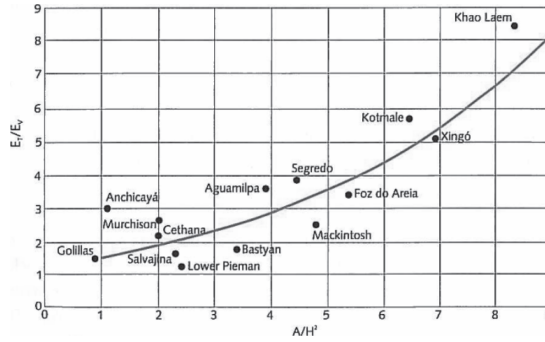


Figure 7. Ratio E_T/E_V as a function of A/H^2 (Pinto & Marques Filho (1998)).

slab movement, i.e. normal to the face slab, under the water load. Considering this transverse modulus the maximum face slab deflection D can be estimated:

$$D = \frac{\gamma_w H_w H_d}{E_T} \quad (2)$$

where γ_w = unit weight of water; H_w = height of water above face slab; H_d = thickness of fill below face slab (perpendicular to face slab), E_T = transverse rockfill modulus.

The transverse modulus E_T is higher than the vertical modulus E_V (E_V is equivalent to the modulus during construction E_{rc} as defined in Equation 1) due to a rotation of the principal stresses within the rockfill and rockfill consolidation during construction. Observed values are generally 1.5 to 5 times higher than the vertical modulus depending greatly on the valley shape factor A/H^2 , but certainly also on the creep characteristics of the rockfill. Knowing the vertical modulus E_V calculated from the measured settlements during construction E_T can be estimated using the graph developed by Pinto & Marques Filho (1998) (Fig. 7).

Considering the valley shape factor of $A/H^2 = 2.7$ and the vertical rockfill modulus $E_V = E_{rc} = 70$ MPa the maximum face slab deflection of the NN2 dam would be in the order of 65 cm occurring at about half of the dam height and full reservoir level.

5 CONCLUSION

The monitoring system of the Nam Ngum 2 dam has provided useful information on the deformation behavior of the dam. The maximum settlements at the end of construction are about 2.2 m which corresponds to 1.2% of the dam height. The measured maximum face slab deflection due to impounding up to 98% of FSL is 0.43 m. The maximum settlement may have reached a value corresponding to 1.5% of the dam height. The deformations will further increase with rising reservoir to full supply level and due to creeping of the rockfill. The deformation monitoring indicates a high rate of creeping.

Measured seepage quantities are in an acceptable range. At present the performance of the dam is good and the visual appearance is excellent.

The back-calculation of dam deformations and prediction of face slab deflection under consideration of deformations measured during construction give reasonable results. A reliable estimation of the in-situ rockfill properties, in particular its creep characteristics, remains the main challenge for deformation prediction.

REFERENCES

- Pinto, N.L.S. 2007. A challenge to very high CFRD dams: Very high concrete face compressive stresses. *5th International Conference on Dam Engineering*. Lisbon, February 2007.
- Pinto, N.L.S. & Marques Filho, P.L. 1998. Estimating the maximum face deflection in CFRDs. *The International Journal on Hydropower & Dams*. Issue 6, 1998: 28–31.